Analysis of an Instrumented Jointless Bridge

By

Mervyn J. Kowlsky
Principal Investigator

Mickey Wing
Graduate Research Assistant

Research Project # 2001-01
FHWA/NC/2002-22

Final Report

In cooperation with the

North Carolina Department of Transportation

Department of Civil Engineering
North Carolina State University
Campus Box 7908
Raleigh, NC 27695-7908

June 2003

Technical Report Documentation Page

1. Report No. **FHWA/NC/2002-22**	2. Government Accession No.	3. Recipient's Catalog No.
4. Title and Subtitle **Analysis of an Instrumented Jointless Bridge**		5. Report Date **June 2003**
		6. Performing Organization Code
7. Author(s) **Mervyn J. Kowalsky and Mickey Wing**		8. Performing Organization Report No.
9. Performing Organization Name and Address **Department of Civil Engineering** **North Carolina State University** **Campus Box 7908** **Raleigh, North Carolina 27695**		10. Work Unit No. (TRAIS)
		11. Contract or Grant No.
12. Sponsoring Agency Name and Address **North Carolina Department of Transportation** **Research and Analysis Group** **1 South Wilmington Street** **Raleigh, North Carolina 27601**		13. Type of Report and Period Covered **Final Report** **August 2000 – July 2002**
		14. Sponsoring Agency Code **2001-01**
Supplementary Notes:		

16. Abstract

Through the use of remote data acquisition, the behavior of an instrumented jointless bridge is explored. The bridge structure, located in Haywood County North Carolina, was recently rehabilitated by the North Carolina Department of Transportation. As part of the rehabilitation, the superstructure was widened and a joint-less link-slab deck employed. The goals of the research are to validate analysis and design assumptions, investigate limit-states design methods, and develop a strategy and guide for long-term monitoring of jointless link-slab bridges.

17. Key Words **Link-slab, joint-less bridges, field monitoring**	18. Distribution Statement		
19. Security Classif. (of this report) Unclassified	20. Security Classif. (of this page) Unclassified	21. No. of Pages **111**	22. Price

Form DOT F 1700.7 (8-72) **Reproduction of completed page authorized**

DISCLAIMER

The contents of this report reflect the views of the author(s) and not necessarily the view of the University. The author(s) are responsible for the facts and the accuracy of the data presented herein. The contents do not necessarily reflect the official views or policies of the North Carolina Department at the time of publication. This report does not constitute a standard, specification, or regulation.

ACKNOWLEDGMENTS

The authors are indebted to many individuals for their support at the various stages of the research. They included, Tim Rountree, Moy Biswas, Robert Woodruff, Rodger Rochelle, and Tom Koch of NCDOT.

The authors would also like to thank the technical staff of the NCSU Constructed Facilities Laboratory, in particular, Jerry Atkinson who assisted in various aspects of instrumentation at the laboratory. The authors also received invaluable help from the following graduate students: Bruce Warren, Matt Wagner, and Bryan Ewing. The assistance from Dr. Paul Zia is also greatly appreciated.

SUMMARY

Through the use of remote data acquisition, the behavior of an instrumented jointless bridge is explored. The bridge structure, located in Haywood County North Carolina, was recently rehabilitated by the North Carolina Department of Transportation. As part of the rehabilitation, the superstructure was widened and a jointless link-slab deck employed. The goals of the research are to validate analysis and design assumptions, investigate limit-states design methods, and develop a strategy and guide for long-term monitoring of jointless link-slab bridges.

TABLE OF CONTENTS

LIST OF FIGURES

LIST OF TABLES

1. Introduction

1.1 Background and Location of Bridge

In 1997, the North Carolina Department of Transportation (NCDOT) Research and Development Unit identified a structure in Haywood County, North Carolina, that was suitable for employing the link slab concept (see Section 1.3). The bridge in question was being widened to accommodate an extra lane of traffic and at the same time, it was decided to utilized link slabs to reduce the total number of joints in the deck. This rehabilitation project provided an excellent opportunity to instrument the link slabs that were replacing the traditional expansion joints and to evaluate their performance in the field. The bridge was instrumented by NSCU and the NCDOT in 1999 (Warren, 2000).

The project site is located in western North Carolina in the city of Waynesville. The actual bridge carries southbound traffic on US 23-74 bypass over Plott Creek and state road 1173 (see Figure 1.1). Design average daily traffic is 25600 vehicles and the design average daily truck traffic is 2050 trucks. The posted speed limit is 55 miles per hour (Warren 2000).

The original structure was built in 1965. It is a four span, steel girder bridge with two lanes of traffic. The substructure units are supported on steel H-piles. New columns and pier extensions were built in 1998 to support the additional girder line that was needed to accommodate the extra two lanes of traffic. Girder spans are simply-supported, but the deck was continuous due to the presence of the link slabs. One expansion joint still remains at the centermost bent (Warren 2000).

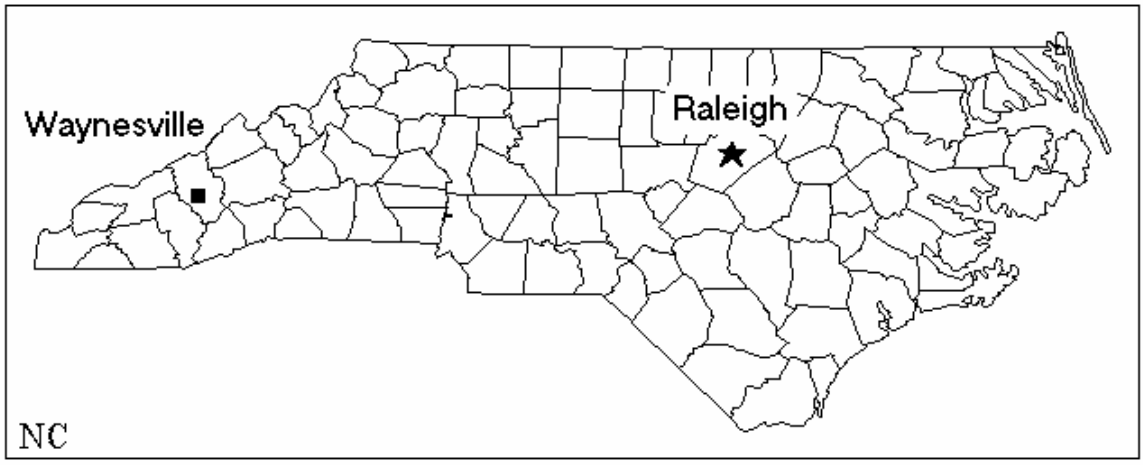

Figure 1.1 Map of North Carolina and project location.


Figure 1.2 Bridge elevation, looking east.

Figure 1.3 Plott Creek and underside of bridge.

1.2 Purpose of Structural Instrumentation

Instrumentation is the process of applying many different instruments to structural members to learn more about the actual behavior of the elements. There are many different instruments that can be applied to members to measure many different responses. Thermal variations, deflections and strains are just some of the quantities that can be measured that are important to an engineer.

Once a structure has been instrumented, data can be collected from the different devices and analyzed. This is important because the data will show how the structure actually behaves. It can then be compared with the anticipated behavior of the structure to see if the design is satisfactory. Long-term analysis of data from instrumentation could also warn an engineer if the system is deteriorating or if the system is susceptible to failure.

1.2.1 Introduction to Structural Instrumentation

The basic data acquisition system includes the following: power source, processing unit (datalogger), multiplexer (collection point for gauges), sensing devices (gauges), data storage device and a retrieval device. Data Acquisition systems may include other components that improve efficiency, but they all must have the above.

The most common power source for data acquisitions systems in the field is a 12-volt battery. This is what is used to power the datalogger. Instead of constantly having to replace dead batteries, a solar panel can be used to charge the battery.

The datalogger is the brains of the data acquisition system. It controls how often measurements are taken, manipulates data to achieve desired output and stores data until it is collected. The datalogger receives instructions for operation from a complex set of computer instructions.

Multiplexers are used as a collection point for a large number of gauge readings. All of the gauges are connected to a multiplexer and the multiplexer is connected to the datalogger. Multiplexers are important because they increase the number of gauges that can be connected to the datalogger and they also reduce the amount of wires that are being connected to the datalogger. If the datalogger is programmed correctly, the datalogger can still control all of the individual devices connected to the multiplexers.

Measuring devices are the heart of the data acquisitions system. The measuring devices are the individual gauges that take readings. Determining the specific types of gauges to be used depends on the information that is needed. Examples of different instruments that are commonly used include: thermocouples, vibrating wire gauges and electrical resistance strain gauges. These types of gauges measure temperature and strain.

The instruments are connected to the multiplexer, which is then connected to the datalogger.

There are several ways to collect the data from the datalogger. One way is through a direct connection to the datalogger. Different variables such as the project site location and datalogger location can hinder this method of data retrieval. A more suitable method would be to use a modem that is connected to the datalogger. Any personal computer with the proper software could use the modem to connect with the datalogger and download the data. This method would be appropriate if the project site is not nearby and if the datalogger is not readily accessible at the project site. The modem could also be used to send a different computer program to the datalogger to alter the measuring instructions.

1.3 Overview of a Link Slab

A jointless bridge deck is a deck in which there are no traditional expansion joints. Instead of expansion joints, the bridge deck has what are known as "Link Slabs." A link slab is the portion of the deck connecting two adjacent simple-span girders (El-Safty 1994).

Traditional bridge deck joints pose many problems with regards to bridge maintenance. Water penetration through the joint can damage the girder end bearings and supporting structures. Debris accumulation within the expansion joint will also prevent the expansion of the deck and ultimately cause damage. Joints and bearings are expensive to install and maintain. A more feasible alternative to expansion joints is the use of link slabs. Link slabs will reduce both the installation and maintenance costs associated with traditional joints. It should also be noted that under normal service loads

that fine cracks might develop in the link slabs and still allow water to penetrate into the slab. However, this situation is more preferable. Figure 1.4 shows the details of the link slab at the Haywood County bridge site. It can be seen that the deck is continuous

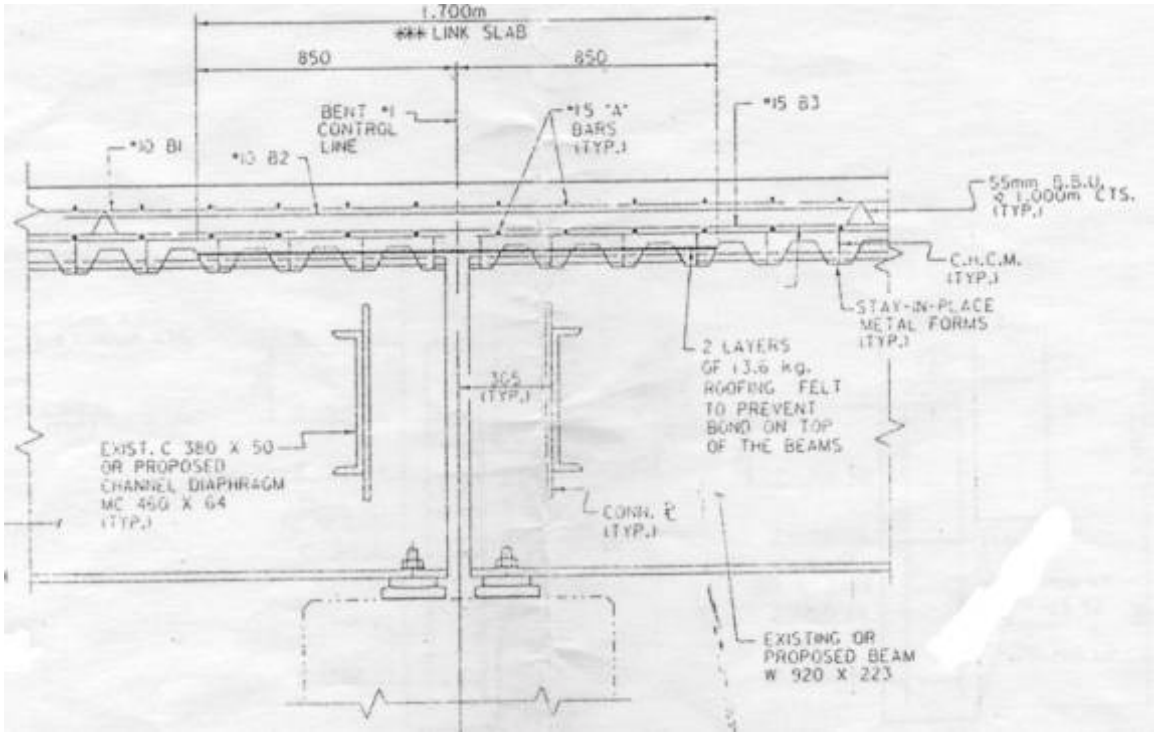

Figure 1.4 Typical link slab.

over the joint between the girders, as well as the reinforcing steel.

At this time, the only formal design approach for link slab bridges was proposed by Zia and Caner (1998). Their method is as follows:

1. Design each span of the bridge as if it was simply-supported, not taking into account the effects of the link slab. This is done because the stiffness of the link slab is much smaller than the stiffness of the composite girders.
2. To further reduce the stiffness of the link slab, provide debonding of 5 percent of the girder spans. The reduction in stiffness of the link slab also minimizes the stresses that will develop. Studies show that debonding up to 5 percent will not affect the force deformation behavior of the structure (El-Safty 1994).
3. Determine the maximum end rotations of the simply-supported girders when subjected to service loads. Impose these rotations on the link slab and determine

the maximum moment in the link slab using gross section properties (which is conservative because cracks will occur in the link slab).
4. Design the link slab reinforcement based on the calculated moment, using a conservative working stress, such as 40 percent of the yield strength of the reinforcing bar.
5. Limit the crack width using the crack control criteria of the AASHTO specifications.

1.4 Equipment at Bridge

Instrumentation placed at the bridge was chosen to monitor the performance of the link slab. Not only is the bridge subjected to live loads (traffic), the bridge is also subjected to thermal loads. Along with the necessary pieces of equipment, such as the power source, datalogger, multiplexers, etc., there are also gauges that can measure strain, temperature and linear displacement. With the instrumentation placed on the structure, it is possible to assess the following quantities:

1. Temperature gradient of the superstructure
2. Ambient Temperature
3. Number of freeze/thaw cycles.
4. Link slab deformation due to thermal loading, service loading, and controlled test loading.
5. Flexural strains and bending moments in the girders.

The power source for the data acquisition system is a BP24 12 Volt, 24 Amp Hour Lead Acid Battery. It is located inside of the instrumentation box with the datalogger. The battery is recharged by solar panel that is located on the top of the bent at the link slab. The voltage of the battery is reported when data is collected to determine if there is sufficient voltage to power the data acquisition system.

There are sixteen linear variable differential transformers (LVDT's) positioned on the bridge. Schaevitz DC-SE Series LVDT's were used. They are attached to stands that were designed by Matt Wagner (2001) which are attached to the bents at the desired

locations. These devices are used to measure the horizontal displacement of the end of the girders (see Figure 1.5).

Figure 1.5 LVDT's on structure.

The LVDT's are used to determine the end rotations of the girders based on the measured displacements. There are three different types of LVDT's in place on the structure. The three stroke lengths of the different devices include: 2 inch, 0.5 inch and 0.25 inch. At each location, there are four devices; two connected to the end of each girder at different heights. Figure 1.6 shows the different locations of the LVDT's.

Table 1.1 lists the different LVDTs located at the bridge site. The channel refers to the channel of the muliplexer. This is important because the data output file lists the data in columns starting with channel one and increasing thereafter. Referring to Table 1.1, it can easily be determined exactly which readings are from which gauges.

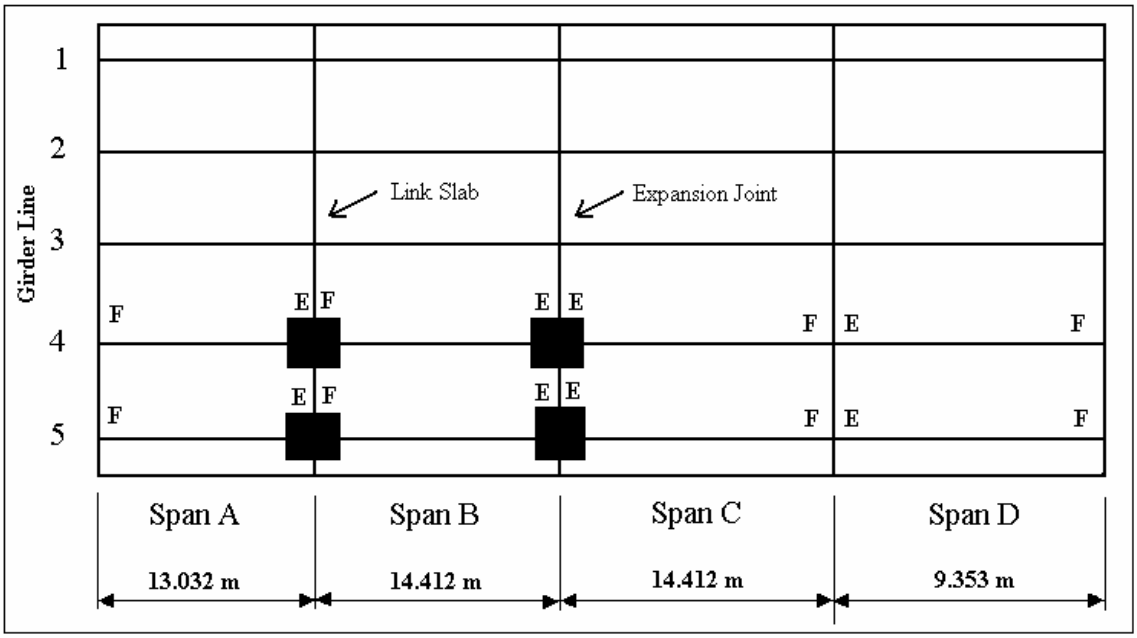

Figure 1.6 Locations of LVDT's.

Table 1.1 LVDT multiplexer channel index.

Channel	Guage Name	Gauge Location
1	A4-1-T-L-1	Top of girder A4 at link slab.
2	A4-1-B-L-2	Bottom of girder A4 at link slab.
3	B4-1-T-M-3	Top of girder B4 at link slab.
4	B4-1-B-S-4	Bottom of girder B4 at link slab.
5	B4-2-T-L-5	Top of girder B4 at expansion joint.
6	B4-2-B-L-6	Bottom of girder B4 at exapnsion joint.
7	C4-2-T-L-7	Top of girder C4 at expansion joint.
8	C4-2-B-L-8	Bottom of girder C4 at expansion joint.
9	A5-1-T-L-9	Top of girder A5 at link slab.
10	A5-1-B-L-10	Bottom of girder A5 at link slab.
11	B5-1-T-M-11	Top of girder B5 at link slab.
12	B5-1-B-S-12	Bottom of girder B5 at link slab.
13	B5-2-T-L-13	Top of girder B5 at expansion joint.
14	B5-2-B-L-14	Bottom of girder B5 at exapnsion joint.
15	C5-2-T-L-15	Top of girder C5 at expansion joint.
16	C5-2-B-L-16	Bottom of girder C5 at expansion joint.

To measure temperature at the structure and also within the deck, there are sixteen thermocouples positioned at different positions along the structure. These devices are FF-K-24 Omega thermocouples. The maximum temperature that these particular gauges can read is 200 degrees Celsius, which is well above the temperature anticipated at the structure. There are twelve thermocouples located inside of the bridge deck and four attached to the steel girders. At each location within the deck, there is a gauge at the top of the slab and one at the bottom of the slab. Figure 1.7 diagrams the locations of the thermocouples.

Table 1.2 lists the different thermocouples located at the bridge site. Again, the channel number refers to the channel of the multiplexer.

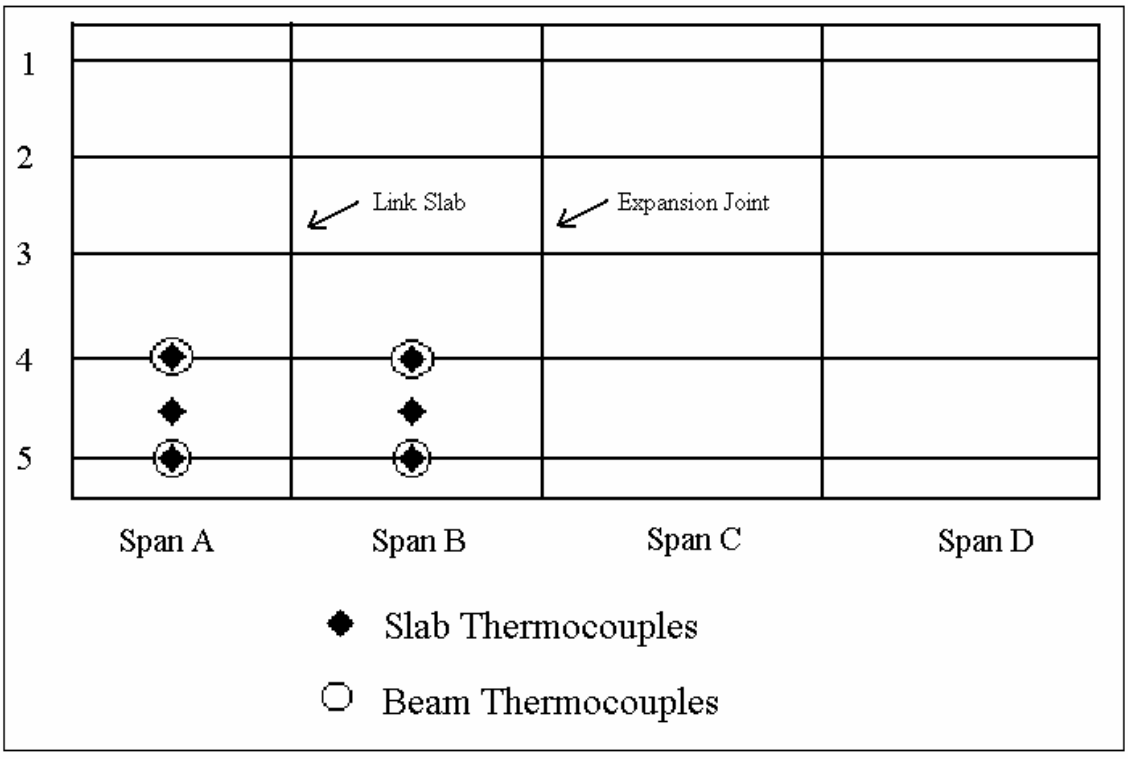

Figure 1.7 Locations of thermocouples.

Table 1.2 AM25T Thermocouple multiplexer channel index (Warren 2000).

Channel	Gauge Name	Gauge Location
1	THB04T	Top of deck, midspan of Beam B4
2	THA04T	Top of deck, midspan of Beam A4
3	THA45T	Top of deck, midspan of Span A, between Beams A4 and A5
4	THB45T	Top of deck, midspan of Span B, between Beams B4 and B5
5	THA05T	Top of deck, midspan of Beam A5
6	THB05T	Top of deck, midspan of Beam B5
7	THA04B	Bottom of deck, midspan of Beam A4
8	THB04B	Bottom of deck, midspan of Beam B4
9	THA45B	Bottom of deck, midspan of Span A, between Beams A4 and A5
10	THB45B	Bottom of deck, midspan of Span B, between Beams B4 and B5
11	THA05B	Bottom of deck, midspan of Beam A5
12	THB05B	Bottom of deck, midspan of Beam B5
13	THB04BSTEEL	Bottom of steel, midspan of Beam B4
14	THB05BSTEEL	Bottom of steel, midspan of Beam B5
15	THA05BSTEEL	Bottom of steel, midspan of Beam A5
16	THA04BSTEEL	Bottom of steel, midspan of Beam A4

To measure strain in the structure there are electrical resistance strain gauges, as well as vibrating wire strain gauges. The electrical resistance strain gauges are type CEA-06-250UW-120 gauges from Micro-Measurements. There are twelve electrical resistance strain gauges located within the structure. Six of the gauges are located in the bridge deck and six are attached to the steel girders. At each location, where the gauges are in the deck, there is a gauge at the top of the deck and also at the bottom of the deck. There is also a gauge at the top, middle and bottom of the girders at two locations (Figure 1.8). They measure the change in electrical resistance of the gauge due to strain, which can be converted to units of strain with the given gauge factor.

The vibrating wire strain gauges are type EM-5 from Roctest. The gauge is approximately 18 centimeters long with two end disks of 2.5 centimeter diameter. The gauge has a range of 3300 microstrains. Not only will these gauges measure strain, they also contain a thermistor, which can determine the temperature at the location of the gauge.

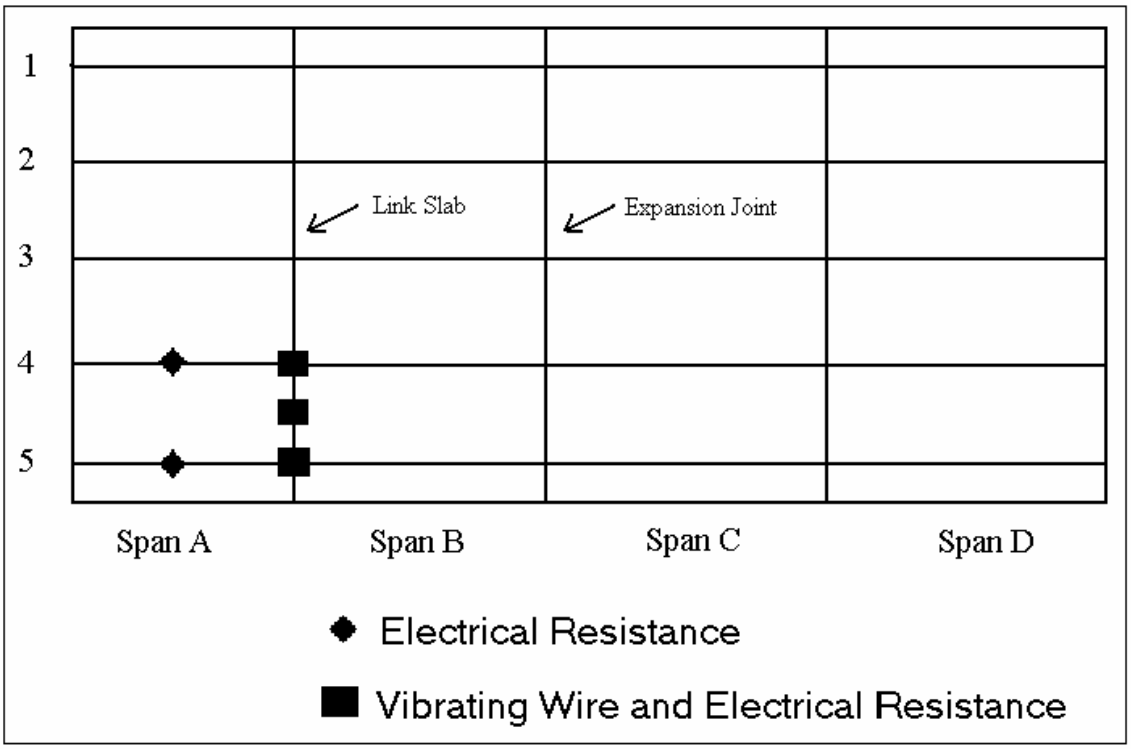

Figure 1.8 Strain Gauge Locations

Tables 1.3 and 1.4 lists the channel number and location of the electrical resistance strain gauges and the vibrating wire strain gauges. Again, the channel number refers to the channel of the multiplexer.

Table 1.3 AM416A Electrical resistance strain gauge multiplexer channel index (Warren 2000).

Channel	Gauge Name	Gauge Location
1	EG104T	Top of deck, above intersection of Beams A4, B4, and centerline of Bent1
2	EG145T	Top of deck, midway between beam lines A4-B4 and A5-B5 and over the centerline of Bent1
3	EG105T	Top of deck, above intersection of Beams A5, B5, and centerline of Bent1
4	EG104B	Bottom of deck, above intersection of Beams A4, B4, and centerline of Bent1
5	EG145B	Bottom of deck, midway between beam lines A4-B4 and A5-B5 and over the centerline of Bent1
6	EG105B	Bottom of deck, above intersection of Beams A5, B5, and centerline of Bent1
7	EGA04BSTEELTOP	2” below the bottom of the top flange, midspan of Beam A4
8	EGA04BSTEELMID	Midheight of beam web, midspan of Beam A4
9	EGA04BSTEELBOT	2” above the top of the bottom flange, midspan of Beam A4
10	EGA05BSTEELTOP	2” below the bottom of the top flange, midspan of Beam A5
11	EGA05BSTEELMID	Midheight of beam web, midspan of Beam A5
12	EGA05BSTEELBOT	2” above the top of the bottom flange, midspan of Beam A5

Table 1.4 AM416B Vibrating wire gauge multiplexer channel index (Warren 2000).

Channel	Gauge Name	Gauge Location
1	VG104T	Top of deck, above intersection of Beams A4, B4, and centerline of Bent1
2	VG145T	Top of deck, midway between beam lines A4-B4 and A5-B5 and over the centerline of Bent1
3	VG105T	Top of deck, above intersection of Beams A5, B5, and centerline of Bent1
4	VG104B	Bottom of deck, above intersection of Beams A4, B4, and centerline of Bent1
5	VG145B	Bottom of deck, midway between beam lines A4-B4 and A5-B5 and over the centerline of Bent1
6	VG105B	Bottom of deck, above intersection of Beams A5, B5, and centerline of Bent1

All of the gauges report readings in English units. A gauge reading of "-6999" or "-417.5" indicates that the gauge is not reading properly. This could mean that the reading is outside of the gauge's range, which is unlikely at this location, or that the gauge is not working properly.

1.5 Literature Review: Jointless Bridge Decks

As of December 2001, approximately 28 percent of all highway bridges are rated as structurally or functionally deficient (FHWA 2002). That is more than one out of every four bridges. With the new technology of jointless bridge decks, hopefully this number can be reduced in the future. These bridge decks will help reduce the high maintenance costs associated with bridges that have expansion joints.

In many newer bridges, traditional expansion joints are either reduced in number or completely eliminated. Some of the bridges with longer spans still have joints, but usually at the abutments only. These bridges still require maintenance work on the joints, but not as much is required as with older bridges with more expansion joints. Bridges with no expansion joints, even at the abutments, are known as integral bridges. These integral bridges are becoming so popular that existing structures are rehabilitated to eliminate the expansion joints to save money on the maintenance of the costly joints (Burke 1993).

The Ohio Department of Transportation is one of the first agencies to use continuous construction. Beginning in the 1930's, they constructed integral continuous steel and concrete bridges up to 15 meters in length (Burke 1994). However, it appears that Tennessee is now leading the way in the construction of jointless bridges. Since 1956, jointless bridge decks have been constructed in Tennessee. The longest concrete

bridge designed and constructed without joints is approximately 283 meters and the longest steel bridge is approximately 127 meters (Wasserman 1987 and Loveall 1985).

In the *News and Information from the Steel Bridge Forum* dated Summer/Fall of 1993, the writers presented a list of the advantages that integral bridges have over jointed bridges. The first advantage on their list is that integral bridges can be built without bearings and joints. This will reduce not only installation costs, but also maintenance costs. The third advantage is that integral bridges can be built much faster and more economical. Another advantage that integral bridges have over jointed bridges is that they minimize deterioration because harmful deicing agents cannot penetrate the deck slab due to the lack of joints. The fifth advantage is that integral bridges will simplify bridge replacement. These bridges will last longer and the adaptability of these structures will allow them to use the existing foundations without replacing them. The last advantage discussed is that integral bridges have extraordinary resistance to illegal overloads by distributing loads along the continuous and full-depth diaphragm at the bridge ends.

While it is common to design new bridges without joints, it is also not uncommon to convert existing bridge decks to jointless bridge decks. Currently, about 30 percent of transportation departments have converted one or more bridges from multiple simple spans to continuous spans (Burke 1990).

2. Objectives and Methods

2.1 Research Objectives

There are three major objectives of this research, which include the following: Validate analysis and design assumptions, investigate limit-states design parameters and simplified design procedure, and develop a strategy and guide for long-term monitoring.

In order to accomplish all of the research objectives, several tasks have been identified. These tasks include the following: live load testing and data collection, collection of data under random and thermal loading, live load test analysis, and random and thermal loading analysis. The instrumentation on the bridge will be used to obtain data from thermal loading, service loading and live load testing. Each one of these loadings will provide different results, which can then be used to accomplish objectives one and two (validate analysis and design assumptions and investigate limit-states design methods). Also, the ongoing data collection will be useful in developing a long-term monitoring strategy, which is object three.

2.2 Validate Analysis and Design Assumptions

There are several assumptions that are made when designing, observing and analyzing a link slab. It is the purpose of this research to determine if these assumptions are in fact valid or not. To determine the validity of these assumptions, the bridge was subjected to several loading conditions including: service loading, thermal loading and a controlled live load test.

The first assumption made when designing a link slab is that the girder spans are simply supported. Because the stiffness of the link slab is much smaller than the stiffness

of the composite girders, the effect of the link slab on the deflection of the girders is neglected. Under service loading conditions, the girders will deflect, which will induce end rotations on the link slab. The link slab can then be treated as a beam and analyzed with the end rotations from adjacent girders applied to the link slab. These rotations will induce a moment in the link slab, from which the reinforcement can be determined.

Another assumption made is that there is compatibility of deformation between girders and the link slab. This follows from the assumption that the girder spans are simply supported. It is assumed that the link slab will deform similarly to the deformation of the end of the girders, which is why the end rotations of adjacent girders are imposed on the link slab in the design process to determine the moment in the link slab.

Analysis of the live load test, service loadings and thermal loadings will be used to validate the design assumptions. In Chapter 3, the results of the analysis of these loadings are presented.

2.3 Investigation of Limit-States Design Methods and Simplified Design Procedure

There are three areas of interest within this objective. The first area of interest is to identify the link slab limit states. These will be determined in conjunction with the DOT. Once the limit-states are known, the rotational demands that the link slab is subjected to will be determined for a wide range of loading conditions. For each of the rotational demand levels, a satisfactory performance, or limit state will be determined. Using this information, as well as Caner and Zia's proposed design method, a simplified design procedure will be explored. The simplified design approach would require only one rotation demand and one corresponding limit state.

All of the aforementioned tasks will aid in completing this objective. Further discussion of a simplified design procedure is presented in Chapter 3.

2.4 Develop Strategy and Guide for Long-Term Monitoring.

In order to fully utilize the equipment at the project site to monitor the performance of the link slab, a long-term monitoring strategy is needed. The purpose of this objective is to develop a strategy and guide for monitoring the long-term performance of the link slab. A computer program was developed using Visual Basic in Microsoft Excel. The program, as well as the datalogger software that will be used to download the data will be described in Chapter 4.

3. Analytical Studies

3.1 Live Load Test Analysis

3.1.1 Overview of Test

The live load test was conducted in June of 2001. The test consisted of using four known loads and positioning them on the bridge at two locations. The first location would produce the maximum positive moment in one of the adjacent spans. The second location would produce the maximum negative moment in the link slab.

The first issue of the live load test was determining the loads with which to load the bridge. The loads were applied to the bridge using a DOT truck loaded with gravel at the local maintenance office.

Figure 3.1 Truck used during live load test.

Figure 3.2 Determining wheel loads with scales.

After discussions with the NCDOT, four loads were chosen. The loads that were selected were based on the capacity of the truck that the DOT decided to use and the maximum allowable overload condition. The first load used was the weight of the truck empty. It turned out to be 137 kN. The third load used was close to the maximum allowable load for the specified truck without the need of a permit. The load was 304 kN as opposed to the maximum allowable load of 305 kN for the truck. The second load used was approximately halfway in between the first and third loads. The load that was used was 214 kN. The fourth and final load that was used for the test was 424 kN. This was the largest allowable load that the Department of Motor Vehicles (DMV) allowed. To be able to use this load, a permit had to be obtained from the DMV. Table 3.1 lists the loads that were used during the test. Figure 3.3 is a

Table 3.1 Loads used during live load test (kN).

	Load 1	Load 2	Load 3	Load 4
	left/right	left/right	left/right	left/right
Axle 1 *	21.53/19.93	20.55/20.19	21.17/21.44	22.95/22.69
Axle 2	13.97/16.28	20.11/22.24	25.98/28.91	40.83/44.66
Axle 3	15.39/14.77	19.39/20.73	25.62/28.38	39.77/44.57
Axle 4	10.05/8.36	28.20/21.44	35.76/45.37	46.88/58.54
Axle 5	8.54/8.36	23.58/17.08	31.05/40.66	46.35/56.40
Total	**137**	**214**	**304**	**424**

* Axle 1 is in the front of the truck.

diagram of the wheels and axles of the truck, in which the above loads were applied.

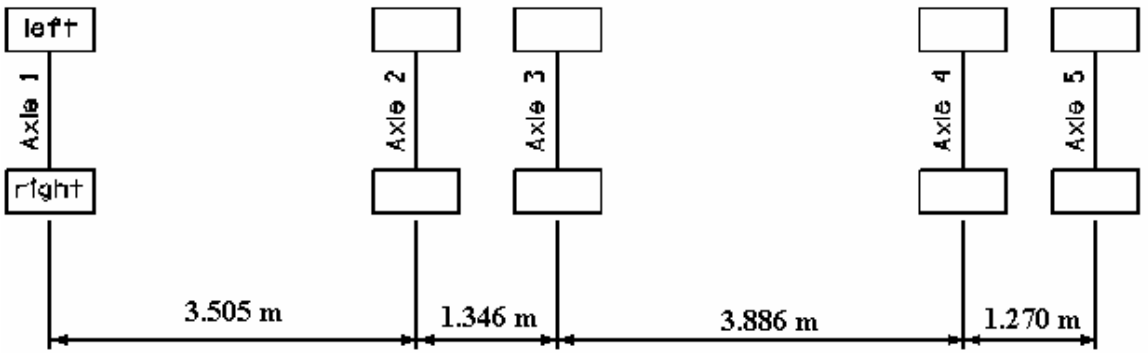

Figure 3.3 Truck layout.

After determining the loads, the position of the truck on the bridge during the test had to be determined. Based on the location of the instruments, it was determined that the truck should be positioned to produce the maximum negative moment in the link slab and also the maximum positive moment in the span between the link slab and the expansion joint (span B). NCDOT used an influence line to determine the exact location of the truck to produce these moments. Figures 3.4 and 3.5 are diagrams of the locations of the truck during the test.

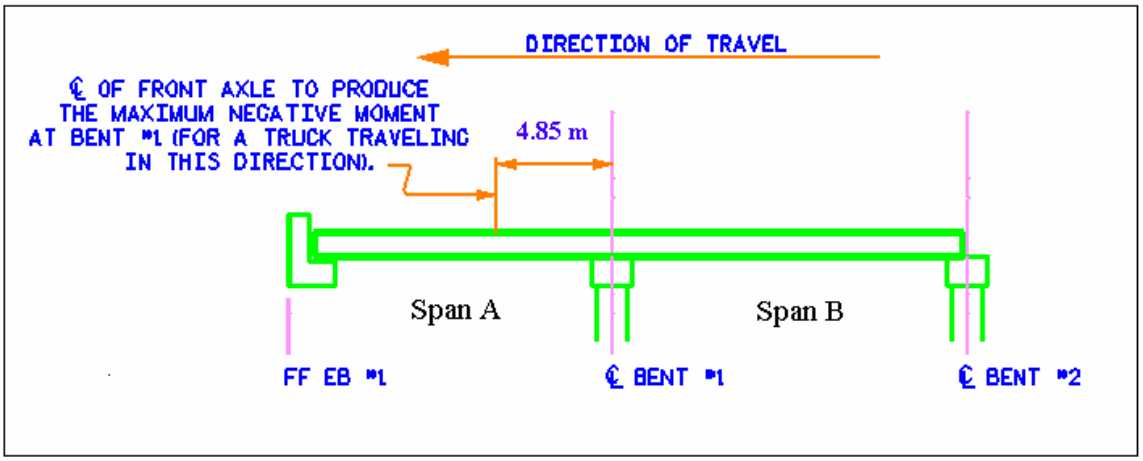

Figure 3.4 Location of truck to produce maximum negative moment in link slab.

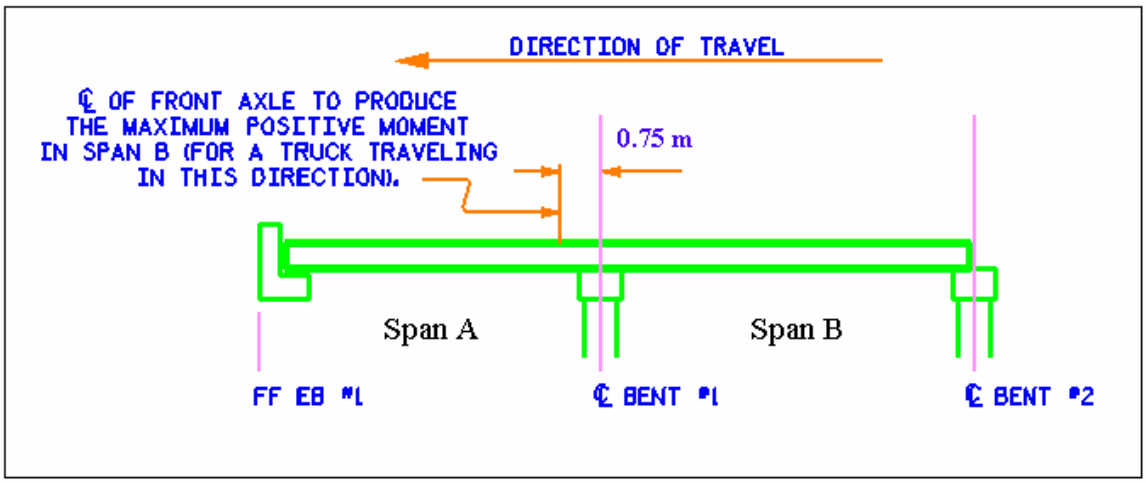

Figure 3.5 Location of Truck to produce maximum positive moment in span B.

Another issue that had to be dealt with during the test was how to collect the data. Due to certain limitations of the data acquisition system, a new program had to be developed which would collect data when the truck was in position. To do this, a program was developed that would take continuous readings during the time the truck was on the bridge and in position. The complete program is listed in Appendix A. The testing procedure involved coordination between individuals above and below the bridge where the computer system is set up. For each load test, traffic on the bridge was stopped, and as the truck approached the computer program was sent to the datalogger to start collecting data. The truck would slowly drive to the first position, which was the

position that produced the maximum positive moment in the span between the link slab and the expansion joint. After the truck was stopped for approximately two minutes, the truck would then slowly drive forward to the next position, which was the position that produced the maximum negative moment in the link slab. After being stopped for another two minutes, the truck would slowly drive off the bridge and return to the DOT office to pick up more gravel for the next load. Then another computer program was sent to the datalogger to stop it from continuously taking data until it was time for the test with the next load increment. This procedure was followed until all four tests were completed. The raw data from the live load test is presented in Appendix B.

Figure 3.6 Truck on bridge during live load test.

3.1.2 Live Load Test Results

To determine the force-rotation response of the link slab, the rotations had to be determined. These rotations were easily obtained from the LVDT readings. The vertical distance between the two LVDT's at the end of each girder is known. Dividing the difference of the LVDT readings by the vertical distance, the rotations are determined. Table 3.2 and Table 3.3 lists the rotations from the live load test. The girder identification is as follows: "A4-N" means span "A," girder line "4," and the north end of the girder. The other girders follow the same identification procedure. The link slab is located between A-N and B-S.

Table 3.2 Rotations (rad) from maximum negative moment in link slab.

Load (kN)	A4-N	B4-S	B4-N	C4-S	A5-N	B5-S	B5-N	C5-S
0	0.000000	0.000000	0.000000	0.000000	0.000000	0.000000	0.000000	0.000000
137	0.000045	0.000026	0.000049	0.000005	0.000019	0.000042	0.000056	0.000001
214	0.000071	0.000046	0.000232	0.000005	0.000062	0.000117	0.000079	0.000002
304	0.000136	0.000102	0.000454	0.000005	0.000114	0.000200	0.000182	0.000006
424	0.000148	-0.000037	0.000524	0.000016	0.000110	0.000272	0.000224	0.000007

Table 3.3 Rotations (rad) from maximum positive moment in span B.

Load (kN)	A4-N	B4-S	B4-N	C4-S	A5-N	B5-S	B5-N	C5-S
0	0.000000	0.000000	0.000000	0.000000	0.000000	0.000000	0.000000	0.000000
137	0.000070	0.000083	0.000119	0.000016	0.000043	0.000080	0.000126	-0.000008
214	0.000094	0.000835	0.000286	0.000022	0.000052	0.000177	0.000176	0.000021
304	0.000171	0.000204	0.000595	0.000027	0.000133	0.000289	0.000397	0.000016
424	0.000234	0.000149	0.000703	0.000076	0.000143	0.000409	0.000452	0.000020

As stated before, fine cracks may appear in the jointless bridge deck at the link slab location under normal service loads. This is the case at the project site. Figure 3.7 shows a picture of the crack located in the link slab. The grooves in the deck are approximately 2 centimeters apart. The crack width is just less than 2 millimeters wide. This is very small as compared to the width of traditional expansion joints. It should also

be noted that during the live load test there was no notable change in the width of the crack.

Figure 3.7 Crack in bridge deck.

3.1.3 Validation of Results

To determine if the results obtained from the live load test were valid or not, a model was developed using the computer program *Visual Analysis.* Only spans *A* and *B* were incorporated into the model. The other half of the bridge is not instrumented and an expansion joint separates the two halves. There were two models that were created to try to emulate the test results. A picture of the model that is presented in this section can be seen in Figure 3.8 without any load on it. A description and results from the other model is located in Appendix C. The two models were compared with each other and the comparison graphs are located in Appendix D. Only one girder line was modeled at a time. The loads were positioned along the girders at the same locations that the wheel

loads were during the test. One point load was used for each axle. The load that was used was a combination of the two wheel loads for each axle using the AASHTO load distribution method. Tables 3.4 and 3.5 list the loads that were entered into the computer model. These loads were obtained by multiplying the wheel loads by the ratio of the distance the wheels were from the girder to the girder spacing. In effect, this is the load that is carried by the modeled girder. The first table lists the loads for the girder 4 run and the second table lists the loads for the girder 5 run. The abutment was modeled with a fixed joint and the expansion joint was modeled with a roller joint. The link-slab was modeled using a pinned connection at the girder end bearings of two adjacent girders. The stiffnesses of the composite girders and link-slab were calculated by hand calculations and then entered into the computer program.

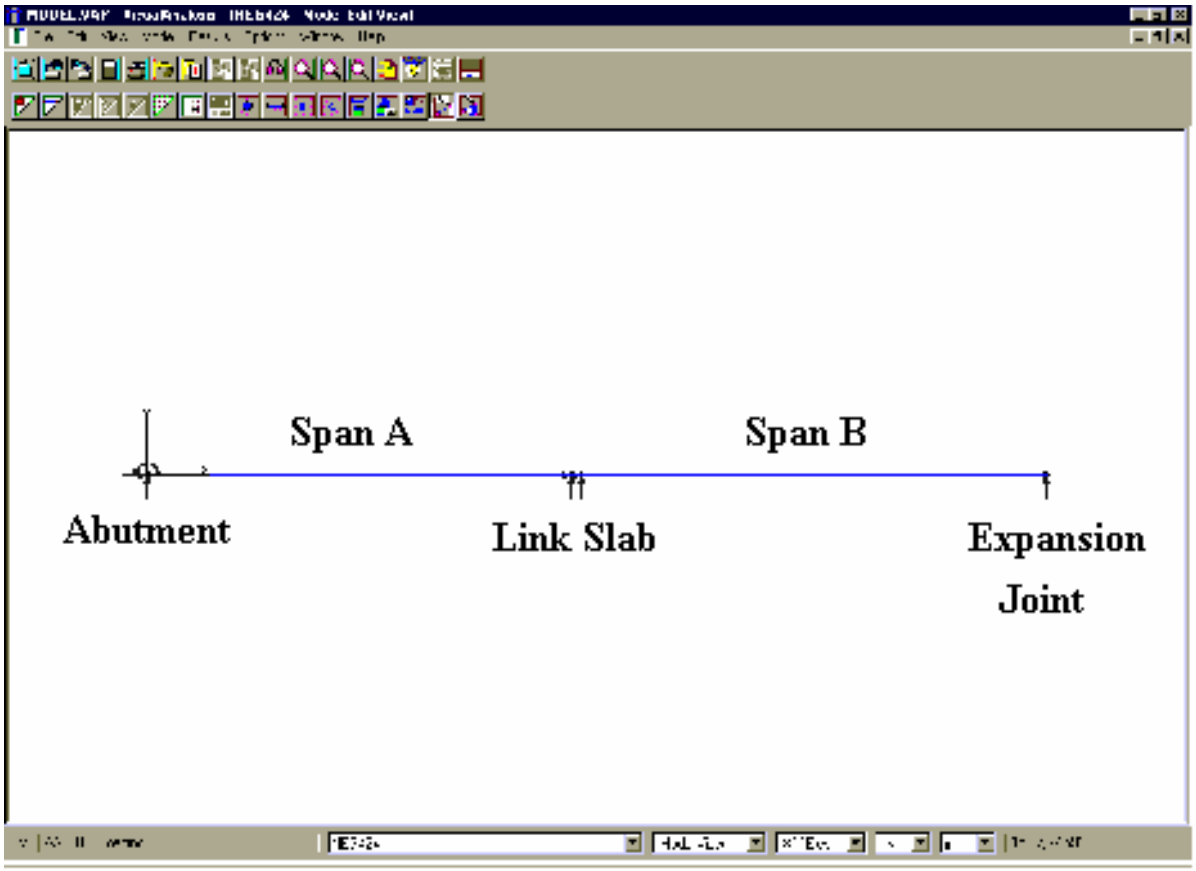

Figure 3.8 Visual Analysis computer model.

Table 3.4 Girder 4 loads.

	Load 1	Load 2	Load 3	Load 4
Axle 1	26.26	25.57	26.62	28.61
Axle 2	18.48	26.08	33.78	52.75
Axle 3	19.00	24.85	33.25	51.84
Axle 4	11.86	32.39	48.89	63.69
Axle 5	10.61	26.72	42.99	62.33
Total	86.20	135.60	185.53	259.23

Table 3.5 Girder 5 loads.

	Load 1	Load 2	Load 3	Load 4
Axle 1	10.95	11.09	11.78	12.46
Axle 2	8.94	12.22	15.88	24.53
Axle 3	8.11	11.39	15.59	24.48
Axle 4	4.59	11.78	24.92	32.16
Axle 5	4.59	9.38	22.33	30.98
Total	37.19	55.86	90.50	124.61

After running the computer model for each load at the location, which produces the maximum positive moment in span B, and the location that produces the maximum negative moment in the link-slab, the results were compared with the actual results from the live load test. Tables 3.6 and 3.7 list the results from the computer model. The girder identification is the same as before.

Table 3.6 Rotations (rad) from maximum negative moment in link slab.

Load (kN)	A4-N	B4-S	B4-N	A5-N	B5-S	B5-N
0	0.000000	0.000000	0.000000	0.000000	0.000000	0.000000
137	0.000080	0.000075	0.000073	0.000031	0.000035	0.000033
214	0.000108	0.000171	0.000176	0.000044	0.000072	0.000072
304	0.000140	0.000267	0.000283	0.000065	0.000143	0.000150
424	0.000182	0.000363	0.000389	0.000084	0.000190	0.000201

Table 3.7 Rotations (rad) from maximum positive moment in span B.

Load (kN)	A4-N	B4-S	B4-N	A5-N	B5-S	B5-N
0	0.000000	0.000000	0.000000	0.000000	0.000000	0.000000
137	0.000122	0.000087	0.000129	0.000084	0.000056	0.000073
214	0.000183	0.000194	0.000300	0.000126	0.000120	0.000157
304	0.000251	0.000304	0.000475	0.000183	0.000232	0.000307
424	0.000382	0.000424	0.000661	0.000279	0.000321	0.000421

When comparing the results from the computer model and the live load test, it can be seen that the results are very similar. The force-rotation response of the end of all the instrumented girders was graphed. Figures 3.9 through 3.20 are the graphs, which compare the model with the live load test results. Included in the graph is a diagram which shows where the girder being graphed is located and the position of the truck during the test which caused these rotations. With two exceptions, all of the graphs are very similar. The two exceptions are both at the south end of girder B4, which is located at the link slab, but during the two different loading positions. It is believed that there was a faulty LVDT at this location. "V.A." and "L.L.T." in the legend of the following graphs refers to *Visual Analysis* and Live Load Test respectively.

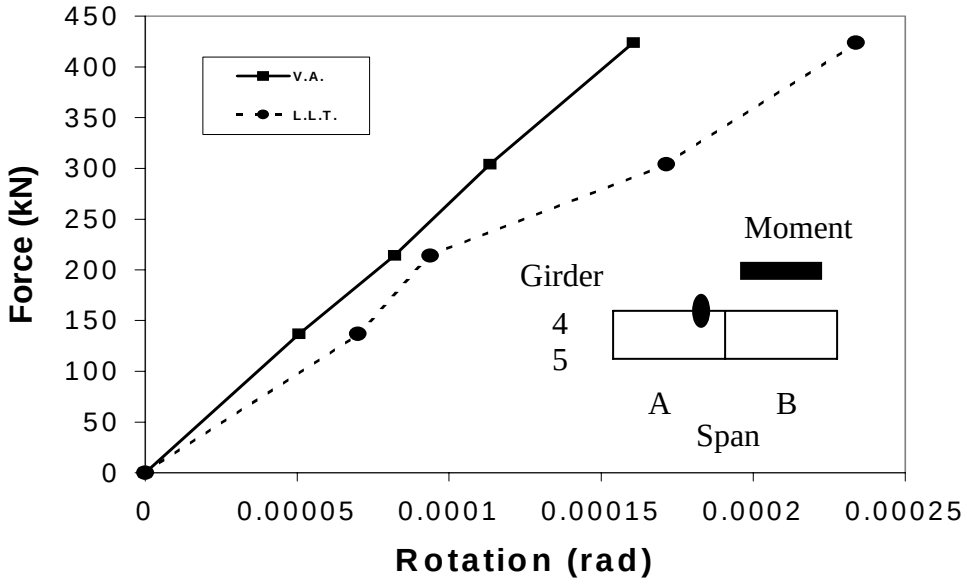

Figure 3.9 North end of girder A4 with maximum moment in span B (link slab).

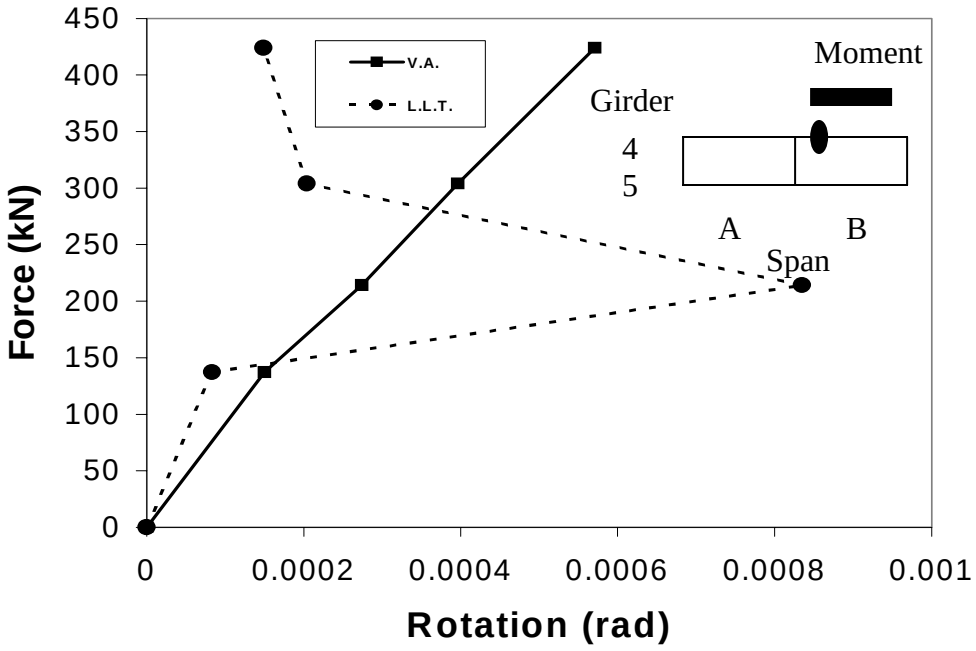

Figure 3.10 South end of girder B4 with maximum moment in span B (link slab).

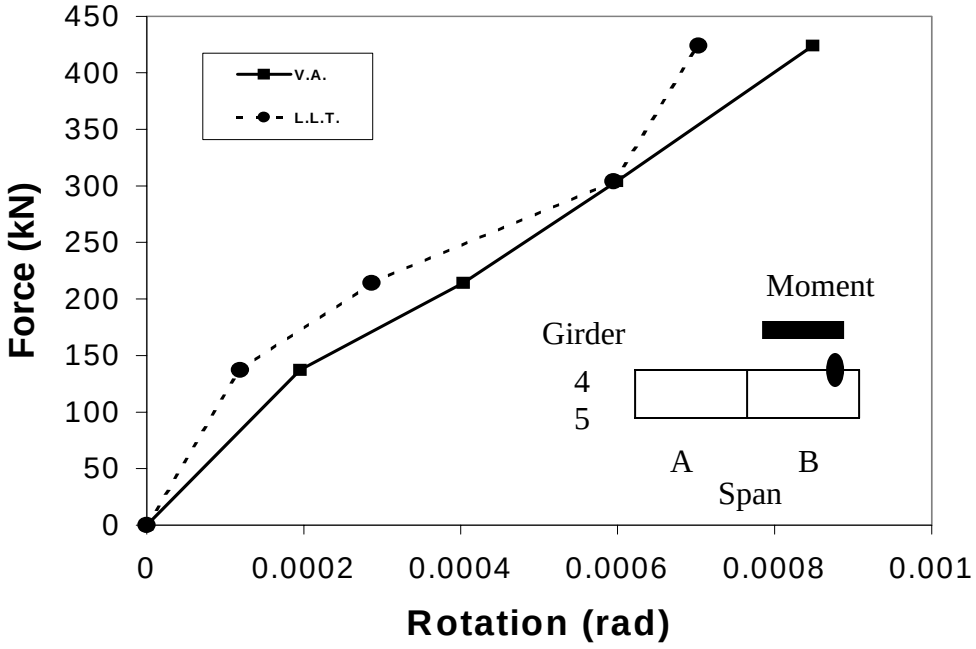

Figure 3.11 North end of girder B4 with maximum moment in span B.

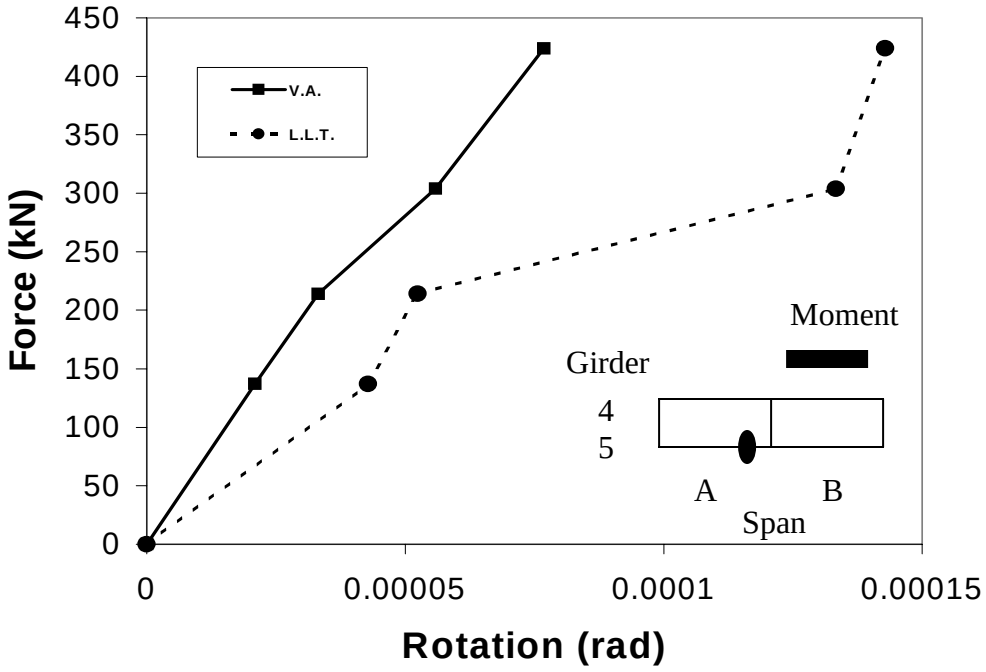

Figure 3.12 North end of girder A5 with maximum moment in span B (link slab).

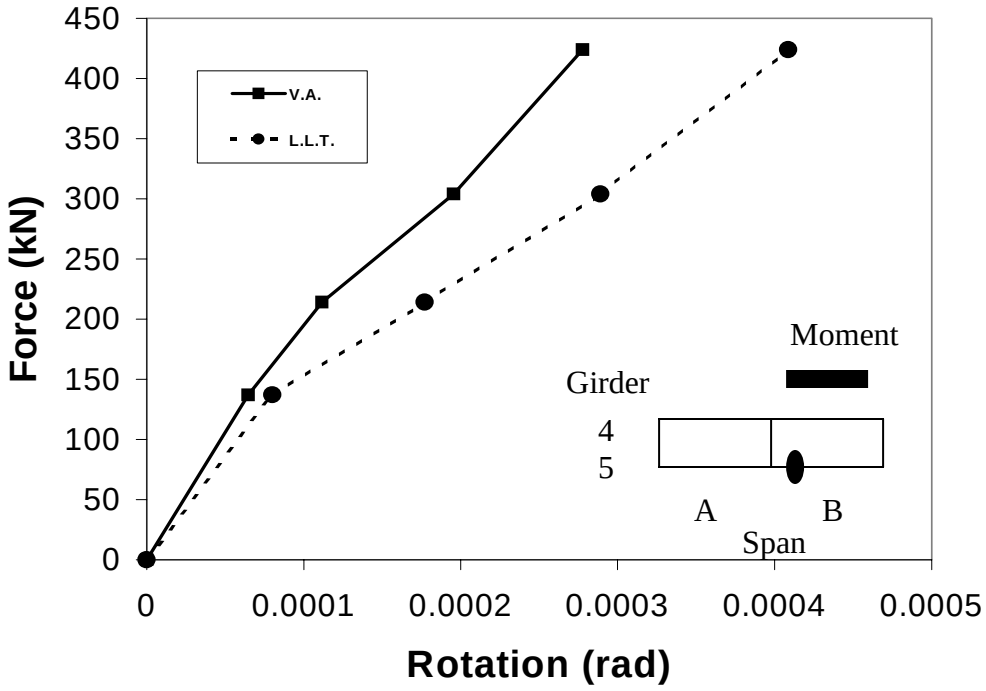

Figure 3.13 South end of girder B5 with maximum moment in span B (link slab).

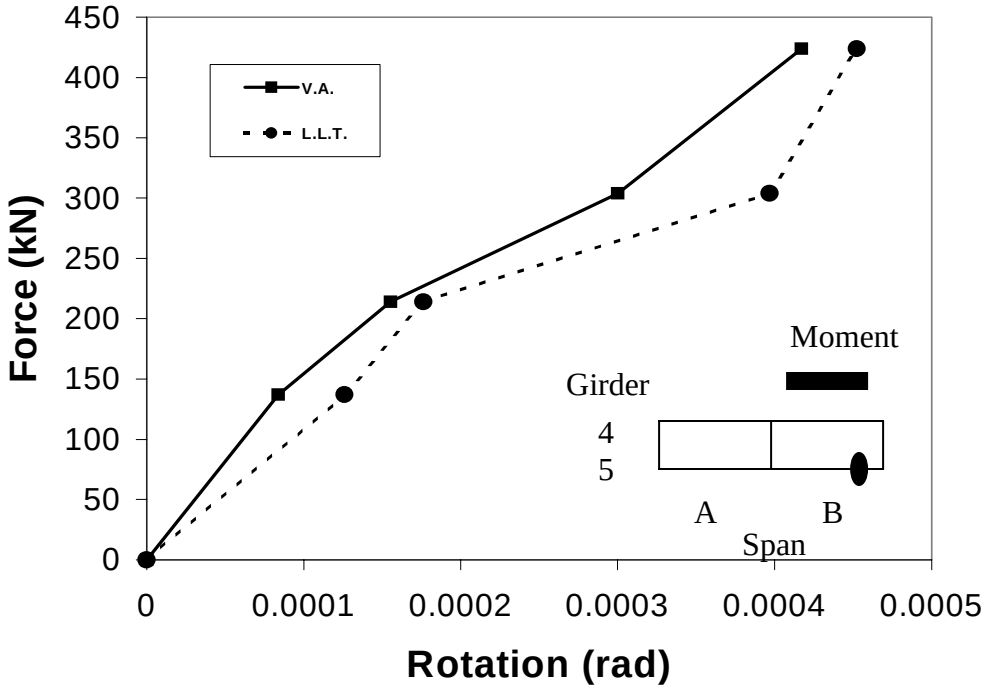

Figure 3.14 North end of girder B5 with maximum moment in span B.

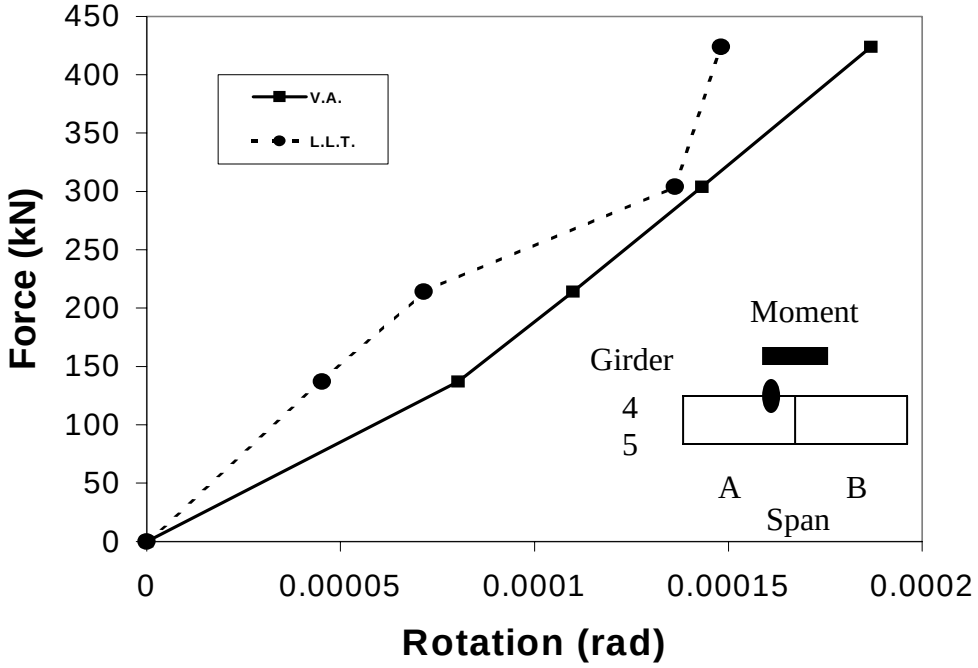

Figure 3.15 North end of girder A4 with negative moment (link slab).

Figure 3.16 South end of girder B4 with negative moment (link slab).

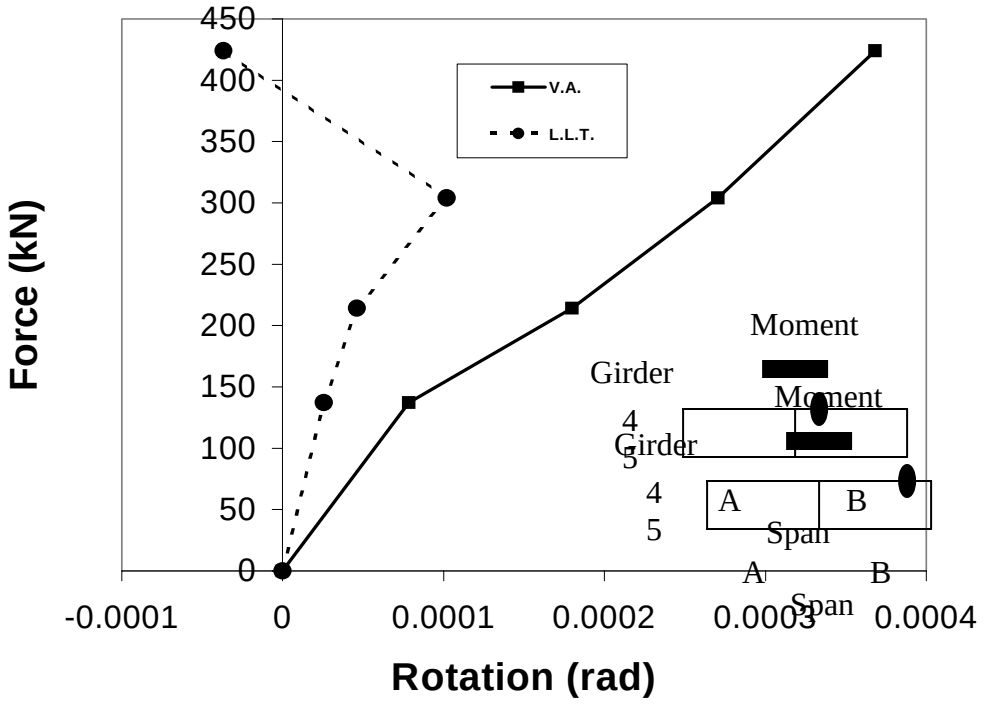

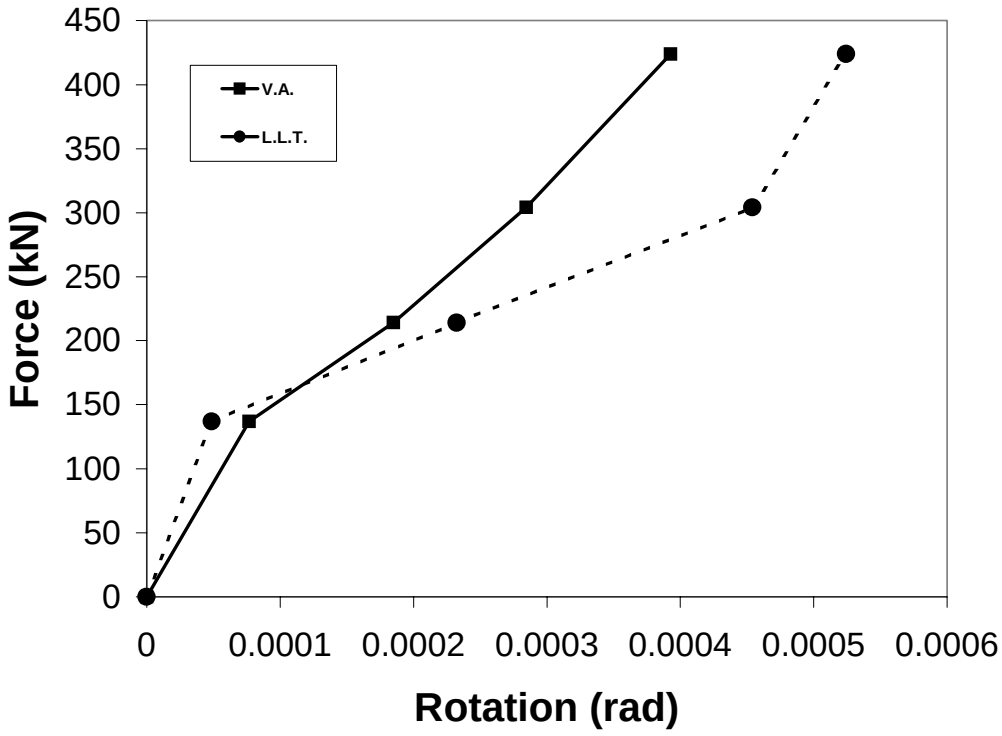

Figure 3.17 North end of girder B4 with negative moment.

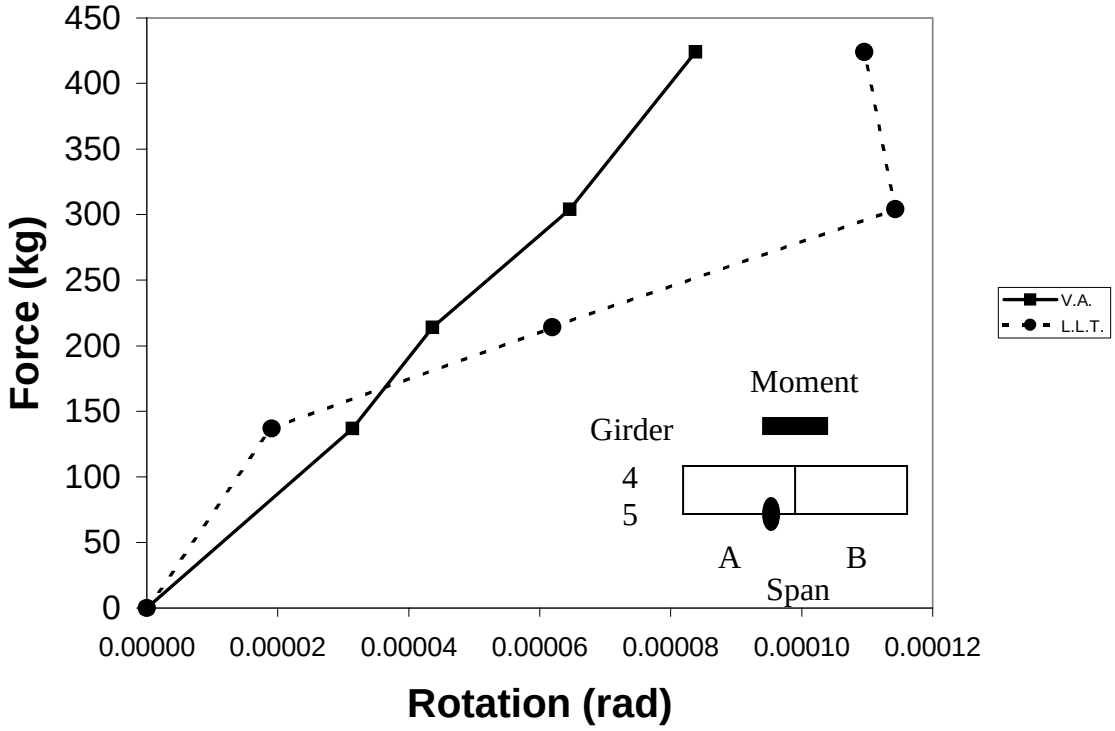

Figure 3.18 North end of girder A5 with negative moment (link slab).

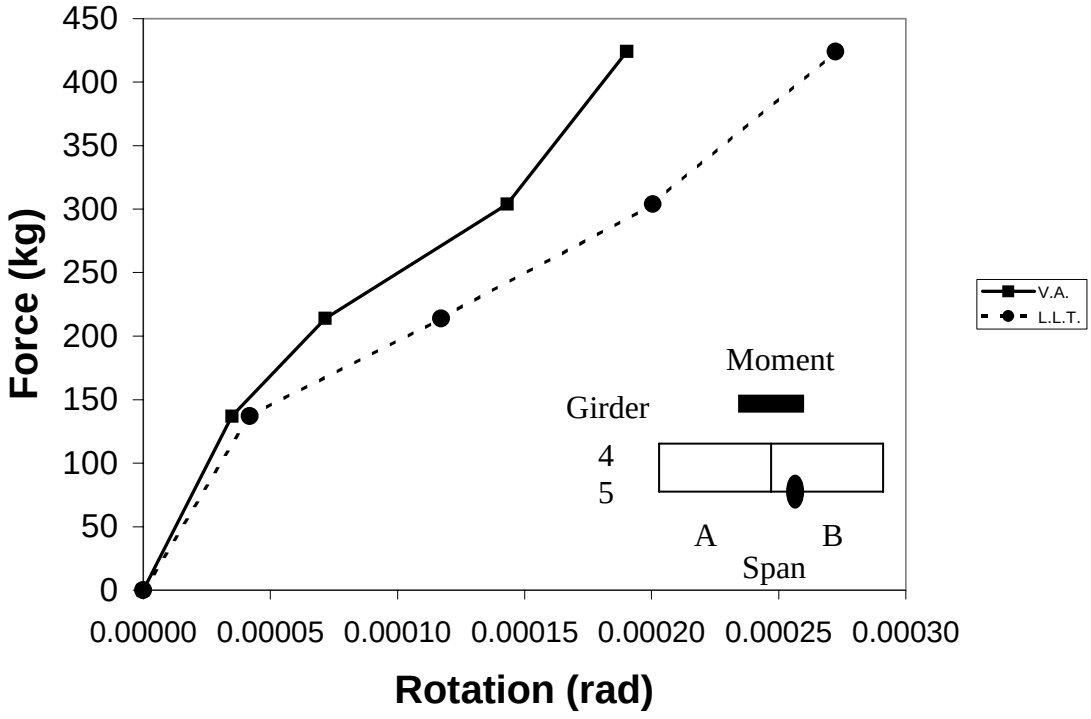

Figure 3.19 South end of girder B5 with negative moment (link slab).

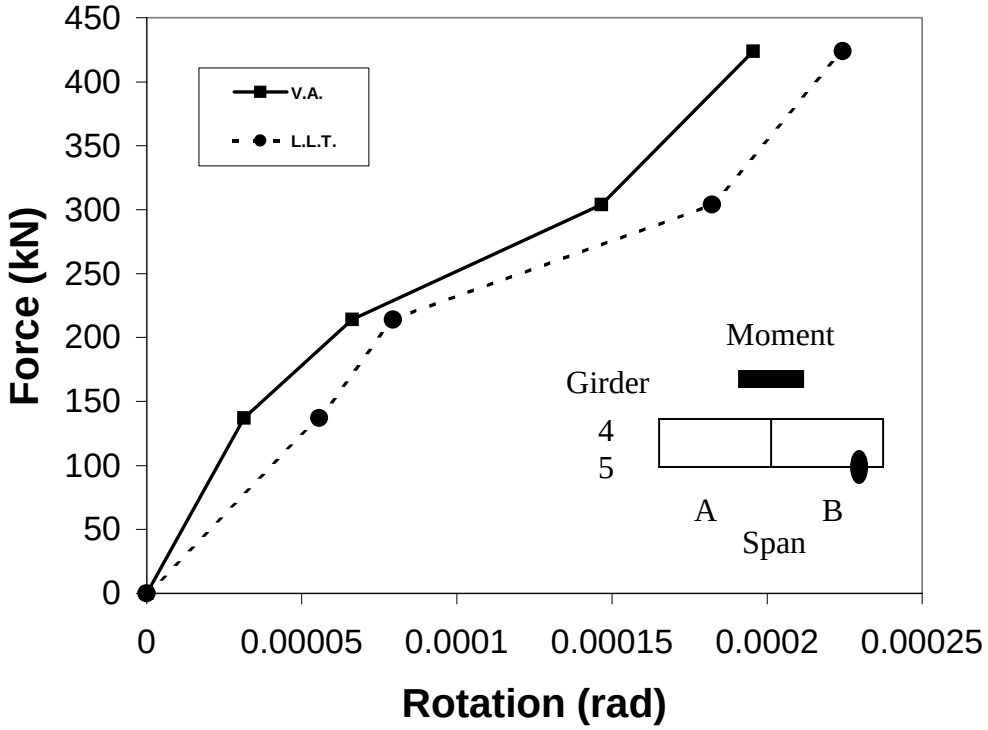

Figure 3.20 North end of girder B5 with negative moment.

The model shown here helps reinforce that the design and analysis assumptions are valid. The girders were modeled as simply supported. After comparing the live load test results and the model, it can be seen that the rotations are very similar. There is also compatibility of deformations between the link slab and the end of the girders. A simple model also easily predicted the force-deformation behavior of the link-slab.

3.2 Random and Thermal Loading Analysis

3.2.1 Service Load Demands

Design average daily traffic and average daily truck traffic are 25600 vehicles and 2050 trucks, respectively. This amount of traffic will be sufficient to obtain data related to the service loading. Also, with the amount of trucks driving across the bridge, which weigh more than passenger vehicles, it should be easy to see different magnitudes of

girder end movements. However, due to the limitations of the instrumentation a service load demand could not be achieved. It takes a vehicle driving the posted speed limit approximately 0.3 seconds to travel across the bridge. The LVDTs can only read about every 0.8 seconds. Figures E.1 and E.2 in Appendix E are examples of what the displacement of a LVDT gauge and the rotation of the end of a girder look like graphed for a fifty second time interval. The strain gauges take readings at a much slower rate than the LVDTs.

3.2.2 Daily Thermal Demands

Due to the severe weather common to the project site, thermal effects must be investigated. It is not uncommon for the range of temperatures throughout the day to be in excess of fifteen degrees Celsius. Figure 3.21 is a graph of the temperature range for a typical thermocouple. Tables 3.8-3.10 display the maximum and minimum temperature ranges for the different thermocouples over the course of a day. The average daily temperature difference is also presented. The gauge located in the top of the deck at the midspan of girder A-5 is not working properly.

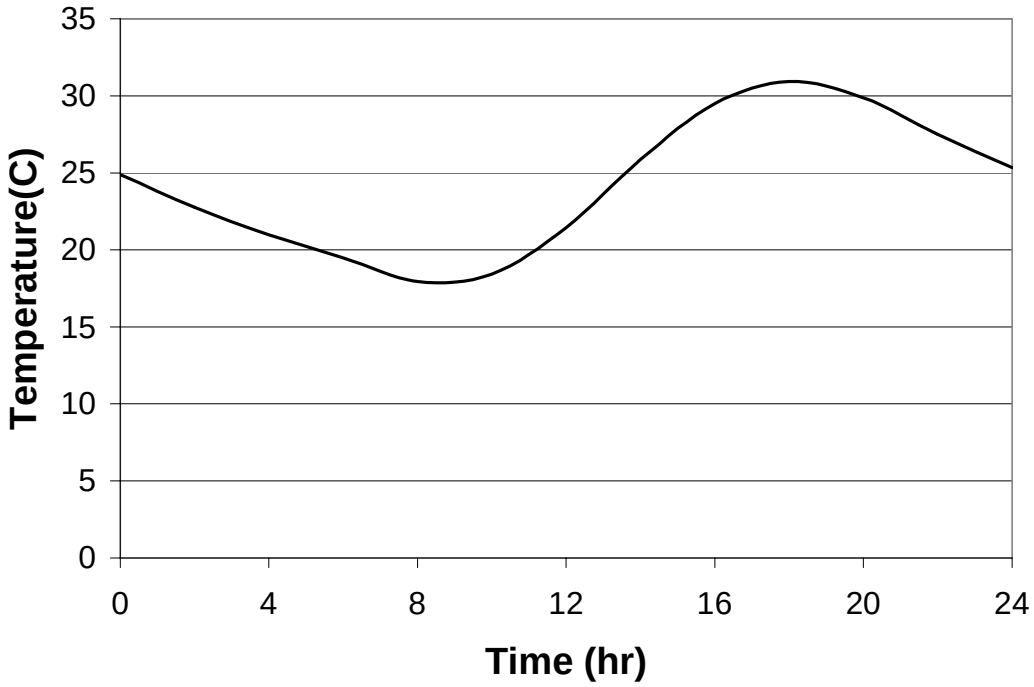

Figure 3.21 Change in temperature for a typical day.

Table 3.8 Temperature ranges (Celsius) for thermocouples near top of the bridge deck.

	Top B4	Top A4	Top A 4-5	Top B 4-5	Top A5	Top B5
Maximum	14.32	18.09	17.10	16.88		18.43
Minimum	0.21	0.55	0.46	0.48		0.60
Average	6.86	9.80	8.99	8.86		9.93

Table 3.9 Temperature ranges (Celsius) for thermocouples near the bottom of the bridge deck.

	Bot B4	Bot A4	Bot A 4-5	Bot B 4-5	Bot A5	Bot B5
Maximum	15.42	20.03	16.05	15.53	16.35	15.96
Minimum	0.45	0.62	0.47	0.47	0.54	0.56
Average	7.82	10.93	8.25	8.01	8.68	8.23

Table 3.10 Temperature ranges (Celsius) for thermocouples on the girders.

	Bot Steel Mid B4	Bot Steel Mid B5	Bot Steel Mid A5	Bot Steel Mid A4
Maximum	16.68	21.81	22.05	21.20
Minimum	0.58	0.00	0.00	0.00
Average	8.53	9.00	9.47	8.94

3.2.3 Seasonal Thermal Demands

While the daily temperature variations can be in excess of fifteen degrees Celsius, the yearly temperature variations can be in excess of forty-five degrees Celsius. Figure 3.22 is a graph representing the temperature variations for one thermocouple over the course of a year. Tables 3.11-3.13 display the maximum and minimum temperature ranges for the different thermocouples over the course of a year. Again, the gauge located in the top of the deck at the midspan of girder A-5 is not working properly.

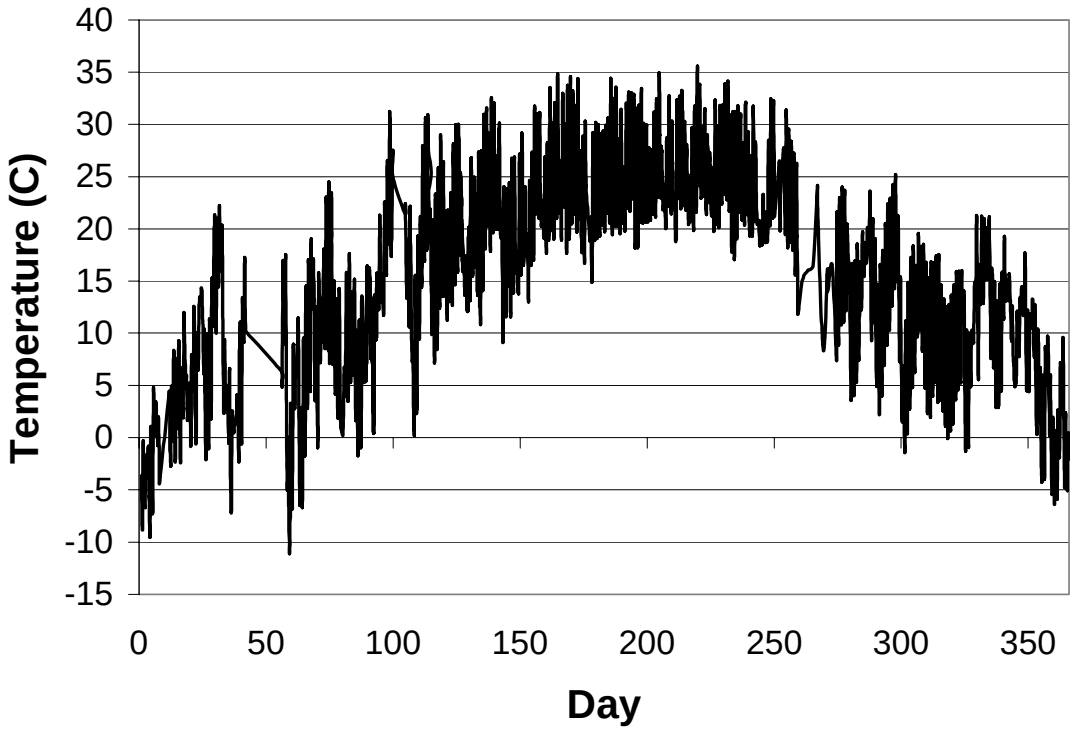

Figure 3.22 Range of temperatures for a thermocouple over the course of a year.

Table 3.11 Temperature ranges (Celsius) for thermocouples near the top of the bridge deck.

	Top B4	Top A4	Top A 4-5	Top B 4-5	Top A5	Top B5
Maximum	27.47	35.54	34.70	35.32	N/A	36.12
Minimum	-8.66	-11.12	-10.77	-10.41	N/A	-10.90

Table 3.12 Temperature ranges (Celsius) for thermocouples near the bottom of the bridge deck.

	Bot B4	Bot A4	Bot A 4-5	Bot B 4-5	Bot A5	Bot B5
Maximum	32.00	37.37	32.32	33.24	34.43	32.67
Minimum	-9.63	-11.26	-9.78	-9.49	-9.82	-9.61

Table 3.13 Temperature ranges (Celsius) for thermocouples on the girders.

	Bot Steel Mid B4	Bot Steel Mid B5	Bot Steel Mid A5	Bot Steel Mid A4
Maximum	33.00	29.51	29.95	29.43
Minimum	-9.65	-10.01	-10.47	-10.10

3.3 Link Slab Rotation Demands

3.3.1 Average Random Service Load Rotations

Due to the nature of the instrumentation at the project site, it is quite difficult to obtain the average random service load rotations. The instrumentation is not capable of taking readings fast enough to be able to determine what the rotations of the girders are due to the traffic. Tables 3.14 and 3.15 list the rotations of the girders during the live load test for all loadings except for the overload condition.

Table 3.14 Rotations (rad) due to maximum positive moment in span B.

Load (kN)	A4-N	B4-S	B4-N	C4-S	A5-N	B5-S	B5-N	C5-S
137	0.000070	0.000083	0.000119	0.000016	0.000043	0.000080	0.000126	-0.000008
214	0.000094	0.000835	0.000286	0.000022	0.000052	0.000177	0.000176	0.000021
304	0.000171	0.000204	0.000595	0.000027	0.000133	0.000289	0.000397	0.000016

Table 3.15 Rotations (rad) due to maximum negative moment at link slab.

Load (kN)	A4-N	B4-S	B4-N	C4-S	A5-N	B5-S	B5-N	C5-S
137	0.000045	0.000026	0.000049	0.000005	0.000019	0.000042	0.000056	0.000001
214	0.000071	0.000046	0.000232	0.000005	0.000062	0.000117	0.000079	0.000002
304	0.000136	0.000102	0.000454	0.000005	0.000114	0.000200	0.000182	0.000006

3.3.2 Overload Conditions

The overload rotational demands were determined from the live load test. Tables 3.16 and 3.17 list the rotations of the end of the girders due to the overload conditions.

Table 3.16 Rotations (rad) due to maximum positive moment in span B.

Load (kN)	A4-N	B4-S	B4-N	C4-S	A5-N	B5-S	B5-N	C5-S
424	0.000234	0.000149	0.000703	0.000076	0.000143	0.000409	0.000452	0.000020

Table 3.17 Rotations (rad) due to maximum negative moment at link slab.

Load (kN)	A4-N	B4-S	B4-N	C4-S	A5-N	B5-S	B5-N	C5-S
424	0.000148	-0.000037	0.000524	0.000016	0.000110	0.000272	0.000224	0.000007

The load that was used for the live load test was approximately 12000 kilograms over the allowable load for the truck that was used.

3.3.3 Seasonal and Daily Thermal Rotations

The thermal rotations that occurred at the Haywood County bridge were calculated using two different types of gauges, thermocouples and LVDTs. The two different calculations produced similar results.

To calculate the rotations using the thermocouples, the differential equation of the deflection curve based on temperature effects was solved. The equation used was as follows:

$$\frac{d^2y}{dx^2} = \frac{\alpha(T_2 - T_1)}{h}$$

where y is deflection, α is the coefficient of thermal expansion, T is the two different temperatures and h is the height between the two different gauges. The coefficient of thermal expansion that was used was 12 E –6, (Gere and Timoshenko 1997) is that of structural steel. The thermocouples used were the ones that were located at the top of the bridge deck and the ones located at the bottom of the steel girder. Solving the differential equation for the maximum rotations over the course of a year produced the results in Table 3.18.

Table 3.18 Rotations (rad) based on thermocouple readings.

A4-N	A5-N	B4-S	B5-S
2.813E-12	4.010E-12	1.560E-12	3.561E-12

Since the LVDTs located on the bridge only measure the horizontal movement of the end of the girders, a different approach was taken to determine the thermal rotations. For the four instrumented girders which intersect the link slab, the rotations from LVDT data for an entire year was graphed. Figure 3.23 is an example of one of the graphs.

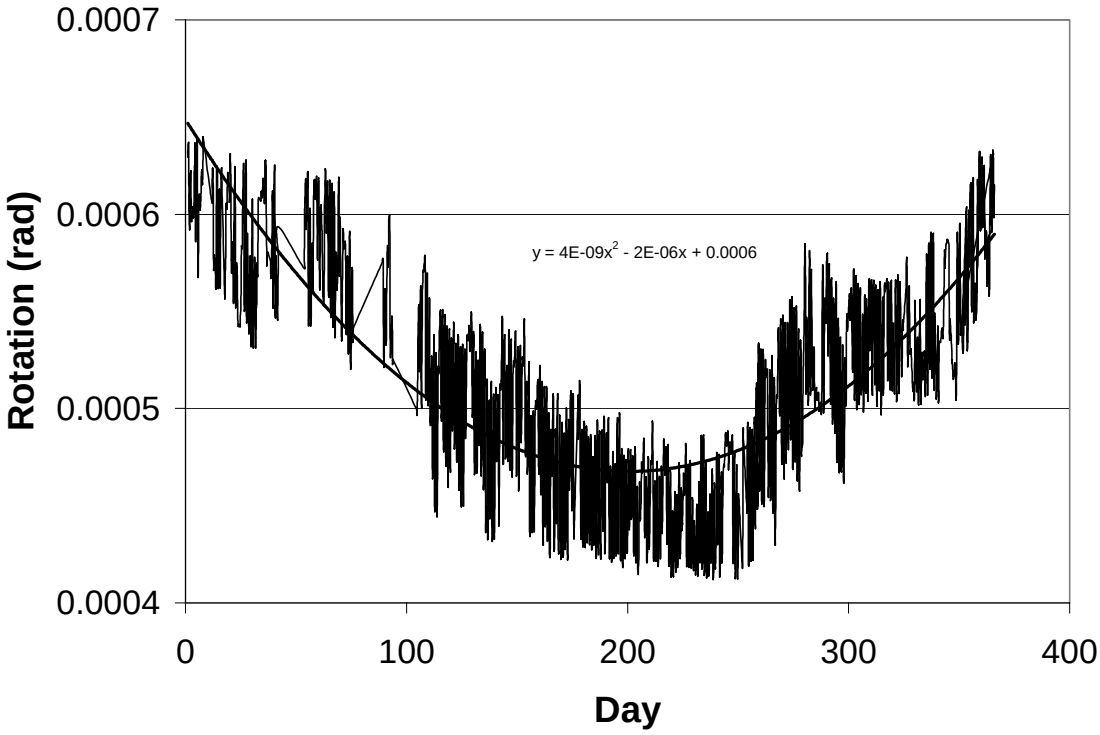

Figure 3.23 Graph of LVDT rotations.

The rotations that are presented in this figure are not actual rotations, but are the rotations that are determined from the LVDT readings. The actual rotation is the difference in the values. To obtain the rotations, a trendline was added to the graph, which can be seen. Solving the equation of the trendline for the maximum and minimum values and then subtracting the two, will result in the rotation of that girder. This process was done for all four girders that intersect at the link slab. Table 3.19 presents the results of this process.

Table 3.19 Rotations (rad) based on LVDT readings.

A4-N	A5-N	B4-S	B5-S
3.454E-05	2.500E-04	6.200E-05	2.304E-05

When comparing the results from the two different processes, it can be seen that the two processes produced very different results. The results from the LVDTs are the actual rotations that are present at the project site. The procedure using the thermocouples produces theoretical results.

The same two processes were also used to calculate and compare the daily rotational demands for one random day (June 29, 2001) during the year. Table 3.20 shows the rotations based on the thermocouple readings. Table 3.21 shows the rotations based on the LVDT readings. The results from the

Table 3.20 Rotations (rad) based on thermocouple readings.

A4-N	A5-N	B4-S	B5-S
9.998E-13	1.076E-12	3.420E-13	1.563E-12

Table 3.21 Rotations (rad) based on LVDT readings.

A4-N	A5-N	B4-S	B5-S
1.018E-05	6.478E-05	5.203E-05	8.035E-06

two methods for determining rotations produce very different results again. It can be seen that the rotations over the course of a day are much smaller than the rotations over the course of a year, which was expected.

After comparing the rotations from the service load, overload and thermal loadings, it can be seen that the rotations due to the overload were the most severe. However, the rotation used to design the steel in the link slab was 0.002 radians, which is larger than any of the calculated rotations from the three different loading conditions. Figure 3.24 is a bar chart comparing the rotational demands from the three different loading cases. The thermal rotations are the rotations calculated from the data from the

LVDTs. The service load rotations are the rotations that were measured during the live load test for the truck loaded to 214 kN. The overload rotations are the measured rotations from the live load test with the truck being overloaded.

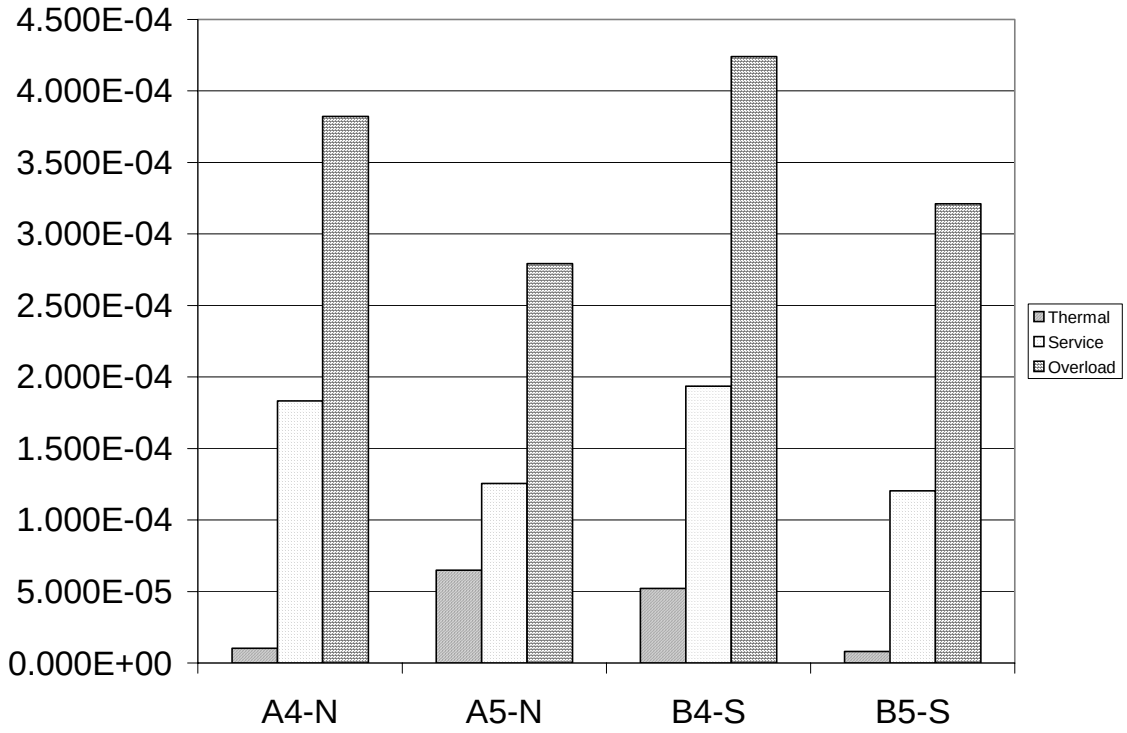

Figure 3.24 Rotational demand comparison (rad).

It can be seen from the above graph that the largest rotational demands are the demands from the overload condition.

3.4 Proposed Limit States Design Process

After the analyses were completed on all the data, the current design procedure was examined. The actual design of the link slab for the Haywood County bridge was to limit the crack width to less than 0.33 mm. The width of the crack that is present at the joint is approximately 1.6 mm. This crack is small, but it is still not less than the design calculations. It is believed that the crack is a result of localized debonding of the concrete and that the steel has not yielded. During the live load test, the crack width did

not change. The crack was already present before the testing was conducted. Even under the overload condtion, the crack width did not change.

The 0.33 mm crack width comes from the AASHTO crack criteria under exposed conditions. This crack width is based on the fact that the cracks are going to be spaced out over the length of the link slab. However, a saw cut was made along the link slab to concentrate the cracks in one place. The result of the saw cut is that the crack width is wider than the allowable crack width, but the crack is not so large that it will cause major damage. One advantage of having one larger crack instead of many smaller cracks is that the one large crack can more easily be repaired. The saw cut and crack can be filled with a hot-poured sealant to improve its serviceability (Zia and Caner 1998). A larger limit for crack width should be investigated for link slabs in which a saw cut is present.

During the design, the crack width limitation was based on the design service load. It is possible that the crack has come from thermal loadings that are present. As shown before, the thermal loadings were the most severe. Nonetheless, the current design procedure produces satisfactory results.

During this research, a limit states design method was investigated. The intention of this investigation was to determine if a more simplified design procedure exists. The idea is for an engineer to determine what rotation the bridge will be subjected to and also determine what crack width is acceptable for the structure. It was shown previously that rotations could come from many different sources. The three sources of rotations shown in this report are the result of thermal, service and overload loadings. Once the engineer knows these two values, he or she could obtain the steel quantities to meet the performance objective.

Several design charts were developed for different steel ratios based on the geometry of the bridge specific to the Haywood County bridge site. The process for developing these design charts is as follows:

M_a = Negative moment induced in the link slab due to applied end rotations.
I_d = Moment of inertia of the link slab.
θ = end rotation of the girder.
L = Length of the link slab.
M_{cr} = Cracking moment of the link slab.
f_r = Flexural modules for the deck concrete.
f_s = Stress in the reinforcing steel.
N = Number of reinforcing bars.
A_b = Area of one reinforcing bar.
ρ = Ratio of tension steel reinforcement.

1. Compute the negative moment (M_a) induced in the link slab due to the applied end rotation using equation 3.1 and the cracking moment (M_{cr}) of the link slab using equation 3.2.

$$M_a = \frac{2 \cdot E_c \cdot I_d \cdot \vartheta}{L} \qquad \text{(EQ. 3.1)}$$

$$M_{cr} = \frac{f_r \cdot I_d}{y} \qquad \text{(EQ. 3.2)}$$

2. Compute the stress in the steel using equation 3.3:

$$f_s = \frac{f_r \cdot M_a}{6 \cdot M_{cr} \cdot \rho \cdot \gamma^2 \left\{1 + \eta\rho / 3 - 0.333\left[(\eta\rho)^2 + 2\eta\rho\right]^{0.5}\right\}} \qquad \text{(EQ. 3.3)}$$

3. Using the Gergely-Lutz expression (EQ 3.4) for crack width, solve for the effective tension area of concrete around the main reinforcement (A), having the same centroid as the reinforcement, using different crack widths.

$$\omega = 0.076 \cdot \beta \cdot f_s \cdot \sqrt[3]{d_c A} \qquad \text{(EQ 3.4)}$$

where
ω = estimated cracking width in units of 0.03 mm (0.001 in)
β = ratio of the distance to the neutral axis from the extreme tension fiber and from centroid of main reinforcement
f_s = steel stress in units of MPa (ksi)
d_c = concrete cover measured from extreme tension fiber to centroid

of nearest reinforcement level in units of mm (in)
A = the effective tension area of concrete around the main reinforcing divided by the number of bars in mm^2 (in^2)
(McCormac 1998)

4. Solve for the spacing of reinforcement using equation 3.5.

$$s = \frac{A}{2 \cdot d_c} \qquad \text{(EQ 3.5)}$$

where
A = effective tension are of concrete in units of mm^2 (in^2).
d_c = concrete cover measured from extreme tension fiber to centroid of nearest reinforcement level in units of mm (in)

5. Compute the number of bars needed using equation 3.6.

$$N = \frac{b}{s} \qquad \text{(EQ. 3.6)}$$

where
s = spacing of reinforcemnt in units of mm (in).
b = width of link slab in units of mm (in).

6. Calculate the area of the reinforcing bars needed to obtain the crack width with the specified girder end rotation using equation 3.7.

$$A_b = \frac{\rho \cdot b \cdot \gamma h}{N} \qquad \text{(EQ 3.7)}$$

7. Eliminate non feasible solutions from the charts such as small spacings and large reinforcement bar diameters.

Tables 3.22-3.27 are the design charts that were produced for a link slab having the same geometry as the link slab at the project site. Specifically, these charts can only be used for link slabs having the same depth and length as the link slab at the Haywood County project site because the above mentioned procedure is dependent on those two

variables. Charts were developed for steel ratios of 0.005 to 0.03 percent, but could be developed for any steel ratio desired using the above procedure.

Table 3.22 Steel ratio of 0.005.

ρ = 0.005	w (mm)			
θ	0.25	0.5	0.75	1.00
0.00025	# 22 @ 530			
0.0005		# 22 @ 530		
0.00075		# 13 @ 157	# 22 @ 530	# 32 @ 1257
0.001			# 13 @ 224	# 22 @ 530

Table 3.23 Steel ratio of 0.010.

ρ = 0.010	w (mm)			
θ	0.25	0.5	0.75	1.00
0.0005	# 29 @ 482			
0.00075	# 16 @ 143			
0.001	# 10 @ 60	# 29 @ 482		
0.00125		# 19 @ 247		
0.0015		# 16 @ 143	# 29 @ 482	
0.00175		# 13 @ 90	# 22 @ 304	# 36 @ 720
0.002		# 10 @ 60	# 19 @ 204	# 29 @ 482

Table 3.24 Steel ratio of 0.015.

ρ = 0.015	w (mm)			
θ	0.25	0.5	0.75	1.00
0.00075	# 32 @ 451			
0.001	# 22 @ 190			
0.00125	# 16 @ 98			
0.0015	# 13 @ 56	# 32 @ 451		
0.00175		# 25 @ 284		
0.002		# 22 @ 190		
0.00225		# 19 @ 134	# 32 @ 451	
0.0025		# 16 @ 98	# 29 @ 329	
0.00275		# 13 @ 73	# 25 @ 247	
0.003		# 13 @ 56	# 22 @ 190	# 32 @ 451

Table 3.25 Steel ratio of 0.020.

ρ = 0.020	w (mm)		
θ	0.25	0.50	0.75
0.00125	# 25 @ 219		
0.0015	# 22 @ 127		
0.00175	# 16 @ 80		
0.002	# 13 @ 54		
0.00225		# 32 @ 301	
0.0025		# 25 @ 219	
0.00275		# 22 @ 165	
0.003		# 19 @ 127	
0.00325		# 19 @ 100	# 32 @ 337
0.0035		# 16 @ 80	# 29 @ 270
0.00375		# 16 @ 65	# 29 @ 219
0.004		# 13 @ 54	# 25 @ 181

Table 3.26 Steel ratio of 0.025.

ρ = 0.025	w (mm)		
θ	0.25	0.50	0.75
0.0015	# 32 @ 238		
0.00175	# 25 @ 150		
0.002	# 19 @ 100		
0.00225	# 16 @ 70		
0.0025	# 16 @ 51		
0.00275	# 13 @ 39	# 36 @ 309	
0.003		# 32 @ 238	
0.00325		# 29 @ 187	
0.0035		# 25 @ 150	
0.00375		# 22 @ 122	
0.004		# 19 @ 100	
0.00425		# 19 @ 84	# 36 @ 282
0.0045		# 16 @ 70	# 32 @ 238
0.00475		# 16 @ 60	# 29 @ 202

Table 3.27 Steel ratio of 0.030.

ρ = 0.030	w (mm)	
θ	0.25	0.50
0.00175	# 36 @ 249	
0.002	# 29 @ 167	
0.00225	# 25 @ 117	
0.0025	# 22 @ 86	
0.00275	# 19 @ 64	
0.003	# 16 @ 50	
0.00325	# 13 @ 39	
0.0035		# 36 @ 249
0.00375		# 32 @ 203
0.004		# 29 @ 167
0.00425		# 25 @ 139
0.0045		# 22 @ 117
0.00475		# 22 @ 100
0.005		# 19 @ 86

To use these charts, the engineer would chose the crack width and come down the chart to the calculated girder end rotations and the intersection of the two would be the amount of reinforcing steel to use in the link slab. Examples of using these design charts are presented in Appendix F.

3.5 Softening of Link-Slab

One concern of the link slab is whether or not it will soften over time. A link slab could soften due to the repeated service loads being applied to it. Fatigue of the link slab will reduce its capacity. Softening of the link-slab would eventually cause the link slab to become damaged and it may need to be replaced.

Using the remote data acquisition system, it can be determined whether the link slab is softening or not. Girder end rotations can be calculated using the same two methods that were used to calculate the rotations based on temperature effects. The rotations can be calculated over the course of a month or over the course of a year. Then,

the rotations can be compared to rotations that were calculated in previous years during the same time of the year in which the temperatures are similar. If the rotations are becoming larger, then softening of the link slab is occurring.

3.6 Girder Elongation.

The elongations of the girders over the course of a year were calculated from data obtained from the LVDTs. The average of the two LVDTs attached to the same girder was calculated over the course of a year. The average was then graphed for the entire year. A trendline was added to the graph so that the maximum and minimum averages could be determined. These two values were then subtracted and the result is the maximum elongation of the girder for a typical year. Figure 3.25 is an example of the graph of the average values for a LVDT for an entire year.

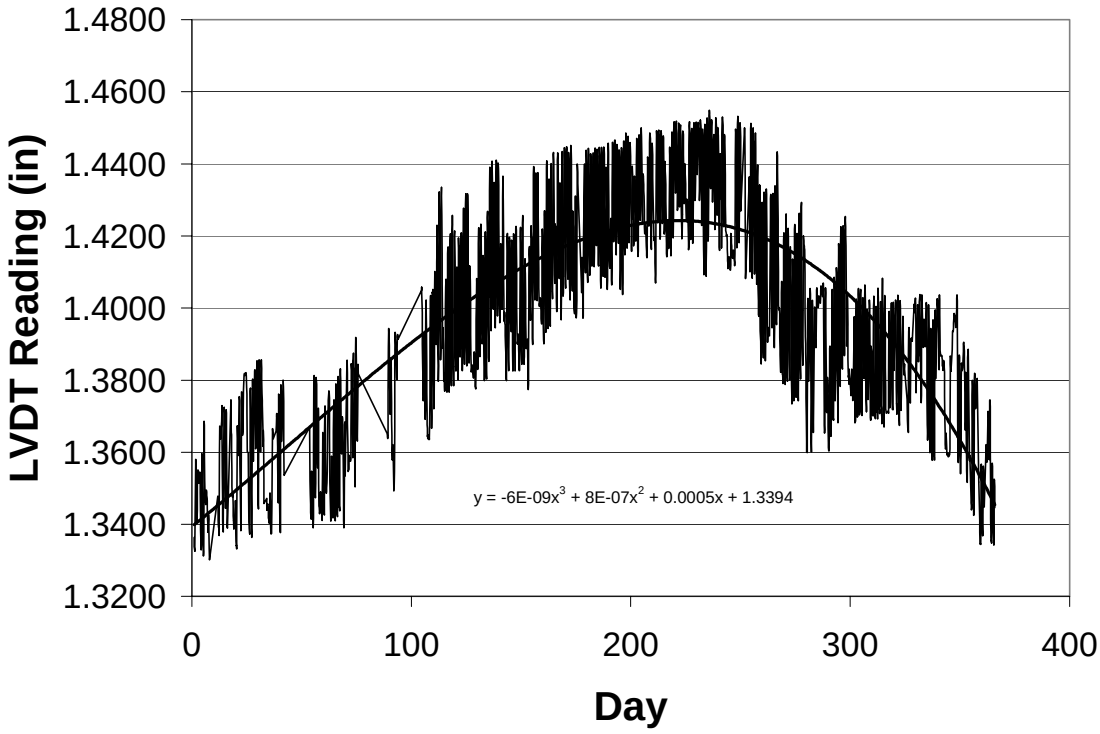

Figure 3.25 Average values for two LVDTs.

This process was done for the eight locations in which there is two LVDTs attached to the end of the girder. Table 3.28 presents the elongations of the girders and also the boundary condition for the end of the girder as shown in the bridge plans.

Table 3.28 Girder Elongations (mm).

A4-N	B4-S	B4-N	C4-S	A5-N	B5-S	B5-N	C5-S
0.16	0.17	2.38	8.99	2.22	0.21	0.58	8.45
EXP.	FIXED	EXP.	EXP.	EXP.	FIXED	EXP.	EXP.

Girders B4-N, C4-S, B5-N and C5-S are located at the traditional expansion joint. The other girders are located at the link slab. It can be seen from Table 3.28 that the largest elongations occur at the expansion joint which is what was expected.

4. Long-Term Monitoring Strategy

4.1 LoggerNet Software

Campbell Scientific provides the software program LoggerNet for interfacing a personal computer with the CR23X datalogger. The software allows the user to create data acquisition programs, transfer programs to the datalogger, retrieve data from the datalogger, and communicate via a telecommunication link. Version 2.0 is a menu driven program compatible with Windows. This software has a copyright date of 2002 and is an upgraded version of the previous software that was used to communicate with the datalogger.

After installing and opening the LoggerNet software, a toolbar with nine buttons will appear on the screen as shown in Figure 4.1. The setup button is used to configure the computer with the datalogger. Information, such as the telephone number used to

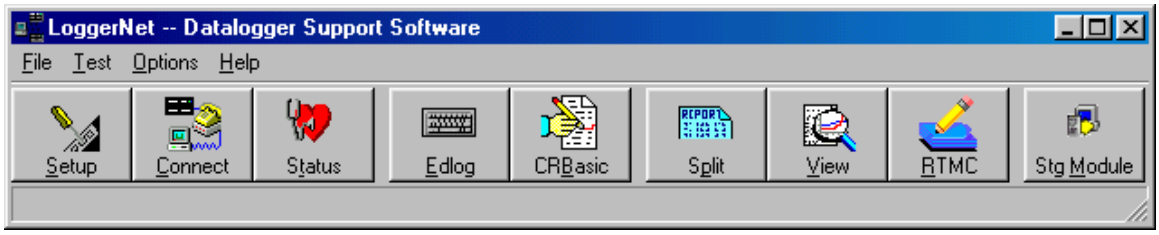

Figure 4.1 LoggerNet main menu bar.

connect to the datalogger, the type of datalogger and the communication port used by the PC are entered under this button. The connect button is selected to communicate with the datalogger. Figure 4.2 is a picture of the toolbar that appears, once the connect button is selected. The Edlog button is used to write and compile data acquisition programs. The Edlog computer language is a unique computer language that has its own specific commands. The datalogger manual has more information about the specifics of the language. The View button is used to examine the data files, once they have been

downloaded. The new LoggerNet software makes available several new options that the previously used software did not have to view the data. One important addition to this software is the graphing capability. It should be noted that this software is relatively new to the author and it has not been used enough for the author to become fully familiar with.

4.1.1 Downloading Data

Once the LoggerNet software has been opened, to download data the user must first connect with the datalogger. To connect with the datalogger, the Connect menu must be accessed. Figure 4.2 is a picture of the Connect menu bar. The user connects

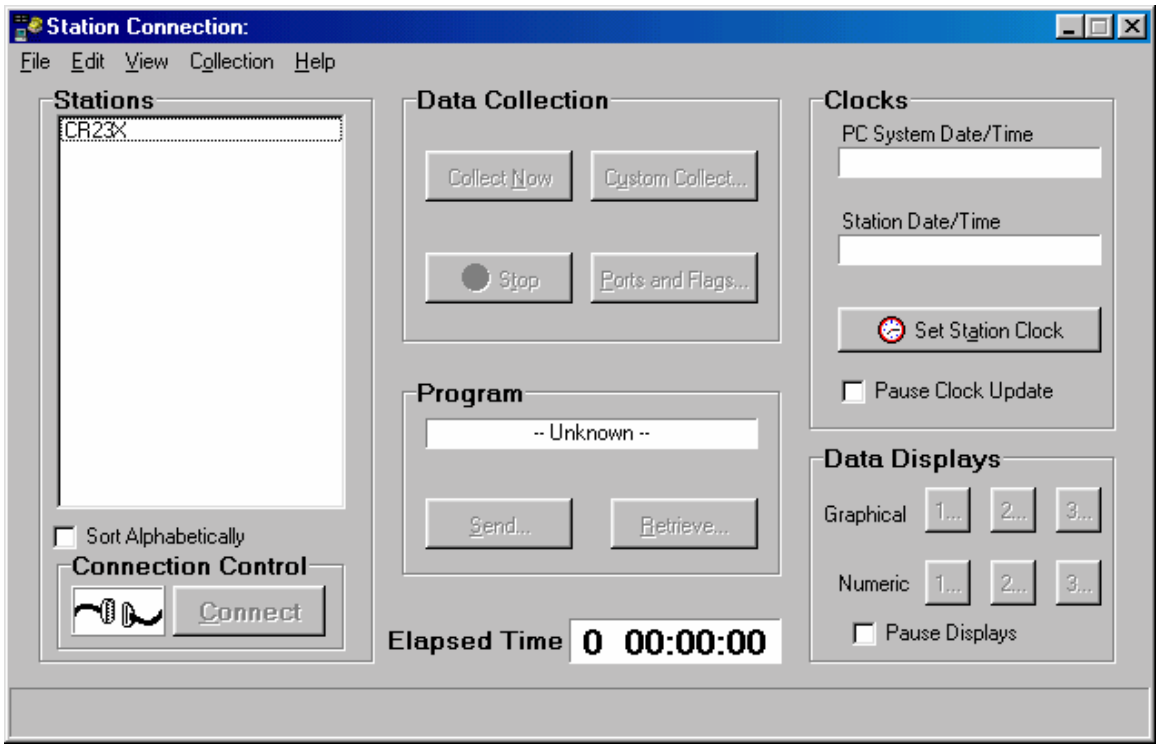

Figure 4.2 Connect menu.

to the datalogger by simply pressing the Connect button in the lower left-hand corner of the open window. It will take several seconds for the software to connect with the datalogger. Once a connection has been made, the buttons that are not accessible in Figure 4.2 will be highlighted and data can then be downloaded. The buttons under the

category Data Collection are used to download data. The buttons under the category Program are used to send and retrieve new data acquisition programs.

To download the data, the user will select the Custom Collect button in the Data Collection category. Once this button has been selected, another window will appear with several options about how the data is to be downloaded. The user will select the desired options and begin downloading the data.

4.1.2 Viewing Data

After data has been downloaded, the user can then examine the data. To view the data, the View button on the LoggerNet menu bar is selected. When this button is selected, another window will appear. Figure 4.3 is a picture of this newly opened window after a data file has been opened. To open file, the process is similar to other

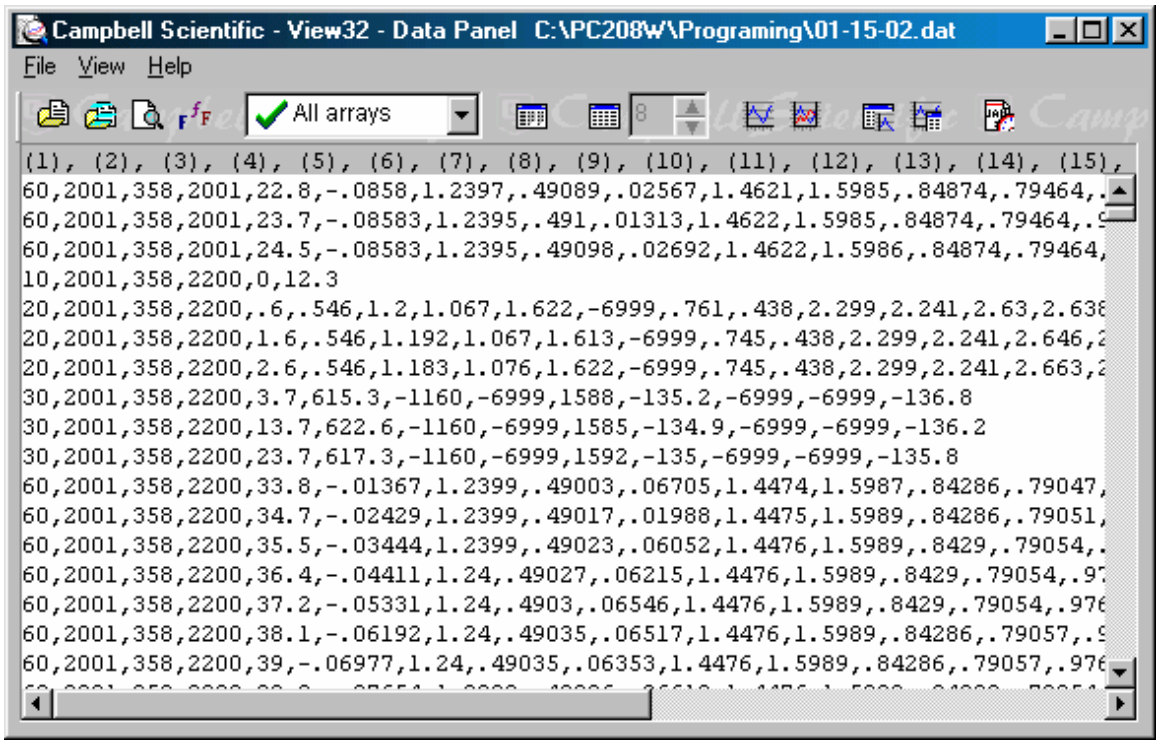

Figure 4.3 View window with a data file opened.

Window applications. The File menu is selected and then the Open File option is selected and the file to be opened is located and opened.

The toolbar buttons at the top of Figure 4.3 are the new options that the LoggerNet software makes available. The Window with All Arrays visible can be selected and only the chosen array can be seen. Figure 4.4 shows the different arrays

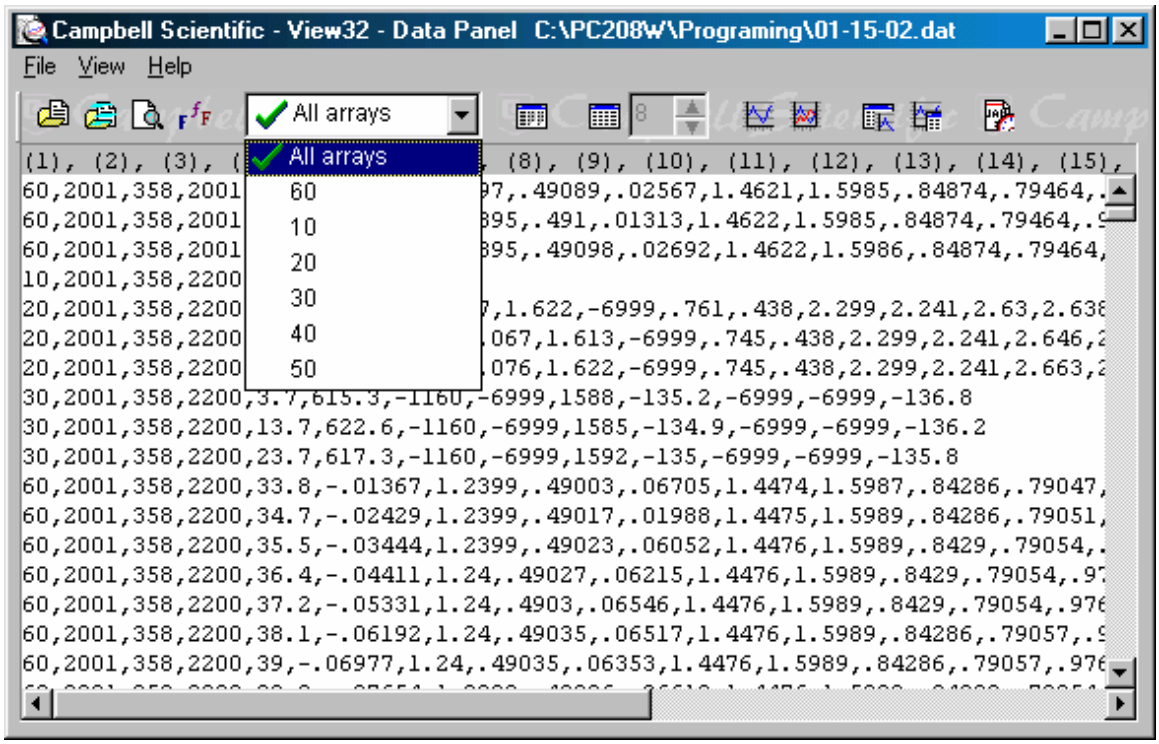

Figure 4.4 View menu with array window open.

that can be seen for this data file. The different arrays in this case are the different types of gauges that are connected to the datalogger and recording data. The first column in the data file label the row of data as to what type of data the row is. For the Haywood County project, 60 is LVDT readings; 10 is voltage readings; 20 is thermocouple readings; 30 is electrical resistance strain gauge readings; 40 is vibrating wire gauge thermistor readings; 50 is vibrating wire gauge strain readings.

To graph the data, the buttons to the right of the array window are used. From left to right, the buttons do the following: toggle hex mode, expands column width, sets column with, graphs with one Y axis, graphs with two y axes, keeps chart on top, keeps data window on top, and sets array definitions. Once an array has been chosen to be

graphed and the graph button is depressed a new window will appear with the graph visible. Figure 4.5 is a picture of a typical graph that can be seen using the LoggerNet software. The new computer program that was developed for the long-term

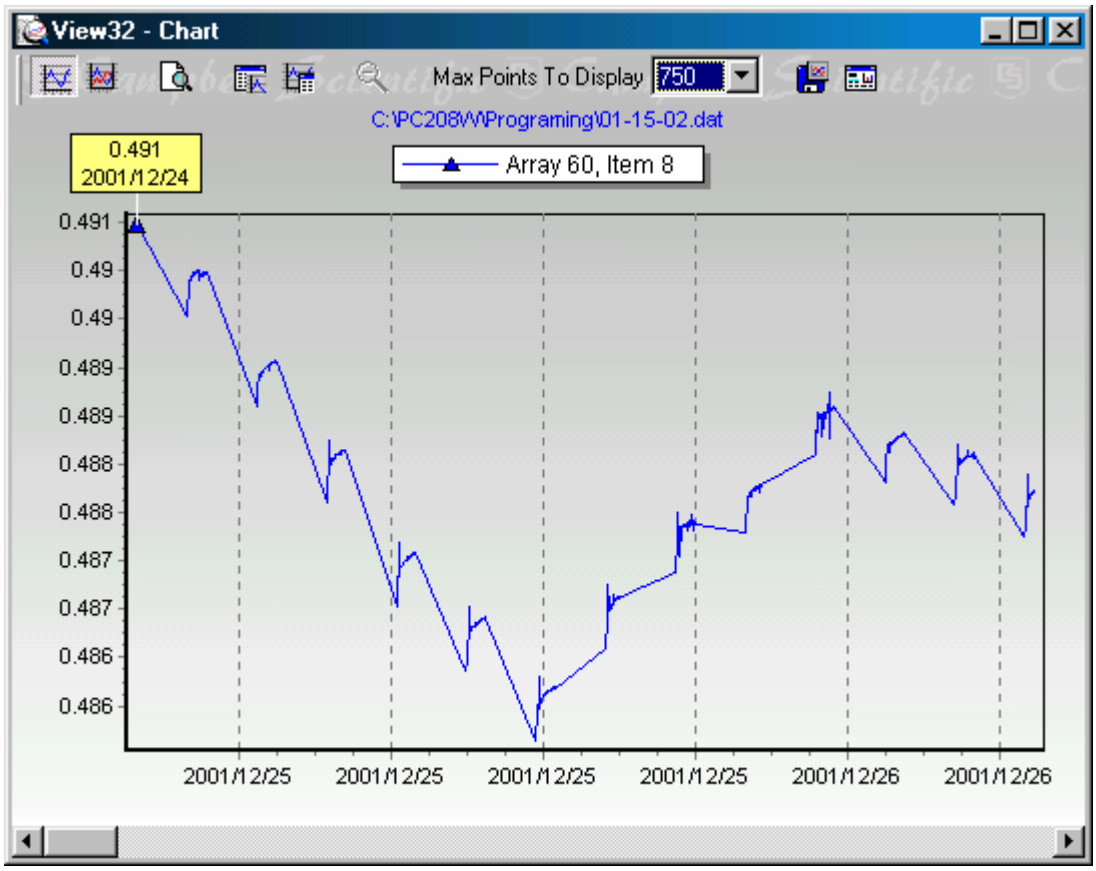

Figure 4.5 Typical graph using LoggerNet software.

monitoring strategy, that will be discussed later, also has graphing capabilities, but was developed before the LoggerNet software was used.

4.2 Computer Program

In order to monitor the long-term performance of the link slab, a computer program was developed using Visual Basic called "AshevilleData." The Excel based program uses the unformatted data files as input and returns the data in a way in which it is easier to use to determine the information of interest.

4.2.1 Overview of Program

Once the data has been downloaded, it must be re-organized to be able to extract pertinent information. The data file is a large notepad file in which the data is separated by commas. Figure 4.6 is an example of the raw data once it has been downloaded. In

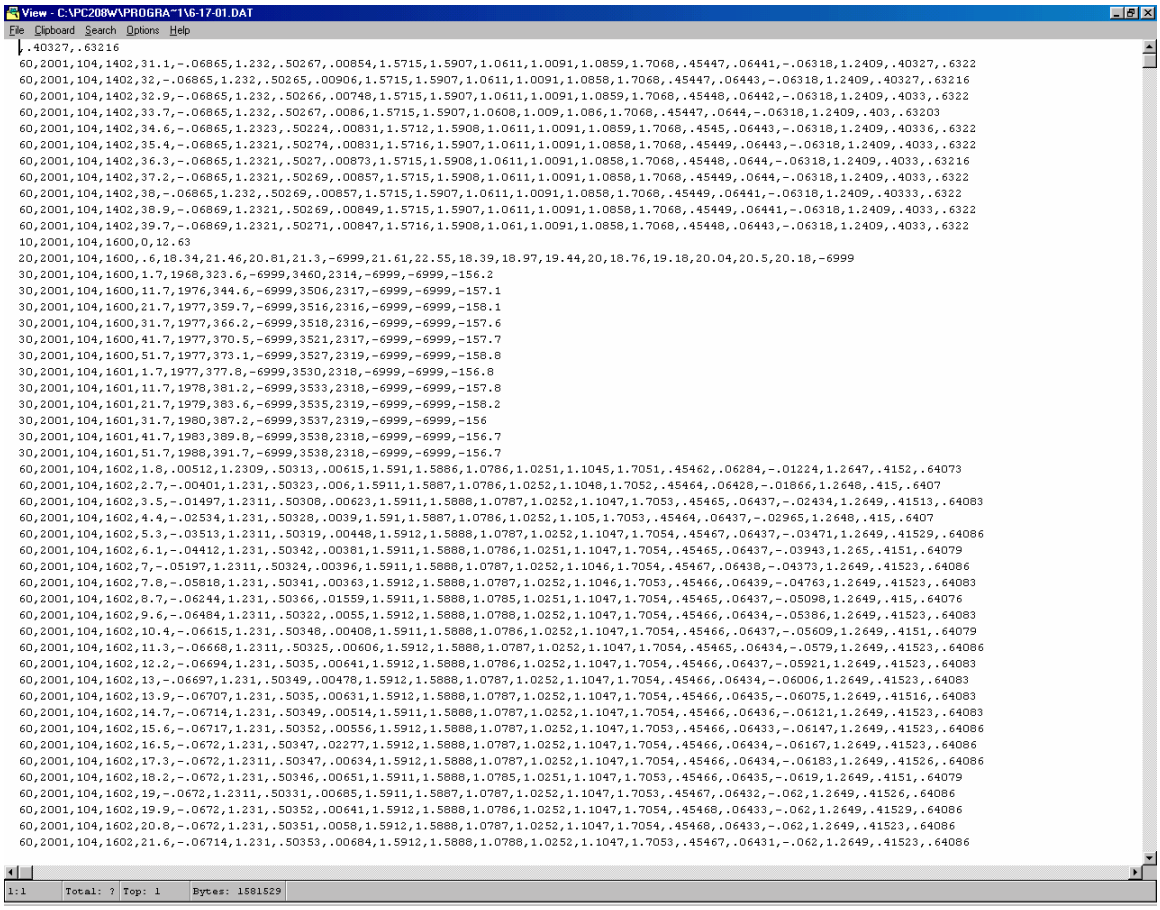

Figure 4.6 Example of raw data.

this data file, each column is separated by a comma. From left to right, the columns display the following: array number (gauge type), year, day, time in hours, time in seconds and the rest of the columns are the different gauge readings.

The program is executed by opening the file "AshevilleData.xls." Figure 4.7 is what the program looks like once it has been opened. To open a data file, the user

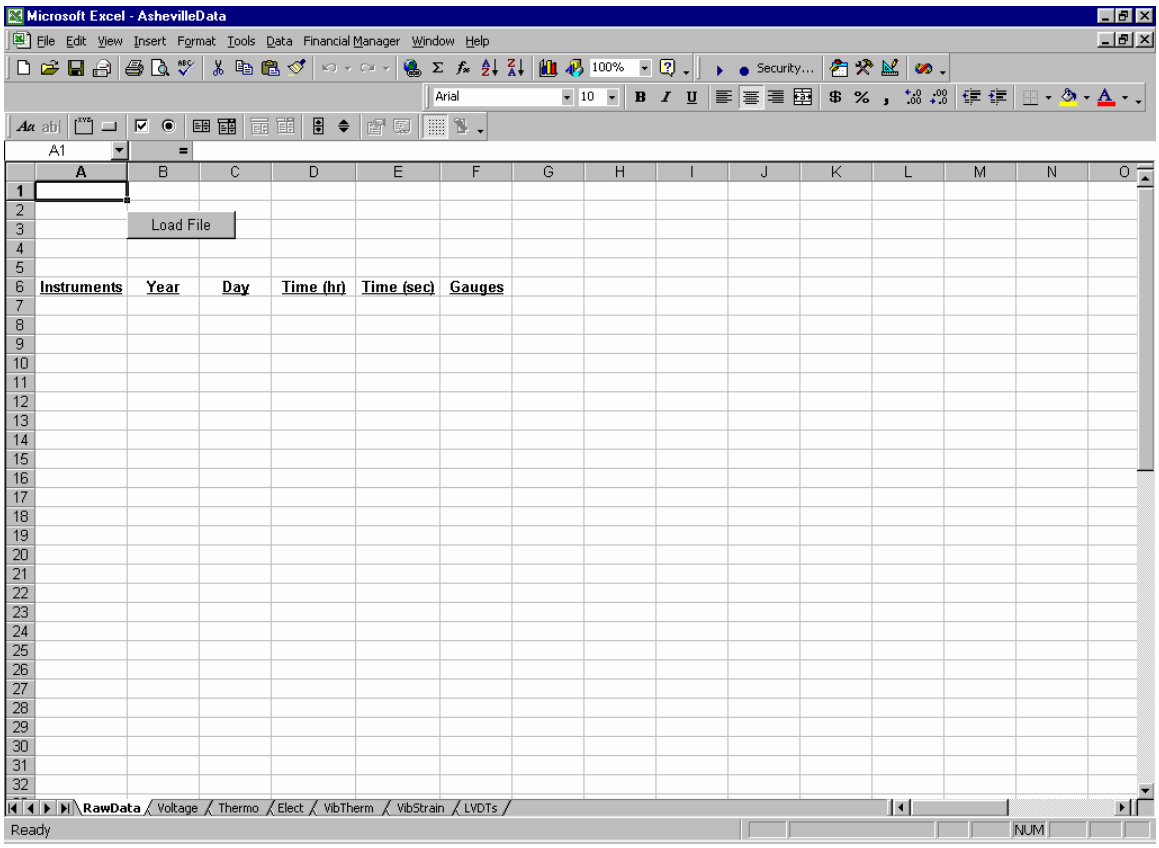

Figure 4.7 AshevilleData.

clicks on the button labeled “Load File.” Once the button has been clicked on, a prompt will appear that asks which data file that the user would like to examine. This program is setup to open files with the “.dat” file extension. The user does not need to re-arrange the data file after it has been downloaded and saved before opening it in this program. When opening a data file, the data is automatically separated by the type of gauge. There are seven active worksheets in this program, which can be seen at the bottom of Figure 4.7. Each worksheet, with the exception of “RawData,” displays the data from the different types of gauges. The worksheet “RawData” displays the whole data file that has been loaded.

Figure 4.8 is what the worksheet “Voltage” looks like. All of the other gauge

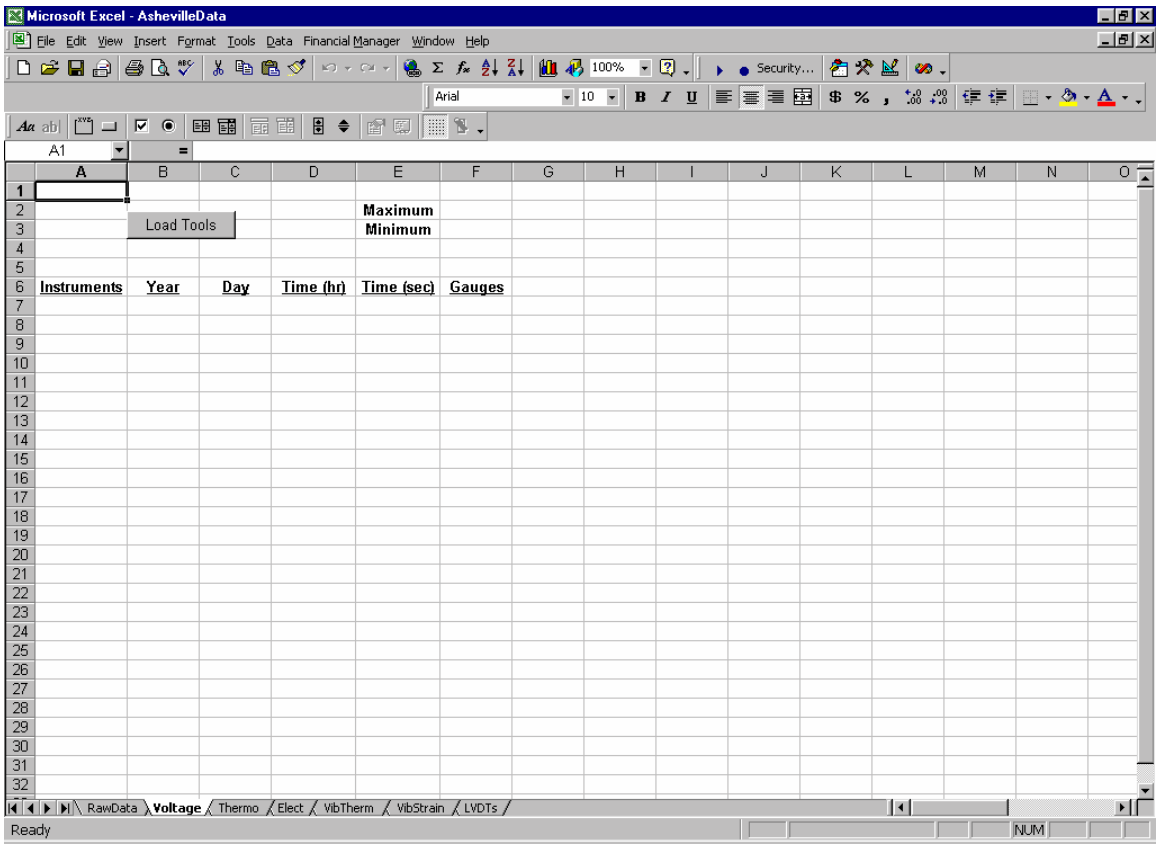

Figure 4.8 Voltage worksheet.

worksheets are very similar to this one. The button that appears on these worksheets "Load Tools" is used to open a toolbar, which makes available several options that make viewing the data easier.

4.2.2 Summary of Options

Once the data file is loaded into the program, there are several options that the user has to re-organize the data and examine it. These options include determining the maximum and minimum values and also the ability to graph. These options are made available by clicking on the "Load Tools" button. Figure 4.9 is a picture of the toolbar

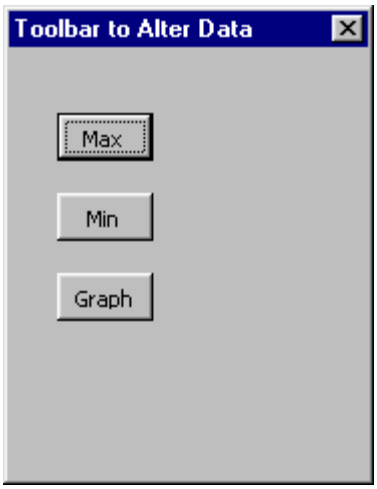

Figure 4.9 “Load Tools” toolbar.

that appears if the “Load Tools” button is depressed.

The “Max” and “Min” buttons will display the maximum and minimum values of the different gauges for the active worksheet that the user is working with. The values are displayed at the top of the worksheet next to the words “Maximum” and “Minimum.”

Microsoft Excel - AshevilleData

	A	B	C	D	E	F	G	H	I	J	K	L	M	N
2					Maximum		0.00748	1.2337	0.50959	0.0009	1.672	1.5754	1.1474	1.0997
3		Load Tools			Minimum		-0.06332	1.2336	0.50901	-0.00028	1.6718	1.575	1	1.0994
6	Instruments	Year	Day	Time (hr)	Time (sec)	Time (min)	Gauges							
8							1	2	3	4	5	6	7	8
9	60	2001	252	0	33.8	0.563	0.00748	1.2336	0.50901	0.0009	1.6718	1.575	1.1473	1.0994
10	60	2001	252	0	34.7	0.578	-0.00243	1.2336	0.50911	0.00028	1.6719	1.5752	1.1473	1.0995
11	60	2001	252	0	35.5	0.592	-0.01388	1.2337	0.50914	0.00025	1.6719	1.5753	1.1474	1.0995
12	60	2001	252	0	36.4	0.607	-0.02425	1.2337	0.50919	0.00016	1.672	1.5753	1.1474	1.0995
13	60	2001	252	0	37.2	0.620	-0.03373	1.2336	0.50921	0.00009	1.6719	1.5753	1.1474	1.0995
14	60	2001	252	0	38.1	0.635	-0.04213	1.2337	0.50923	0.00001	1.672	1.5753	1.1474	1.0995
15	60	2001	252	0	39	0.650	-0.04918	1.2336	0.50927	-0.00009	1.672	1.5753	1.1474	1.0995
16	60	2001	252	0	39.8	0.663	-0.05463	1.2337	0.50927	-0.00007	1.672	1.5753	1.1474	1.0995
17	60	2001	252	0	40.7	0.678	-0.0583	1.2336	0.50929	-0.00008	1.6719	1.5753	1.1474	1.0995
18	60	2001	252	0	41.5	0.692	-0.06053	1.2337	0.50929	-0.00011	1.6719	1.5753	1.1474	1.0995
19	60	2001	252	0	42.4	0.707	-0.06172	1.2336	0.50932	-0.00016	1.6719	1.5753	1.1474	1.0995
20	60	2001	252	0	43.2	0.720	-0.06231	1.2337	0.50931	-0.00011	1.6719	1.5753	1.1474	1.0995
21	60	2001	252	0	44.1	0.735	-0.06263	1.2337	0.50932	-0.00012	1.6719	1.5753	1.1474	1.0995
22	60	2001	252	0	45	0.750	-0.0628	1.2337	0.50932	-0.00014	1.6719	1.5753	1.1474	1.0995
23	60	2001	252	0	45.8	0.763	-0.06286	1.2337	0.50932	-0.00007	1.6719	1.5753	1.1474	1.0995
24	60	2001	252	0	46.7	0.778	-0.06293	1.2337	0.50959	0.00037	1.6719	1.5753	1.1474	1.0995
25	60	2001	252	0	47.6	0.793	-0.06286	1.2337	0.50937	-0.00028	1.672	1.5753	1.1474	1.0995
26	60	2001	252	0	48.4	0.807	-0.06296	1.2336	0.50937	-0.00009	1.672	1.5754	1.1474	1.0995
27	60	2001	252	0	49.3	0.822	-0.06306	1.2337	0.50936	-0.00013	1.6719	1.5753	1.1474	1.0995
28	60	2001	252	0	50.1	0.835	-0.06306	1.2337	0.50935	-0.00011	1.672	1.5753	1.1474	1.0995
29	60	2001	252	0	51	0.850	-0.063	1.2336	0.50937	-0.00012	1.6719	1.5753	1.1474	1.0995
30	60	2001	252	0	51.9	0.865	-0.06309	1.2337	0.50936	-0.00027	1.6719	1.5753	1.1474	1.0995
31	60	2001	252	0	52.7	0.878	-0.06316	1.2337	0.50934	-0.00003	1.6718	1.5754	1.1474	1.0995
32	60	2001	252	0	53.6	0.893	-0.06319	1.2337	0.50932	-0.00001	1.672	1.5753	1.1474	1.0995

Figure 4.10 Example of data in program.

Figure 4.10 is an example of what the program would look like after the maximum and minimum values for each gauge, for a typical data file, have been determined. It should be noted that it might take some time to determine the maximum and minimum values. This program is written in Visual Basic, which is not one of the most efficient computer programming languages.

If the graph button is pressed on the toolbar, another window will appear that looks like the toolbar in Figure 4.11. This toolbar give the user the option of graphing a particular gauge for a specified day. Only one gauge can be graphed at a time due to differences in the readings of the gauges. The user types in the day and instrument

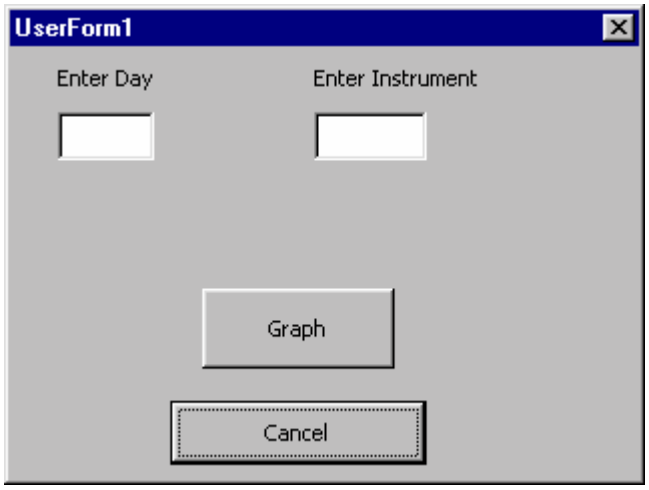

Figure 4.11 Graph toolbar.

number that he or she would like to graph, and then presses the graph button to see the data graphed.

All Excel functions are still available to the user, since it is an Excel file. This includes the ability to save the file. It is suggested that the file not be saved once the user is done viewing the data. The program contains several macros, which would also be saved. This would cause the files to be large and would quickly reduce the amount of

space available on the computer that is being used. An alternative would be to determine the maximum and minimum values for the gauges and copy and paste those values into another Excel file that can be saved and would not use as much disk space.

4.3 Periodic Visits

Not only will the computer program be useful for monitoring the long-term performance, but periodic visits should be made to the project site as well. Visits to the bridge will be important because the link slab can be visually inspected. During the visits, the data acquisition equipment can also be inspected. Problems with the link slab or data acquisition system might be discovered during these visits that might not have been noticed from examining the data alone.

4.3.1 Visual Inspection of Link Slab

As noted before, there is currently a crack visible within the central joint of the link slab. There is no way to measure the width of this crack from the data acquisition system alone. The crack must be visually inspected to determine if it is becoming larger, or if more cracks are appearing outside the control joint. If the crack becomes too large, remediation actions must be taken. Again, this could not be determined from examining the data.

4.3.2 Ensure Equipment is in Good Condition

During visits to the project site, the data acquisition system equipment should also be inspected. Since some of the gauges are exposed to the weather, it is possible that they may have become inoperable and may be giving false readings. There are sixteen LVDTs, six electrical resistance strain gauges, and four thermocouples that are exposed

and can be replaced if they become faulty. The rest of the gauges are embedded in the bridge deck and there is no way to inspect or replace them.

The solar panel and instrumentation boxes should also be inspected. The solar panel was vandalized in the past, which caused the data acquisition system to stop working. In the past, the battery has also died, which caused the system to lose power. Downloading data can check both of these situations. If data cannot be downloaded, it is possible that the solar panel is damaged or the battery has died. The datalogger and mulitplexers are protected in boxes located on top of the bent directly below the instrumented link slab. It would also be a good idea to inspect these pieces of equipment to make sure that there are no loose wires and that they are working properly. Figure 4.12 is a picture of the instrumentation boxes positioned on the bridge bent.

Figure 4.12 Instrumentation boxes at project site.

5. Conclusions and Recommendations

5.1 Conclusions

The primary objectives of this project were to validate design assumptions, investigate limit-states design methods and develop a strategy and guide for long-term monitoring of the link slab. These three objectives were accomplished successfully by the analysis of the data from different loading conditions. The different loads were service load, thermal load and a controlled live load test.

The first objective, validate design assumptions was mainly accomplished by analyzing the data from the live load test. Several assumptions were made when designing the link slab. Some of these assumptions include: girder spans are simply supported and compatibility of deformations between girders and link slab. A computer model was developed to determine if the results of the live load test were valid or not. The model reinforced the results that were obtained from the live load test. It was shown that these assumptions are in fact valid assumptions.

A more simplified design procedure for link-slab bridges was also investigated during this research. The intention of the investigation was to develop a procedure in which the link slab could be designed for a certain level of rotation and also an allowable crack width. A procedure was developed to produce design charts in which the engineer could choose a crack width and rotational degree and obtain the steel reinforcement for the link-slab. The design charts presented in this report are specific to the Haywood County project because they are dependent on the depth and length of the link-slab. However, it is not difficult to develop these charts for other configurations of depth and length. To use these charts the engineer would determine the rotation that the bridge will

be subjected to due to the applied load and also choose an acceptable crack width. The engineer would then go to these charts and find the intersection of the rotation and crack width that was chosen and obtain the amount of reinforcement needed.

The last objective, develop a strategy and guide for long-term monitoring of the link slab, was accomplished by the creation of a computer program using Visual Basic. The Excel based program imports the unformatted data from a file and formats the data in a way that it is easier to work with and discern the information, which is of interest. It is also suggested that not only should the program be used to monitor the long-term performance of the link slab, but also, periodic visits should be made to the project site. During these visits, the link slab can be visually inspected to determine if the crack width is increasing. The data acquisition system equipment can also be inspected to ensure that it is still working properly.

5.2 Recommendations

As the project progressed, it was apparent that several aspects could be changed to improve the efficiency and reliability of the data acquisition system. The following are suggestions for future research in highway instrumentation projects.

The first suggestion is, if at all possible, to select the project site closer to Raleigh so that the site could be visited more frequently. This would allow for more site visits to visually inspect the link slab and data acquisition system. During the inspections, the underside of the link slab should also be examined to determine if the crack present has propagated through the depth of the slab. If the crack has propagated through the depth of the slab, then the link slab is subjected to tension as well as bending. Also, if during one of the inspections, the crack width in the link slab is determined to be too great, the

crack could be filled with a hot poured sealant to improve the serviceability of the link slab and also increase its life.

Another suggestion is to use a more reliable power source. The solar panel, which charges the battery in Haywood County, was damaged due to vandalism in the past. There was also an incident in which the battery had died, both of which make the data acquisition system inoperable. The best solution would be to use a direct power source instead of the solar panel and battery. However, if this is not feasible, some sort of protection for the solar panel should be provided to prevent against vandalism.

The instruments being used for this project provide good results for a controlled live load test. However, due to the time in which the vibrating wire gauges need to give readings, it is hard to get accurate service loading readings. The gauges have a +/- 5 second response time. It takes a vehicle traveling at the posted speed limit approximately 0.3 seconds to cross the entire bridge. Strain sensors with a faster response time would allow for accurate service loading readings. Investigation should be continued to find a more efficient data acquisition system. The state of Connecticut has two bridges that instrumented with data acquisition systems that are manufactured by Agilent Technologies (formerly Hewlett Packard). One system in particular is a E1301A Series B VXI portable mainframe. Connnecticut uses this system to monitor tilt, temperature, strain and acceleration, but it is capable of monitoring different types of sensors. They also have another project where they will be measuring strain inside of a precast-prestressed concrete beam, in which the system will be purchased from Slope Indicator. Further investigations should be made to determine an alternate system in which faster

readings could be made for future projects similar to the Haywood County project if data from traffic loading is desired.

References

Burke, Martin P., "Semi-Integral Bridges Movements and Forces" Transportation Research Record 1460, National Academy Press, Washington, D.C., December 1994.

Burke, Martin P., "The Design of Integral Bridges, " Concrete International, Vol. 15, No. 6, June 1993, pp 37-42.

Burke, Martin P., "Integral Bridges," Transportation Research Board's 69th Annual meeting, January 1990, Burgess & Niple, Limited, Engineers and Architects.

Caner, A. and Zia, P., "Behavior and Design of Link Slabs for Jointless Bridge Decks," PCI Journal, Vol. 43, No. 3, May/June 1998, pp 68-80.

Campbell Scientific Inc., CR23X Micrologger Operator's Manual, October 1998.

Campbell Scientific Inc., PC208W Datalogger Support Software Instruction Manual, February, 1998.

Campbell Scientific Inc., LoggerNet User's Manual, March, 2002.

El-Safty, A. K., "Analysis of Jointless Bridge Decks with Partially Debonded Simple Span Beams," Ph.D. Dissertation, North Carolina State University, Raleigh, NC 1994.

FHWA, "All Systems Highway Bridges Chart," December 2001, http://www.fhwa.dot.gov/bridge/defbr01.xls

Loveall, C. L., "Jointless Bridge Decks," Civil Engineering, ASCE, November 1985.

McCormac, Jack C. *Design of Reinforced Concrete.* Menlo Park, California: Addison-Wesley, 1998.

"Steel Bridge," News and Information From the Steel Bridge Forum, Summer/Fall 1993, http://www.steel.org/markets/infrastructure/sbfall93.pdf

Visual Analysis. By Integrated Engineering Software. Student Version. (1998).

Wagner, Matt, The Behavior of Prestressed High Performance Concrete Bridge Girders for US Highway 401 Over the Neuse River in Raleigh, NC, MSCE Thesis, North Carolina State University, Raleigh, NC 2001.

Warren, Bruce, Development of a Data Acquisition System for an Instrumented Highway Structure, MSCE Thesis, North Carolina State University, 2000. 139 pp.

Wasserman, E. P., "Jointless Bridge Decks," Engineering Journal, AISC, Vol. 24, No. 3, 3rd Quarter 1987.

Appendices

A. Computer Program for Live Load Test

```
;{CR23X}

;***Program Girdergages***
;***Revised: Mickey Wing
;***06/01
;***Edited for Haywood County Project

; This program processes and converts data from a Data Acquisition
; system. It reads vibration wire gages, strain gages, thermocouples
; and lvdts. This program was
; developed for use in both the link slab project B-2985, Haywood
; County near Asheville, NC and Highway 401 in Raleigh, NC.
; Table 1 contains the strain gage, thermocouple adn lvdt subroutines.
; Table 2 contains the vibrating wire gage subroutines.

;****STRAIN GAGE****
; This program will multiplex 16 full bridge strain gauges on one AM416
; multiplexer unit. Micro Measurements electrical resistance strain
; gages type CEA-06-250UW-120 with a gage factor of 2.07 are assumed.
; The program is written for the gages to be in connection with a
; CSI 4WFB120 full bridge completion module.
; The strain gages are measured at the beginning of every 4 hour
; interval. Continuous measurements are taken for 15 seconds at a rate
; of 1/3 hertz (1 measurement every 3 seconds, 5 measurements in 15
; seconds).

; Wiring for this program must be connected in the following manner:
;
;       AM416                   CR23X
;
;       12V                     12V
;       GND                     G (near 12V)
;       Clk                     EX2
;       Res                     C3
;       L1                      G(SYMBOL near EX)
;       H1                      EX3
;       L2                      SE4
;       H2                      SE3
;       SHIELD                  G(SYMBOL near SE4)

; All strain gages must be connected to a full bridge completion module.
;
;       AM416                   4WFB120       3 Wire Strain Gage
;       H                       L2            Terminal 1
```

```
;       L                   H2          Terminal 2
;       G                   L1          Ground
;       Free Wire               H1

; Output format:
;           All ustrain values.....microstrain

;***THERMOCOUPLE****
; This program will multiplex 25 thermocouples on one AM25T multiplexer
; unit. Chrome/Aluminum thermocouples are measured with reference to the
; internal datalogger temperature device.  The thermocouples are
; measured at the beginning of every 4 hour interval.  Continuous
; measurements are taken for 30 seconds at a rate of 1/3 hertz (1
; measurement every 3 seconds, 5 measurements in 15 seconds).

; Wiring for this program must be connected in the following manner:
;
;       AM25T                   CR23X
;
;       12V                     12V
;       G(SYMBOL)                   G
;       Clk                     C1
;       Res                     C2
;       EX                      EX1
;       AG                      GSYMBOL)near EX1
;       HI                      1H
;       LO                      1L
;       G(SYMBOL)                   G(SYMBOL)

; All thermocouples must be connected with Yellow(chromega) HI and
; Red(alumega) LO.

; Output format:
;           BattV.....volts
;           RefTmp.....degrees Celsius
;           All TC.....degrees Celsius

;****LVDT****
; This program will multiplex 16 lvdts on one AM416 multiplexer unit.
; Lucas schaevitz lvdt's are used.  Type DC-SE units with different
; ranges are used. Most gages are 0.25", 0.5", or 2.5" The lvdt's are
; measured at the beginning of every 4 hour interval. Continuous
; measurements are taken for 15 seconds at a rate of 1/3 hertz
; (1 measurement every 3 seconds, 5 measurements in 15 seconds).

; Wiring for this program must be connected in the following manner:
```

```
;
;       LVDT            AM416                   CR23X
;
;       RED             12V                     12V
;       BLACK             G(SYMBOL)                     G (near 12V)
;                   Clk                     C8
;                   Res                     C7
;       GREEN           COM 1H                  Diff 4H
;       WHITE           COM 1L                  Diff 4L
;       RED             COM 2H                  12V
;       BLACK             COM 2L                  GRPUND

; Output format:
;             displ.....inches

;****PROGRAM GIRDERGAGES****

*Table 1 Program
  01: 1         Execution Interval (seconds)

; P92 synchronizes measurement cycle to real time
; (every 240 minutes, 4 hours)
;
1:  If time is (P92)
 1: 1        Minutes (Seconds --) into a
 2: 2        Interval (same units as above)
 3: 30       Then Do

; Measure battery voltage
;
2:  Batt Voltage (P10)
 1: 86       Loc [ BattV     ]

; Set output flag and output Battery Voltage
;
3:  Do (P86)
 1: 10       Set Output Flag High (Flag 0)

; Set storage array for:
; Battery voltage       = array id 10
;
4:  Set Active Storage Area (P80)
 1: 1        Final Storage Area 1
 2: 10       Array ID

; Record real time with each measurement
```

```
;
5:  Real Time (P77)
 1: 1111     Year,Day,Hour/Minute,Seconds (midnight = 0000)

6:  Sample (P70)
 1: 1        Reps
 2: 86       Loc [ BattV     ]

;****THERMOCOUPLES****
; This loop makes measurements every 3 seconds for 15 seconds (5 count)
;
7:  Beginning of Loop (P87)
 1: 0        Delay
 2: 1        Loop Count

; Measure thermocouples connected to AM25T, the reference temperature
; parameter is left blank because it has already been measured.
;
8:  Panel Temperature (P17)
 1: 87       Loc [ RefTmp    ]

9:  AM25T  Multiplexer (P134)
 1: 16       Reps
 2: 21       10 mV, 60 Hz Reject, Slow Range
 3: 1        Channel
 4: 1        DIFF Channel
 5: 0        Do not Measure Reference, Use Current Value
 6: 1        Clock Control
 7: 2        Reset Control
 8: 3        Type K (Chromel-Alumel)
 9: 87       Ref Temp (Deg. C) Loc [ RefTmp    ]
10: 88       Loc [ TC_1      ]
11: 1        Mult
12: 0        Offset

; Set output flag and output all data measured in the loop
;
10:  Do (P86)
 1: 10       Set Output Flag High (Flag 0)

; Set storage array for:
; Reference temperature &
; thermocouple data     = array id 20
;
11:  Set Active Storage Area (P80)
 1: 1        Final Storage Area 1
```

```
 2: 20       Array ID

; Record real time with each measurement
;
12:  Real Time (P77)
 1: 1111     Year,Day,Hour/Minute,Seconds (midnight = 0000)

13:  Sample (P70)
 1: 1        Reps
 2: 87       Loc [ RefTmp    ]

14:  Sample (P70)
 1: 16       Reps
 2: 88       Loc [ TC_1      ]

15:  End (P95)

;****STRAIN GAGES****
; Load the constant 4e6 (for units conversion) into an input location
;
16:  Z=F (P30)
 1: 4        F
 2: 6        Exponent of 10
 3: 1        Z Loc [ unitsconv ]

; Load gage factor into an input location (all gages have same gf)
;
17:  Z=F (P30)
 1: 2.065    F
 2: 00       Exponent of 10
 3: 2        Z Loc [ gagefac   ]

; Calculate multiplier to use with strain calculation
;
18:  Z=X/Y (P38)
 1: 1        X Loc [ unitsconv ]
 2: 2        Y Loc [ gagefac   ]
 3: 3        Z Loc [ mult      ]

; Portions of this routine are taken from the manual for full bridge
; terminal input modules for CR21X.
; (Datalogger CR23X is not referenced in the manual)

; Loop for 5 measurements (3 second intervals for 15 seconds)
;
19:  Beginning of Loop (P87)
```

```
 1: 0        Delay
 2: 3        Loop Count

; Set control port C3 to high, this turns on the multiplexer connected
; to port C3
;
20:  Do (P86)
 1: 43       Set Port 3 High

; Loop for 16 channels of the multiplexer
;
21:  Beginning of Loop (P87)
 1: 0        Delay
 2: 8        Loop Count

; Excite the strain gage for voltage mesurements
;
22:  Delay w/Opt Excitation (P22)
 1: 2        Ex Channel
 2: 1        Delay W/Ex (units = 0.01 sec)
 3: 1        Delay After Ex (units = 0.01 sec)
 4: 5000     mV Excitation

23:  Full Bridge (P6)
 1: 1        Reps
 2: 21       10 mV, 60 Hz Reject, Slow Range
 3: 2        DIFF Channel
 4: 3        Excite all reps w/Exchan 3
 5: 2500     mV Excitation
 6: 4     -- Loc [ rawsg_1   ]
 7: 1.0      Mult
 8: 0.0      Offset

; Change the full bridge reading from from mv/v to v/v
;
24:  Z=X*F (P37)
 1: 4     -- X Loc [ rawsg_1   ]
 2: 0.001    F
 3: 21    -- Z Loc [ vlts_1    ]

; Calculate microstrain
;
25:  Z=X*F (P37)
 1: 21    -- X Loc [ vlts_1    ]
 2: -2       F
 3: 37    -- Z Loc [ _2vlts_1_ ]
```

```
26:  Z=Z+1 (P32)
 1: 37    -- Z Loc [ _2vlts_1_ ]

27:  Z=X/Y (P38)
 1: 21    -- X Loc [ vlts_1    ]
 2: 37    -- Y Loc [ _2vlts_1_ ]
 3: 54    -- Z Loc [ strn_1    ]

28:  Z=X*Y (P36)
 1: 54    -- X Loc [ strn_1    ]
 2: 3       Y Loc [ mult      ]
 3: 70    -- Z Loc [ ustrn_1   ]

29:  End (P95)

; Turn off multiplexer
;
30:  Do (P86)
 1: 53       Set Port 3 Low

; Set storage array
;
31:  Do (P86)
 1: 10       Set Output Flag High (Flag 0)

32:  Set Active Storage Area (P80)
 1: 1        Final Storage Area 1
 2: 30       Array ID

33:  Real Time (P77)
 1: 1111     Year,Day,Hour/Minute,Seconds (midnight = 0000)

34:  Sample (P70)
 1: 8        Reps
 2: 70       Loc [ ustrn_1   ]

35:  End (P95)


;****LVDTs****
;Turn on lvdt multiplexer
;
36:  Do (P86)
 1: 47       Set Port 7 High
```

```
; This loop makes measurements every 3 seconds for 15 seconds
; (5 count)
;
37:  Beginning of Loop (P87)
 1: 0        Delay
 2: 25       Loop Count

; Loop for 16 channels of the multiplexer
;
38:  Beginning of Loop (P87)
 1: 0        Delay
 2: 16       Loop Count

39:  Do (P86)
 1: 78       Pulse Port 8

40:  Delay w/Opt Excitation (P22)
 1: 1        Ex Channel
 2: 0000     Delay W/Ex (units = 0.01 sec)
 3: 2        Delay After Ex (units = 0.01 sec)
 4: 0000     mV Excitation

; Make the voltage measurement across the multiplexer channels
;
41:  Volt (Diff) (P2)
 1: 1        Reps
 2: 25       5000 mV, 60 Hz Reject, Fast Range
 3: 4        DIFF Channel
 4: 177   -- Loc [ lvdtvlt1  ]
 5: .001     Mult
 6: 0        Offset

42:  End (P95)

; Load gage factor into an input location (all gages have diff gf)
;
43:  Z=F (P30)
 1: 2.5011   F
 2: 0        Exponent of 10
 3: 161      Z Loc [ gagefac1  ]

44:  Z=F (P30)
 1: 2.4972   F
 2: 0        Exponent of 10
 3: 162      Z Loc [ gagefac2  ]
```

45: Z=F (P30)
1: 10.0450 F
2: 0 Exponent of 10
3: 163 Z Loc [gagefac3]

46: Z=F (P30)
1: 19.931 F
2: 0 Exponent of 10
3: 164 Z Loc [gagefac4]

47: Z=F (P30)
1: 2.5089 F
2: 0 Exponent of 10
3: 165 Z Loc [gagefac5]

48: Z=F (P30)
1: 2.5029 F
2: 0 Exponent of 10
3: 166 Z Loc [gagefac6]

49: Z=F (P30)
1: 2.5258 F
2: 0 Exponent of 10
3: 167 Z Loc [gagefac7]

50: Z=F (P30)
1: 2.5029 F
2: 0 Exponent of 10
3: 168 Z Loc [gagefac8]

51: Z=F (P30)
1: 2.4958 F
2: 0 Exponent of 10
3: 169 Z Loc [gagefac9]

52: Z=F (P30)
1: 2.4883 F
2: 0 Exponent of 10
3: 170 Z Loc [gagefac10]

53: Z=F (P30)
1: 10.0074 F
2: 0 Exponent of 10

```
 3: 171      Z Loc [ gagefac11 ]

54:  Z=F (P30)
 1: 19.9838  F
 2: 0        Exponent of 10
 3: 172      Z Loc [ gagefac12 ]

55:  Z=F (P30)
 1: 2.5032   F
 2: 0        Exponent of 10
 3: 173      Z Loc [ gagefac13 ]

56:  Z=F (P30)
 1: 2.4983   F
 2: 0        Exponent of 10
 3: 174      Z Loc [ gagefac14 ]

57:  Z=F (P30)
 1: 2.5053   F
 2: 0        Exponent of 10
 3: 175      Z Loc [ gagefac15 ]

58:  Z=F (P30)
 1: 2.5063   F
 2: 0        Exponent of 10
 3: 176      Z Loc [ gagefac16 ]

; Convert LVDT voltages to displacements in inches
;
59:  Z=X/Y (P38)
 1: 177      X Loc [ lvdtvlt1  ]
 2: 161      Y Loc [ gagefac1  ]
 3: 193      Z Loc [ lvdt_1    ]

60:  Z=X/Y (P38)
 1: 178      X Loc [ lvdtvlt2  ]
 2: 162      Y Loc [ gagefac2  ]
 3: 194      Z Loc [ lvdt_2    ]

61:  Z=X/Y (P38)
 1: 179      X Loc [ lvdtvlt3  ]
 2: 163      Y Loc [ gagefac3  ]
 3: 195      Z Loc [ ldvt_3    ]

62:  Z=X/Y (P38)
 1: 180      X Loc [ lvdtvlt4  ]
```

2: 164 Y Loc [gagefac4]
3: 196 Z Loc [ldvt_4]

63: Z=X/Y (P38)
1: 181 X Loc [lvdtvlt5]
2: 165 Y Loc [gagefac5]
3: 197 Z Loc [lvdt_5]

64: Z=X/Y (P38)
1: 182 X Loc [lvdtvlt6]
2: 166 Y Loc [gagefac6]
3: 198 Z Loc [lvdt_6]

65: Z=X/Y (P38)
1: 183 X Loc [lvdtvlt7]
2: 167 Y Loc [gagefac7]
3: 199 Z Loc [lvdt_7]

66: Z=X/Y (P38)
1: 184 X Loc [lvdtvlt8]
2: 168 Y Loc [gagefac8]
3: 200 Z Loc [lvdt_8]

67: Z=X/Y (P38)
1: 185 X Loc [lvdtvlt9]
2: 169 Y Loc [gagefac9]
3: 201 Z Loc [lvdt_9]

68: Z=X/Y (P38)
1: 186 X Loc [lvdtvlt10]
2: 170 Y Loc [gagefac10]
3: 202 Z Loc [lvdt_10]

69: Z=X/Y (P38)
1: 187 X Loc [lvdtvlt11]
2: 171 Y Loc [gagefac11]
3: 203 Z Loc [lvdt_11]

70: Z=X/Y (P38)
1: 188 X Loc [lvdtvlt12]
2: 172 Y Loc [gagefac12]
3: 204 Z Loc [lvdt_12]

71: Z=X/Y (P38)
1: 189 X Loc [lvdtvlt13]
2: 173 Y Loc [gagefac13]

```
 3: 205      Z Loc [ lvdt_13   ]

72:  Z=X/Y (P38)
 1: 190      X Loc [ lvdtvlt14 ]
 2: 174      Y Loc [ gagefac14 ]
 3: 206      Z Loc [ lvdt_14   ]

73:  Z=X/Y (P38)
 1: 191      X Loc [ lvdtvlt15 ]
 2: 175      Y Loc [ gagefac15 ]
 3: 207      Z Loc [ lvdt_15   ]

74:  Z=X/Y (P38)
 1: 192      X Loc [ lvdtvlt16 ]
 2: 176      Y Loc [ gagefac16 ]
 3: 208      Z Loc [ lvdt_16   ]


; Set output flag and output all data measured in the loop
;
75:  Do (P86)
 1: 10       Set Output Flag High (Flag 0)

; Set storage array for lvdt
;
76:  Set Active Storage Area (P80)
 1: 1        Final Storage Area 1
 2: 60       Array ID

; Record real time with each measurement
;
77:  Real Time (P77)
 1: 1111     Year,Day,Hour/Minute,Seconds (midnight = 0000)


78:  Resolution (P78)
 1: 1        High Resolution

79:  Sample (P70)
 1: 16       Reps
 2: 193      Loc [ lvdt_1    ]

; Turn off the multiplexer
;

80:  End (P95)
```

```
81:  Do (P86)
 1: 57       Set Port 7 Low

82:  End (P95)


;****VIBRATING WIRE GAGE****
; This program will multiplex 16 full bridge Roctest EM-5 strain gages
; on one AM416 multiplexer unit. Roctest vibrating wire strain gages
; type EM-5 with a gage factor of 4062.4 are assumed. The program is
; written for the gages to be in connection with a CSI AVW1 or AVW100
; signal conditioner.
; The gauges are measured 1 minute into every 4 hour interval.
; Continuous measurements are taken for 17 minutes at a rate
; of 0.01hertz (1 measurement every 100 seconds, 10 measurements in
; 16.667 minutes, loop count).

; Wiring for this program must be connected in the following manner:
;
;       AM416                   CR23X
;
;       12V                     12V
;       GND                     G (near 12V C8)
;       Clk                     C6
;       Res                     C5
;
;
;       AVW1                    CR23X
;
;       T                       SE5
;       F                       SE6
;       EX                      EX4
;       AG                      G(symbol near EX4)
;       Vx                      12V
;       G                       G(near C4)
;       G(symbol, in sensor group)    G(near 5V)
;
;
;       EM-5 Gauge              AM416                   AVW1
;
;       Temp Hi                 H1                      T+
;       Temp Lo                 L1                      T-
;       Freq Hi                 H2                      C+
;       Freq Lo                 L2                      C-
;       Shield                  Shield                  G
```

```
;Output format:
;              All ustrain values......microstrain
;              All temperatures........degrees celsius


;****Vibrating Wire Gage****



; 5 measurement cycles at 90 second intervals
; (it takes 80 seconds to read all 16 vib wire gages)
83:  Beginning of Loop (P87)
 1: 0        Delay
 2: 1        Loop Count

; Turn on Multiplexer
;
84:  Do (P86)
 1: 45       Set Port 5 High

85:  Beginning of Loop (P87)
 1: 0        Delay
 2: 16       Loop Count

86:  Do (P86)
 1: 76       Pulse Port 6

87:  Delay w/Opt Excitation (P22)
 1: 4        Ex Channel
 2: 0000     Delay W/Ex (units = 0.01 sec)
 3: 5        Delay After Ex (units = 0.01 sec)
 4: 0000     mV Excitation

88:  Excite-Delay (SE) (P4)
 1: 1        Reps
 2: 15       5000 mV, Fast Range
 3: 5        SE Channel
 4: 4        Excite all reps w/Exchan 4
 5: 2        Delay (units 0.01 sec)
 6: 2500     mV Excitation
 7: 113   -- Loc [ vtemp_1   ]
 8: .001     Mult
 9: 0.0      Offset
```

```
89:  Vibrating Wire (SE) (P28)
 1: 1        Reps
 2: 6        SE Channel
 3: 4        Excite all reps w/Exchan 4
 4: 4        Starting Freq. (units = 100 Hz)
 5: 10       End Freq. (units = 100 Hz)
 6: 200      No. of Cycles
 7: 0        Rep Delay (units = 0.01 sec)
 8: 129   -- Loc [ ustrain_1 ]
 9: 4062.4   Mult
10: 0.0      Offset

90:  Polynomial (P55)
 1: 1        Reps
 2: 113   -- X Loc [ vtemp_1   ]
 3: 145   -- F(X) Loc [ vibtmp_1  ]
 4: -416.7   C0
 5: 1577.9   C1
 6: -2469.1  C2
 7: 1954.8   C3
 8: -767.33  C4
 9: 120.34   C5

91:  End (P95)

92:  Do (P86)
 1: 55       Set Port 5 Low

; Output Termperature readings
;
93:  Do (P86)
 1: 10       Set Output Flag High (Flag 0)

94:  Set Active Storage Area (P80)
 1: 1        Final Storage Area 1
 2: 40       Array ID

95:  Real Time (P77)
 1: 1111     Year,Day,Hour/Minute,Seconds (midnight = 0000)

96:  Sample (P70)
 1: 7        Reps
 2: 145      Loc [ vibtmp_1  ]

;Output Strain Readings
;
```

```
97:  Do (P86)
 1: 10       Set Output Flag High (Flag 0)

98:  Set Active Storage Area (P80)
 1: 1        Final Storage Area 1
 2: 50       Array ID

99:  Real Time (P77)
 1: 1111     Year,Day,Hour/Minute,Seconds (midnight = 0000)

100:  Sample (P70)
 1: 7        Reps
 2: 129      Loc [ ustrain_1 ]

101:  End (P95)



*Table 2 Program
  02: 0.0000    Execution Interval (seconds)


*Table 3 Subroutines


End Program
```

B. Second Computer Model and Results.

To determine if the results obtained from the live load test were valid or not, a model was developed using the computer program *Visual Analysis.* Only spans *A* and *B* were incorporated into the model. The other half of the bridge is not instrumented and an expansion joint separates the two halves. All five girder lines were present in the model even though only girder line four and girder line five are instrumented. The abutment was modeled with a fixed joint and the expansion joint was modeled with a roller joint. The link-slab was modeled using a pinned connection at the girder end bearings of two adjacent girders. The stiffnesses of the composite girders and link-slab were calculated

by hand calculations and then entered into the computer program. Loads were positioned on the model at the exact location they were during the live load test. Figure C.1 is an example of what the computer model looks like before it is loaded.

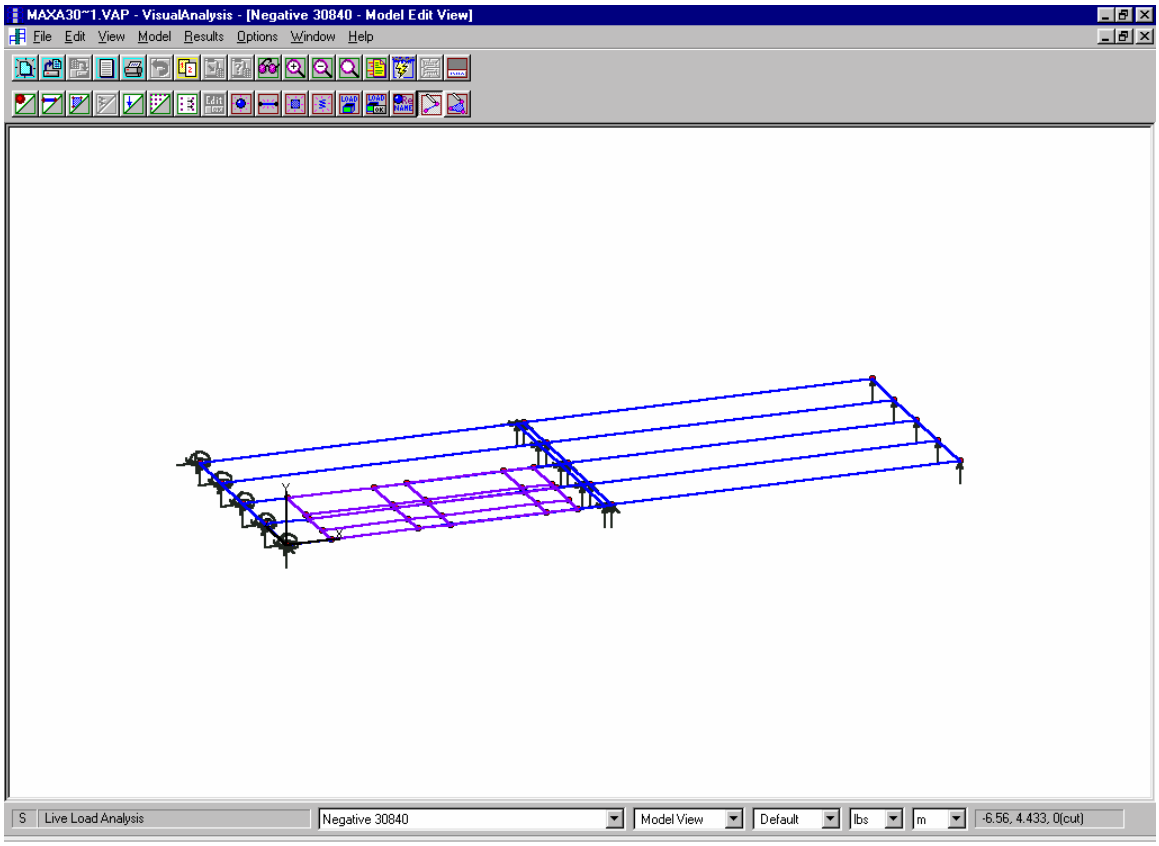

Figure B.1 Visual Analysis computer model.

After running the computer model for each load at the location, which produces the maximum positive moment in span B, and the location that produces the maximum negative moment in the link-slab, the results were compared with the actual results from the live load test. Tables B.1 and B.2 list the results from the computer model. The girder identification is the same as before.

Table B.1 Rotations from maximum negative moment in link slab (rad).

Load (kN)	A4-N	B4-S	B4-N	A5-N	B5-S	B5-N
0	0	0	0	0	0	0
137	8.03E-05	7.50E-05	7.33E-05	3.14E-05	3.49E-05	3.32E-05
214	0.000108	0.000171	0.000176	4.36E-05	7.16E-05	7.16E-05
304	0.00014	0.000267	0.000283	6.46E-05	0.000143	0.00015
424	0.000182	0.000363	0.000389	8.38E-05	0.00019	0.000201

Table B.2 Rotations from maximum positive moment in span B (rad).

Load (kN)	A4-N	B4-S	B4-N	A5-N	B5-S	B5-N
0	0	0	0	0	0	0
137	0.000122	8.73E-05	0.000129	8.38E-05	5.59E-05	7.33E-05
214	0.000183	0.000194	0.0003	0.000126	0.00012	0.000157
304	0.000251	0.000304	0.000475	0.000183	0.000232	0.000307
424	0.000382	0.000424	0.000661	0.000279	0.000321	0.000421

When comparing the results from the model and the live load test, it can be seen that the results are very similar. The force-rotation response of the end of all the instrumented girders was graphed. Figures B.2 through B.13 are the graphs, which compare the model with the live load test results. Included in the graph is a diagram which shows where the girder being graphed is located and the position of the truck during the test which caused these rotations. With two exceptions, all of the graphs are very similar. The two exceptions are both at the south end of girder B4, which is located at the link slab, but during the two different loading positions. It is believed that there was a faulty LVDT at this location.

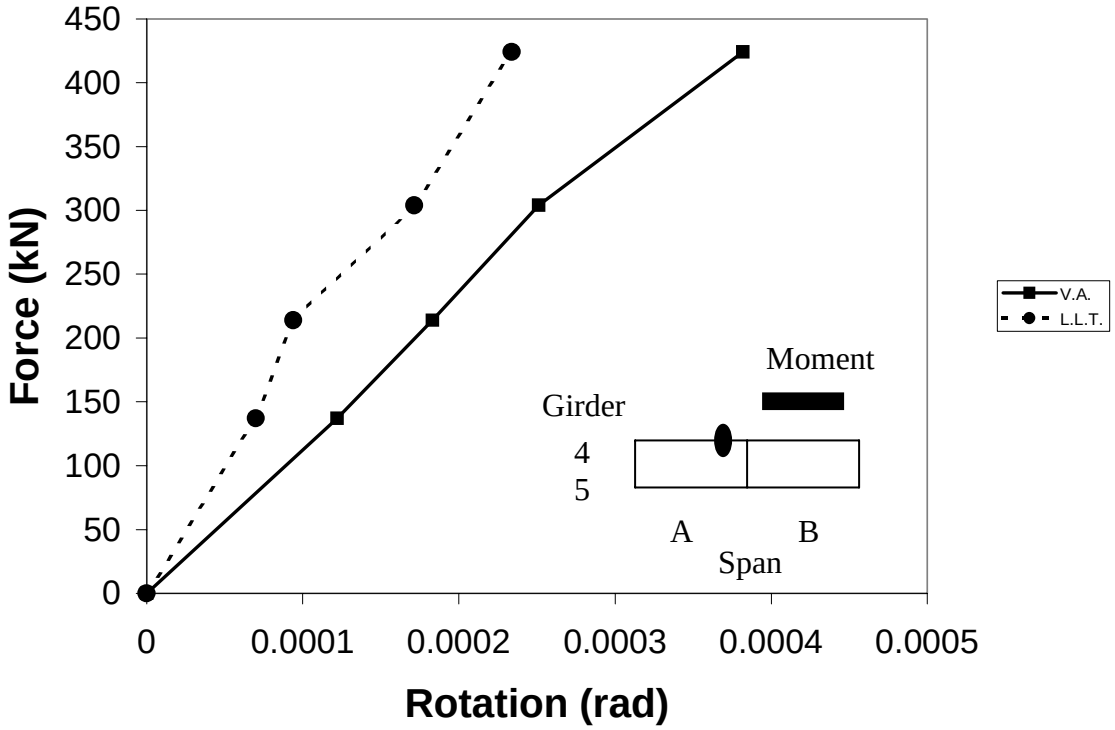

Figure B.2 North end of girder A4 with maximum moment in span B (link slab).

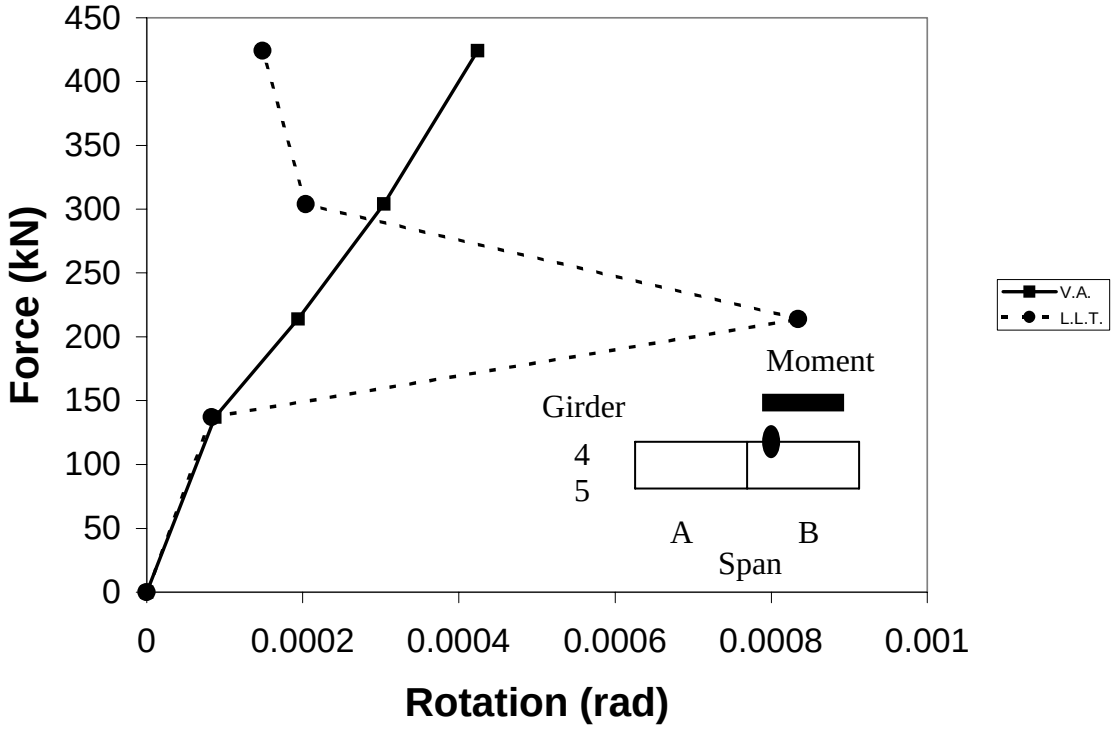

Figure B.3 South end of girder B4 with maximum moment in span B (link slab).

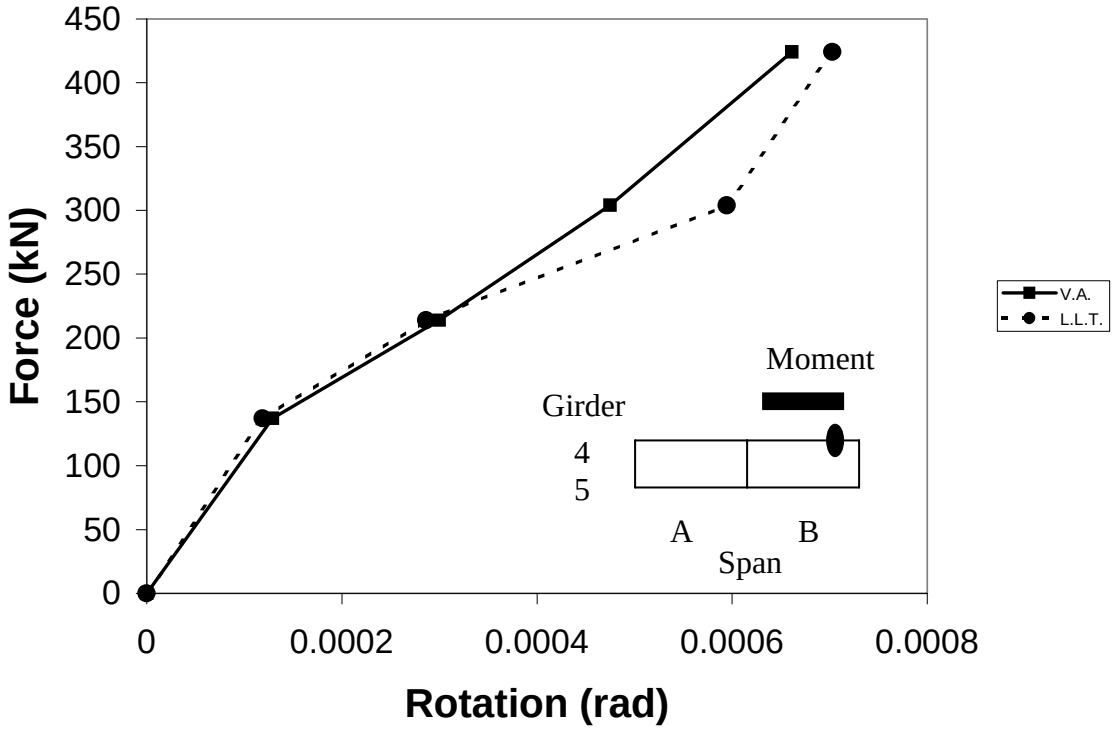

Figure B.4 North end of girder B4 with maximum moment in span B.

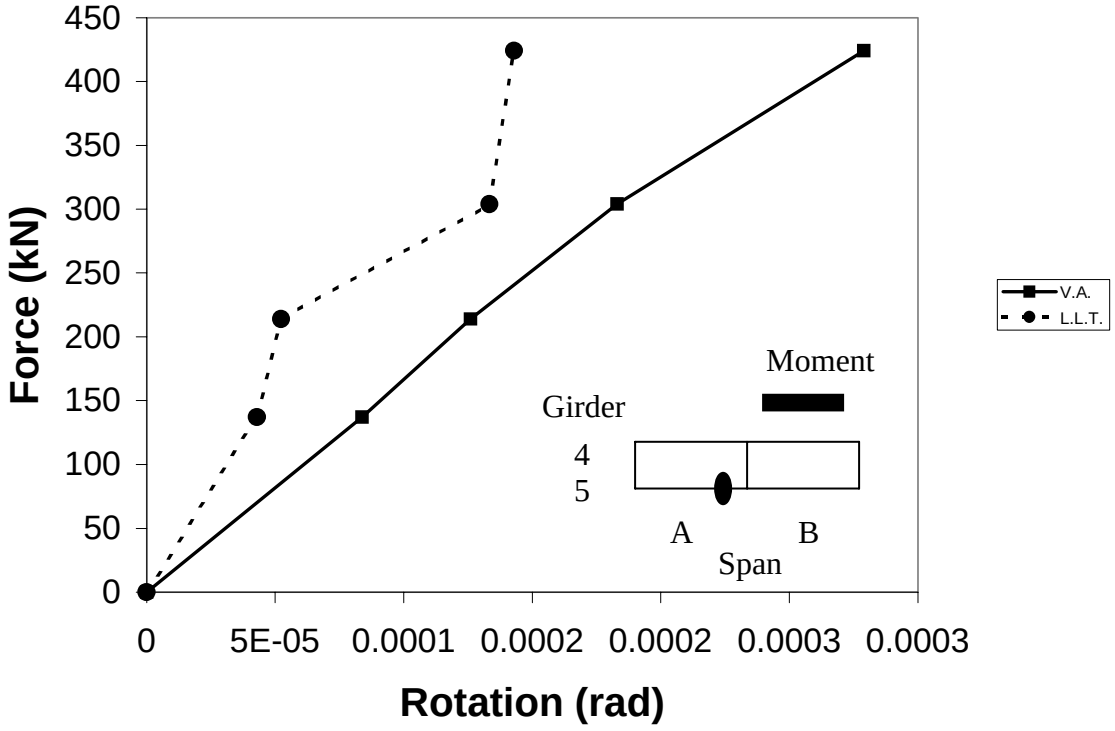

Figure B.5 North end of girder A5 with maximum moment in span B (link slab).

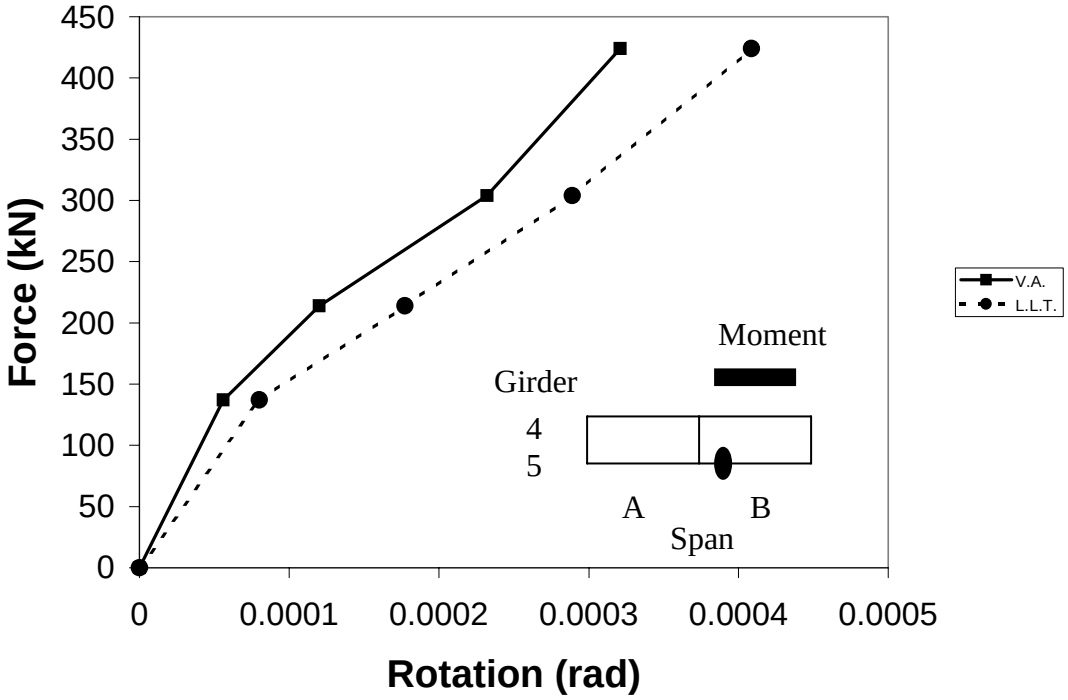

Figure B.6 South end of girder B5 with maximum moment in span B (link slab).

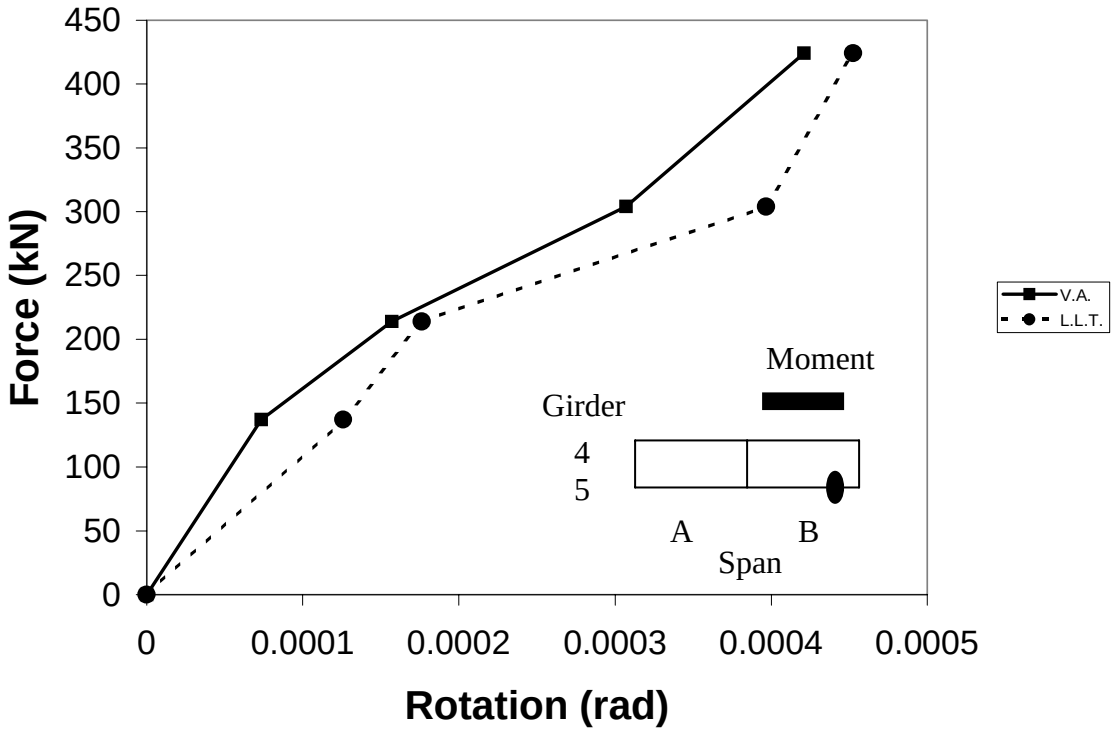

Figure B.7 North end of girder B5 with maximum moment in span B.

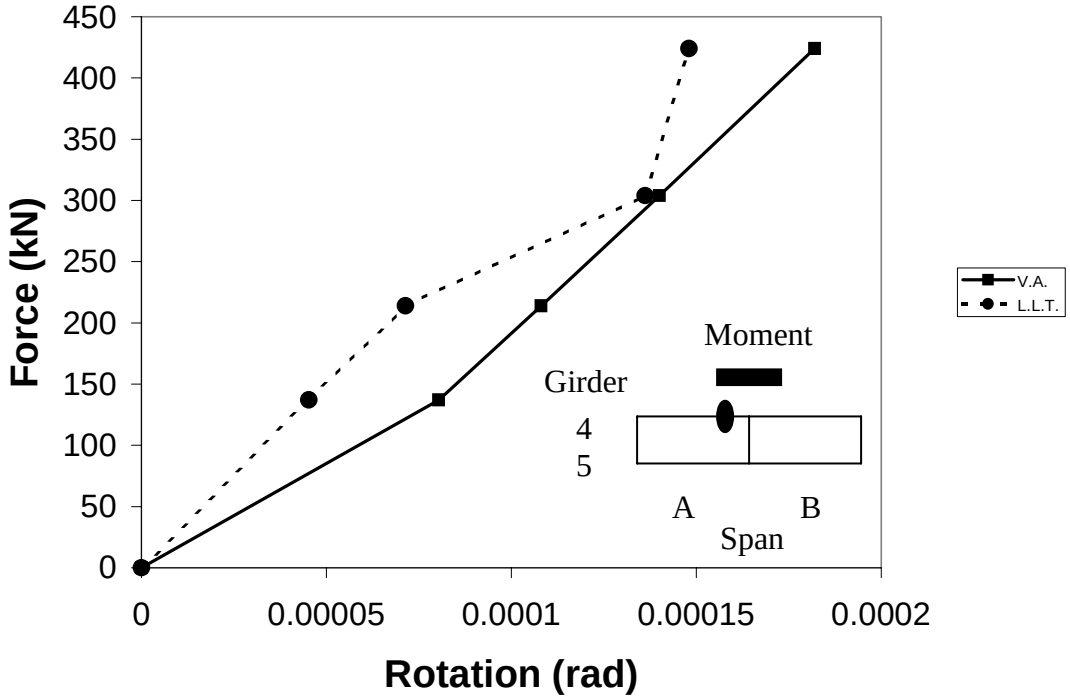

Figure B.8 North end of girder A4 with negative moment (link slab).

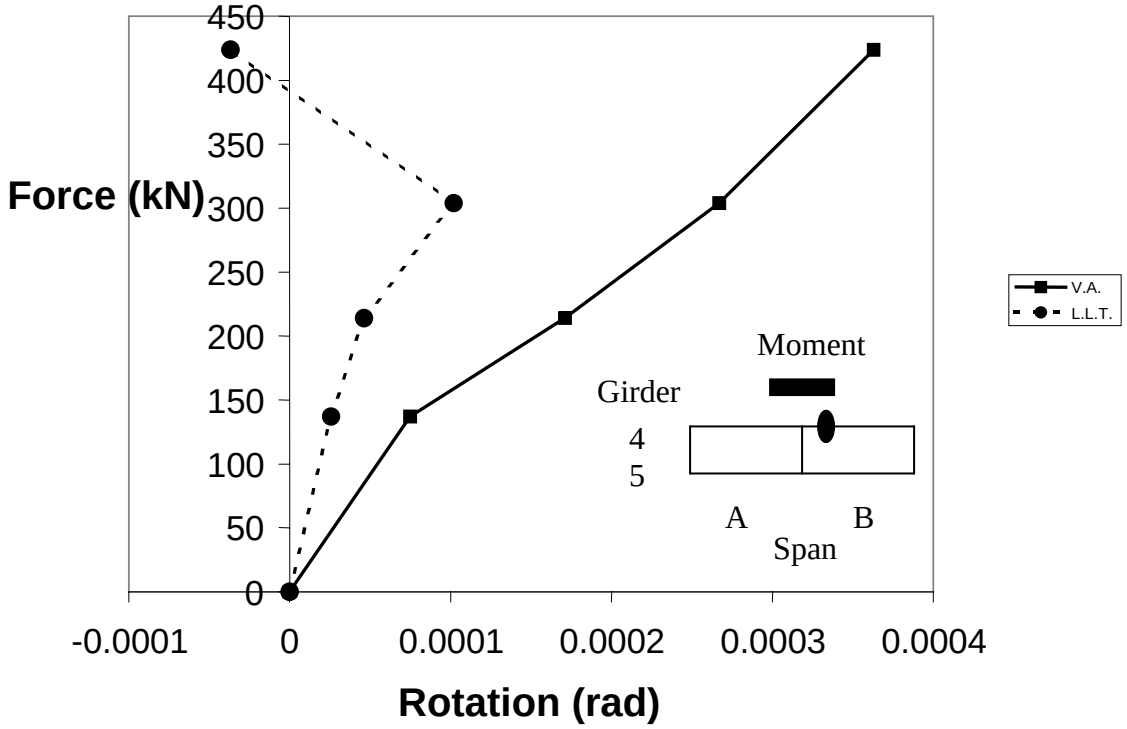

Figure B.9 South end of girder B4 with negative moment (link slab).

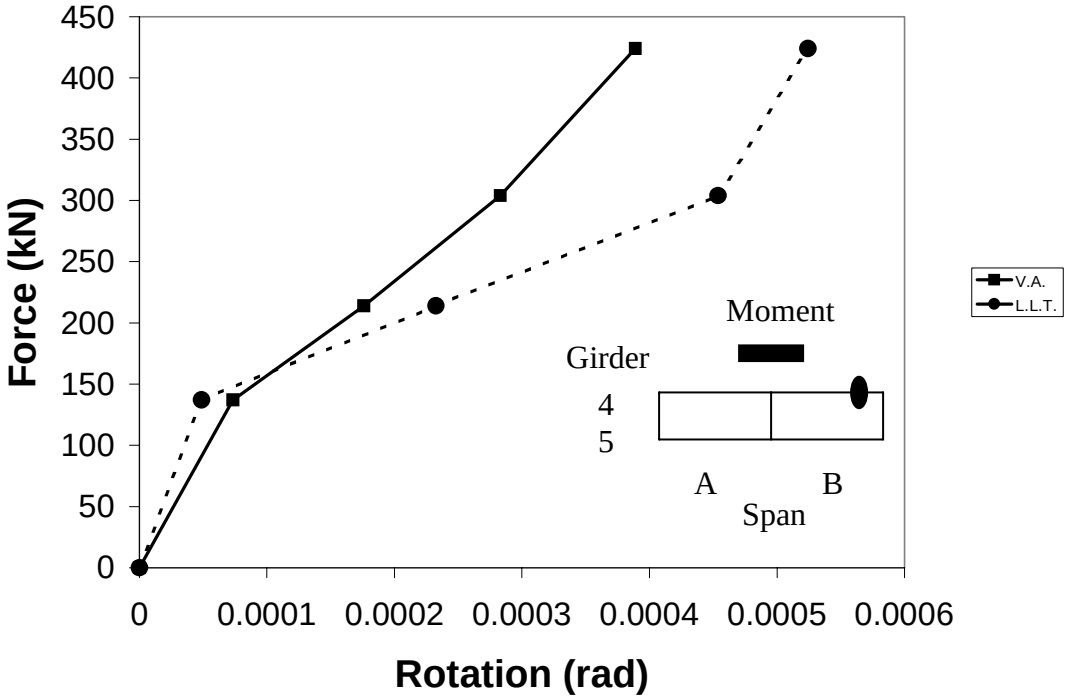

Figure B.10 North end of girder B4 with negative moment.

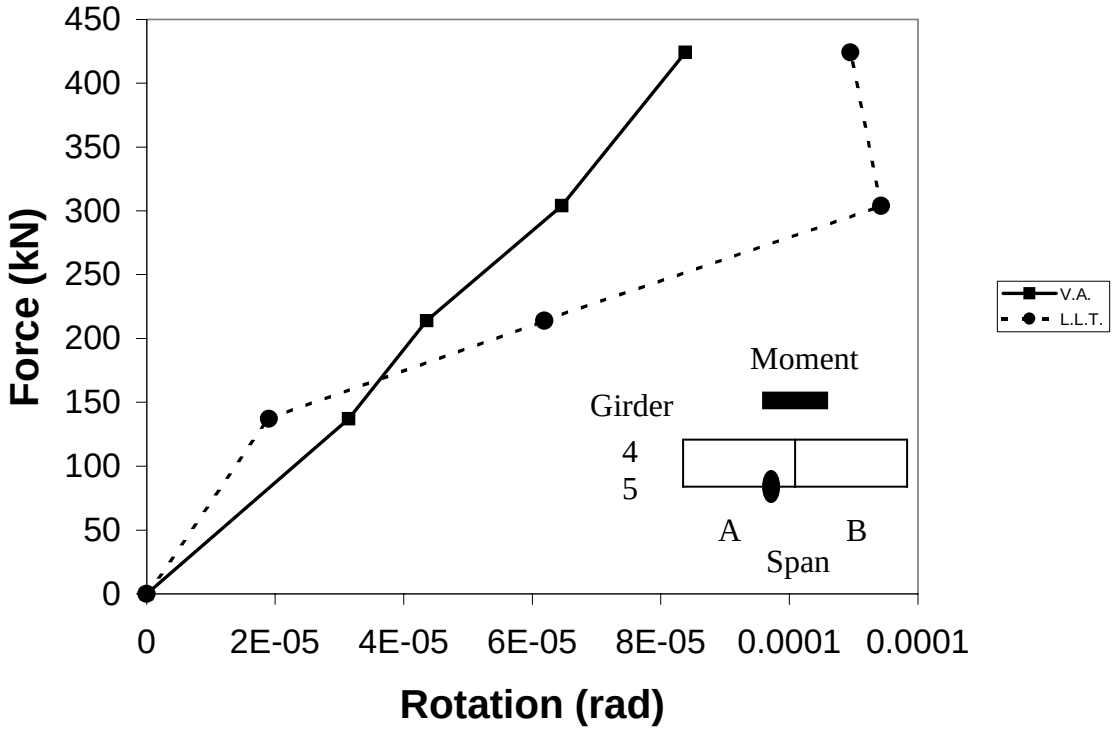

Figure B.11 North end of girder A5 with negative moment (link slab).

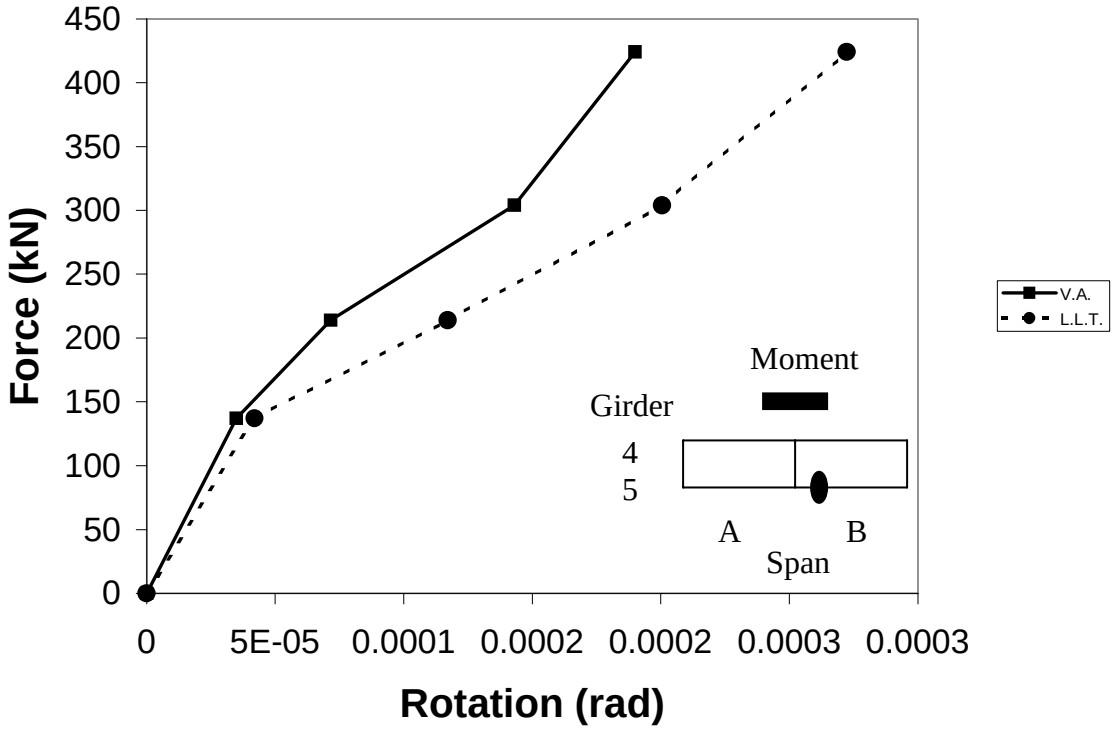

Figure B.12 South end of girder B5 with negative moment (link slab).

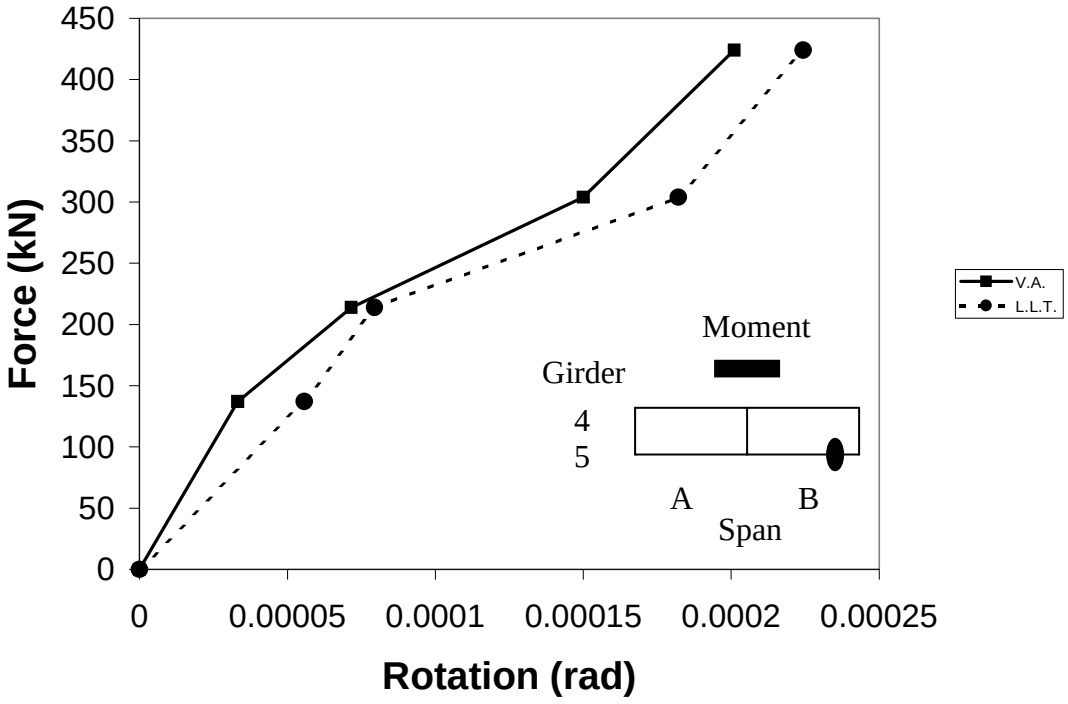

Figure B.13 North end of girder B5 with negative moment.

C. Computer Model Comparison.

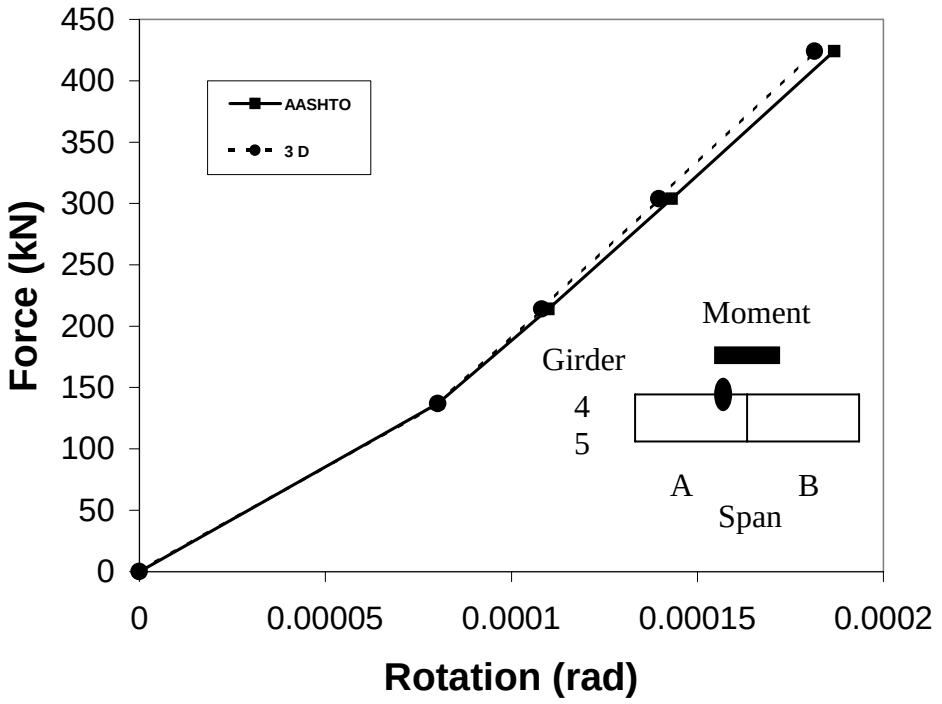

Figure C.1 North end of girder A4 with negative moment (link slab).

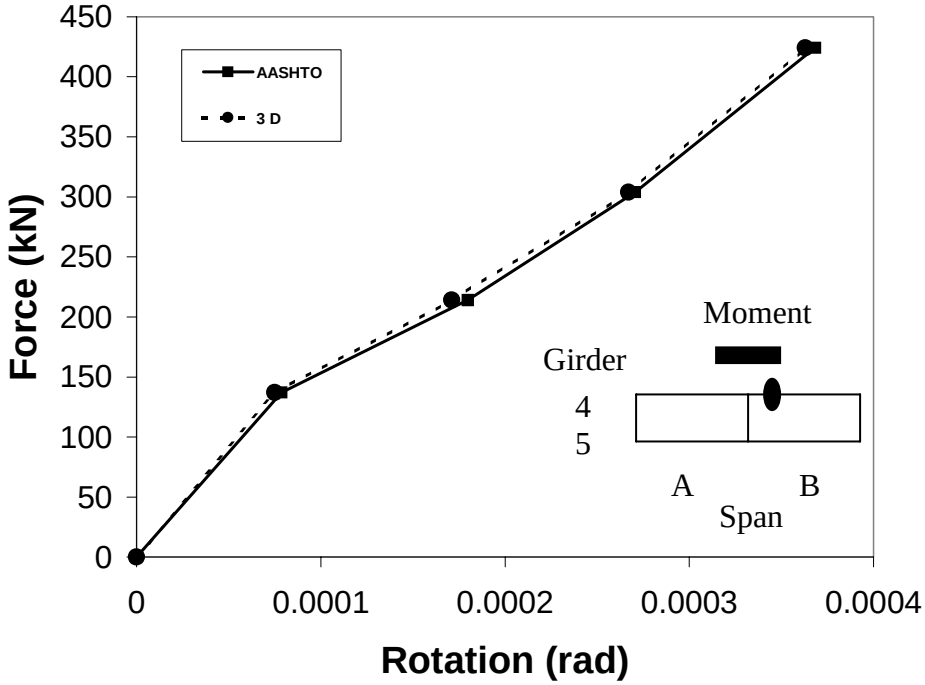

Figure C.2 South end of girder B4 with negative moment (link slab).

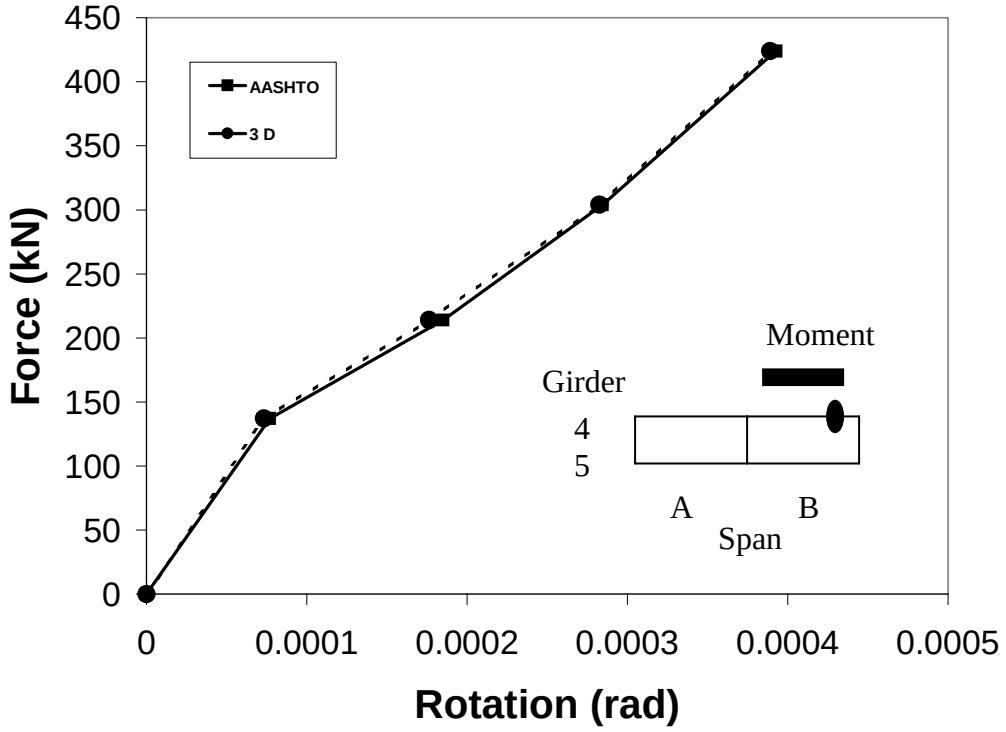

Figure C.3 North end of girder B4 with negative moment.

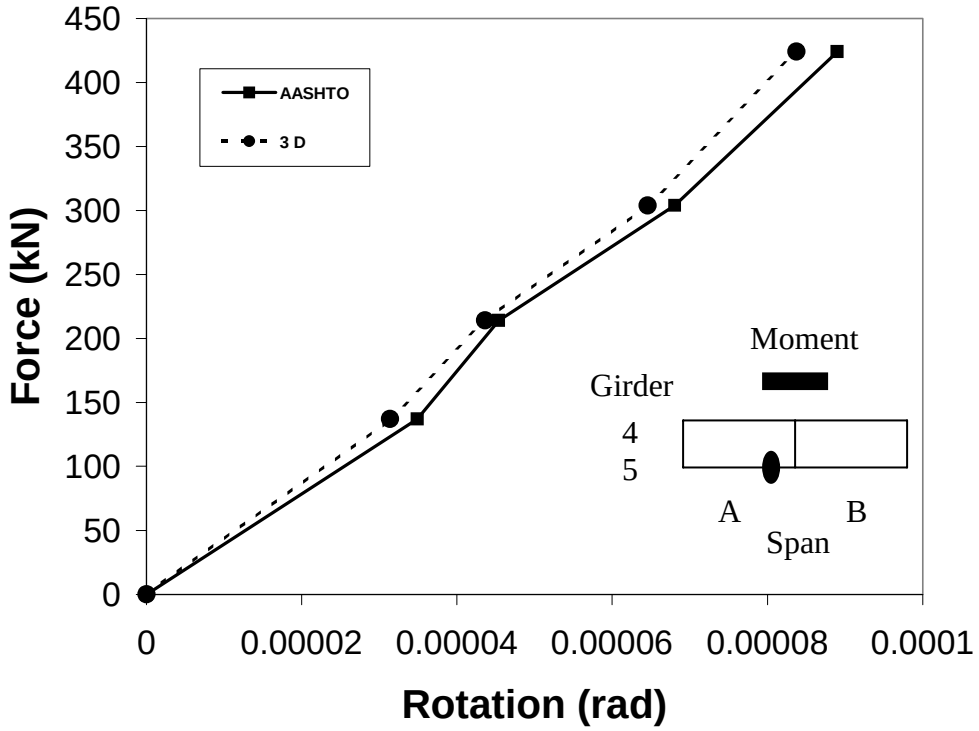

Figure C.4 North end of girder A5 with negative moment (link slab).

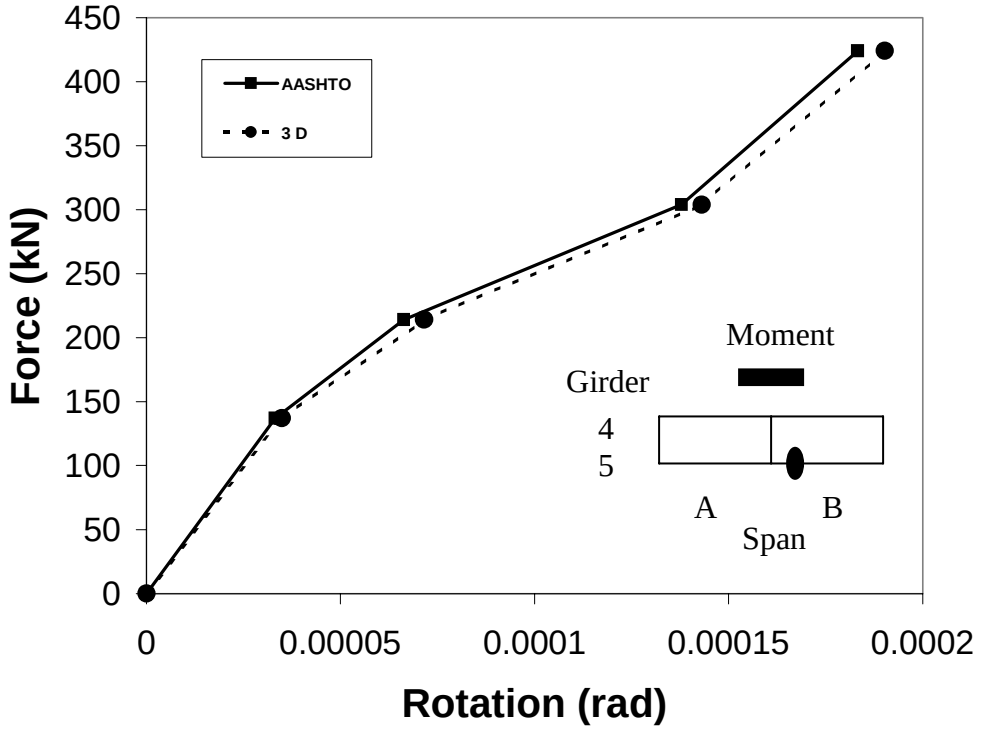

Figure C.5 South end of girder B5 with negative moment (link slab).

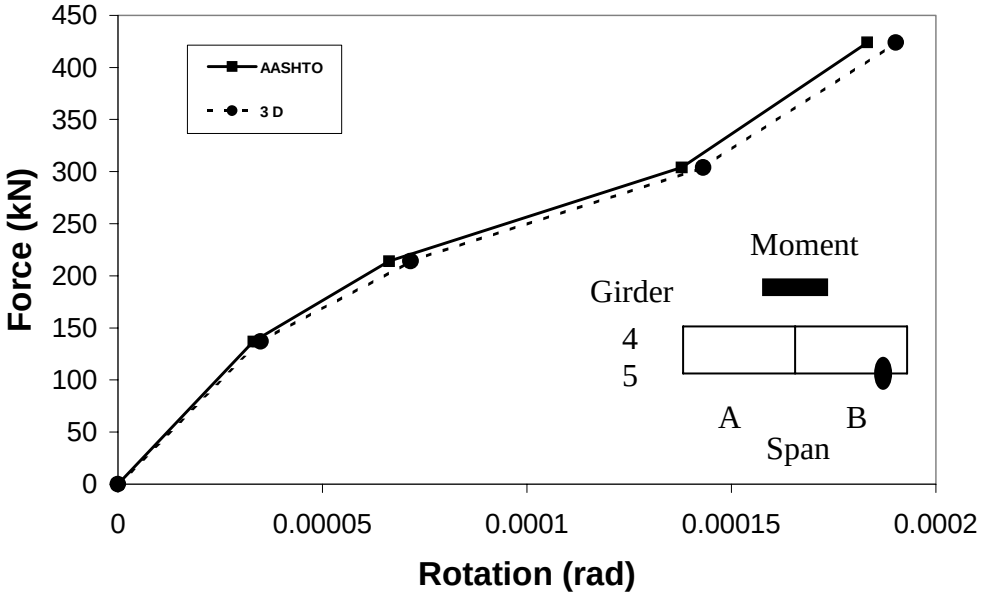

Figure C.6 North end of girder B5 with negative moment.

D. Service Load Graphs.

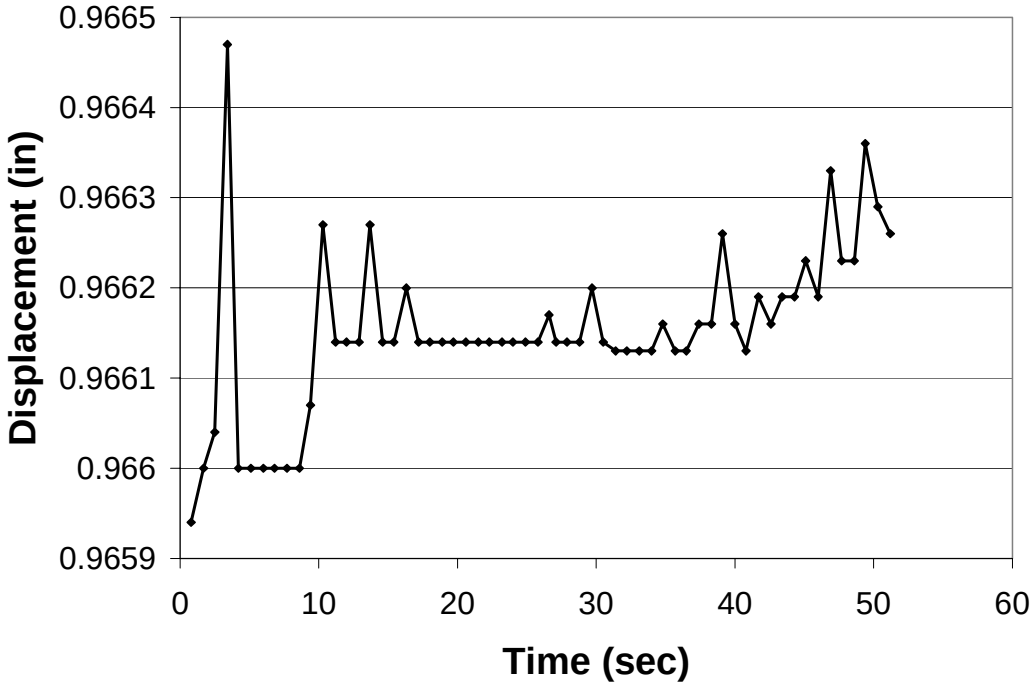

Figure D.1 LVDT reading for approximately fifty seconds.

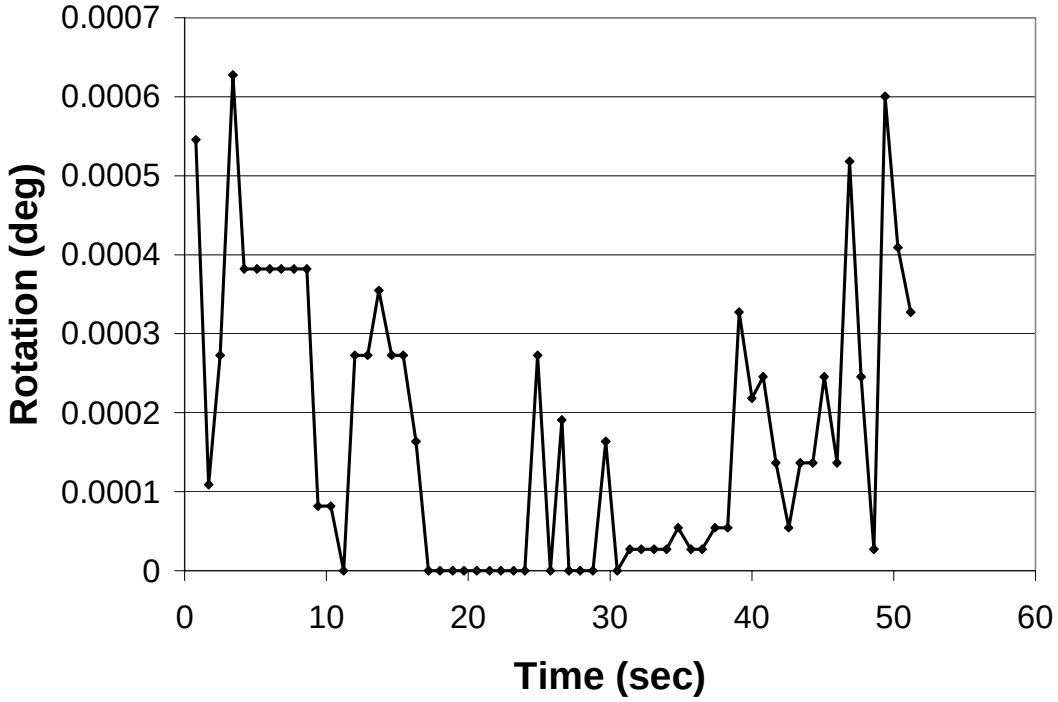

Figure D.2 Rotation of girder end for approximately fifty seconds.

E. Design Procedure Examples.

E.1 Use of Design Charts.

Suppose a link slab with the following geometric properties was going to be designed:

h =	9	
ρ =	0.01	
γ =	0.599969	
β =	1.2	
h =	215	mm
d =	129	mm
b =	2437	mm
Ec =	2.62*10^10	Pa
L =	1500	mm
y =	108	mm
I =	2.019*10^9	mm^4
fr =	3.447*10^6	Pa

These properties are the same properties that were used in the formulation of the design charts previously shown. The steel ratio is 0.01 percent and suppose the engineer wanted to design the link slab for a crack width of 0.75 mm and a rotation of 0.00175 radians. The engineer would go to the following design chart and see that the amount of reinforcing steel needed is #22 bars at 304mm on center:

ρ = 0.010	w (mm)			
θ	0.25	0.5	0.75	1.00
0.0005	# 29 @ 482			
0.00075	# 16 @ 143			
0.001	# 10 @ 60	# 29 @ 482		
0.00125		# 19 @ 247		
0.0015		# 16 @ 143	# 29 @ 482	
0.00175		# 13 @ 90	# 22 @ 304	# 36 @ 720
0.002		# 10 @ 60	# 19 @ 204	# 29 @ 482

E.2 Formulation of Design Charts.

To develop the first column of the design chart with a steel ratio of 0.01 percent, the procedure mentioned in section 3.4 should be followed. Listed in the following chart is the negative moment induced in the link slab by the end rotations and the steel stress based on a cracking moment of 64.8 kilonewton meters:

θ	Ma (N-m)	fs(0.01) (Pa)
0.0005	35266	98160030
0.00075	52899	147240045
0.001	70532	196320060
0.00125	88165	245400075
0.00147	103682	288590488
0.0015	105798	294480090
0.00175	123431	343560105
0.002	141064	392640120

The effective tension area of concrete based on a crack width of 0.25 mm is as follows:

θ	A (mm^2)
0.0005	82979
0.00075	24586
0.001	10372
0.00125	5311
0.00147	3265
0.0015	3073
0.00175	1935
0.002	1297

The spacing of reinforcement is as follows:

θ	s (mm)
0.0005	482
0.00075	143
0.001	60
0.00125	N/A
0.00147	N/A
0.0015	N/A
0.00175	N/A
0.002	N/A

Based on the number of bars required, the area of the bar needed was calculated and the following bar designations were assigned:

θ	Ab
0.0005	29
0.00075	16
0.001	10
0.00125	N/A
0.00147	N/A
0.0015	N/A
0.00175	N/A
0.002	N/A

This is the same procedure that was used to calculate the steel quantities for the other steel ratios. The bars that are not applicable in the above chart were eliminated because the calculated spacings were too close. The procedure is not complicated and can be developed for link slabs having different widths, lengths and depths.

F.3 Example

Design a link slab for a bridge with four equal spans of 20 meters in length. The girder center to center spacing is 3 meters and the depth of the slab is 225 mm. The deck is reinforced with #16 bars in the transverse direction with a concrete cover of 65 mm.

Use E_c = 26.3 MPa for the deck. Assume that the reinforcement ratio for the link slab is 0.01 percent. Also assume that the flexural modulus f_r = 3.5 MPa.

Solution:

Moment of inertia of the link slab = $2.848*10^9$ mm^4

Use rotations of 0.0005, 0.00075, 0.001, 0.00125, 0.0015, 0.00175 and 0.002 to formulate the design charts. The negative moments induced in the link slab due to the applied end rotations are the following:

Negative Moments.

θ	Ma (kN-m)
0.0005	37.45
0.00075	56.18
0.001	74.90
0.00125	93.63
0.0015	112.35
0.00175	131.08
0.002	149.80

Using a cracking moment, which was calculated, of 88.2 kN-m, the stress in the reinforcement using the above calculated negative moments is the following:

Steel Stress.

θ	fs(0.01) Mpa
0.0005	55.30
0.00075	82.96
0.001	110.61
0.00125	138.26
0.0015	165.91
0.00175	193.56
0.002	221.21

Now, using the Gergely-Lutz expression with crack widths of 0.1, 0.25, and 0.4 mm, the effective tension area of concrete is the following:

Effective Tension area of concrete.

θ	0.1	0.25	0.4
0.0005	39500	617187	2527997
0.00075	11704	182870	749036
0.001	4937	77148	316000
0.00125	2528	39500	161792
0.0015	1463	22859	93630
0.00175	921	14395	58962
0.002	617	9644	39500

Using these areas, the spacing of reinforcement, and the size of the bars can be determined The spacing and bar sizes after the unfeasible solutions have been eliminated are the following:

Spacing.

θ	0.1	0.25	0.4
0.0005	304		
0.00075	90		
0.001		593	
0.00125		304	
0.0015		176	
0.00175		111	454
0.002		74	304

Bar Sizes.

θ	0.1	0.25	0.4
0.0005	10		
0.00075	33		
0.001		5	
0.00125		10	
0.0015		17	
0.00175		27	7
0.002		40	10